THE DEVELOPMENT OF AFFECTIVE AND COGNITIVE STRIATAL NEUROBIOLOGY AND CONNECTIVITY DURING ADOLESCENCE

by

Bart Larsen

B.A., Lewis and Clark College, 2010

Submitted to the Graduate Faculty of

The Dietrich School of Arts and Sciences in partial fulfillment

of the requirements for the degree of

Doctor of Philosophy

University of Pittsburgh

2017

UNIVERSITY OF PITTSBURGH

DIETRICH SCHOOL OF ARTS AND SCIENCES

This dissertation was presented

by

Bart Larsen

It was defended on

November 30, 2017

and approved by

Kirk Erickson, Professor, Psychology

Jamie Hanson, Assistant Professor, Psychology

Timothy Verstynen, Assistant Professor, Psychology, Carnegie Mellon University

Dissertation Advisor: Beatriz Luna, Staunton Professor, Psychiatry and Psychology

THE DEVELOPMENT OF AFFECTIVE AND COGNITIVE STRIATAL NEUROBIOLOGY AND CONNECTIVITY DURING ADOLESCENCE

Bart Larsen, PhD

University of Pittsburgh, 2017

Adolescence is characterized by heightened reward-drive and sensation seeking behavior. Current neurodevelopmental theories hypothesize that this behavior is driven by the development of the brain's dopaminergic reward system and a developmental imbalance in the influence of the reward system on behavior relative to in cognitive control systems. The striatum is an ideal target for investigating these hypotheses because it is a central hub of the dopaminergic reward system, receives inputs affective and cognitive control systems, and functions to influence action selection. Current evidence for the development of striatal dopaminergic neurobiology during adolescence has been limited to animal models of adolescence due to limitations on the available techniques to assess striatal dopaminergic neurobiology *in vivo* in the human adolescent. Studies 1 and 2 of this dissertation assess this limitation by assessing a novel tissue property that has been linked multiple aspects of striatal dopamine neurobiology: tissue iron. We first use two MRI metrics sensitive to tissue iron concentration to investigate age-related differences in striatal tissue iron in a developmental sample spanning from adolescence to adulthood (ages 12 – 30) and then conduct a combined PET/MRI experiment in an adult sample (ages 18 - 30) to evaluate the relationship between striatal tissue iron concentration and indices of dopamine neurobiology. We find age-related increases in striatal tissue iron throughout adolescence and a positive association between an MR metric of tissue iron concentration and a PET metric of dopamine concentration in the aspect of the striatum most strongly associated with reward processing, the ventral striatum. Finally, study 3 assesses the hypothesis that there is a developmental imbalance between the

influence of affective reward systems and cognitive control systems of behavior during adolescence by investigating corticostriatal connectivity. Specifically, we identify areas of the striatum that integrate corticostriatal projections for brain areas involved affect and cognitive control and investigate age-related differences in the balance of these inputs. We find that the relative integrity of affective projections, in relation to projections from cognitive control systems, decreases with age and is positively associated with an index of reward-driven behavior.

TABLE OF CONTENTS

LIST OF TABLES

LIST OF FIGURES

LIST OF EQUATIONS

1.0 **INTRODUCTION**

Adolescence is a unique stage of development occurring between childhood and adulthood, starting with the onset of puberty and sexual maturation and spanning the second decade of life. This developmental stage has been found to be prominently characterized by heightened reward drive (sometimes referred to as incentive motivation), leading to a peak in sensation seeking behavior that is evident across cultures and species (see Spear, 2000 for review). Several lines of evidence support this model of adolescence. Large-scale self-report studies have found that sensation seeking and openness to new experience peak during late adolescence and decrease into adulthood (Steinberg 2010; Harden and Tucker-Drob 2011) (McCrae et al. 2002). These findings are supported by rodent studies that find that rodents show greater preference for novelty and greater exploratory behavior in novel environments during puberty as compared to adult rats (Adriani et al. 1998; Stansfield and Kirstein 2006). Increases in sensation seeking are thought to play an adaptive role in motivating individuation and specialization during the transition to adulthood because they promote the exploration of novel environments, creating a drive to seek new and more complex experience (Spear 2000; Steinberg 2008, 2010; Telzer 2016). Experience accumulation under novel contexts is critical for shaping and specializing complex behaviors and for establishing new social relationships during the transition to adulthood. Indeed, adolescence is the period when rodents begin to leave the nest, forage for food, and interact socially with rodents outside the family nest (Spear 2000). Though generally adaptive, heightened sensation seeking can

lead to a propensity for risk-taking during adolescence that can have maladaptive consequences (e.g. substance use, reckless behavior, unprotected sex). These risky behaviors can undermine survival during this stage; despite being a period of prime physical health, there is a transient increase in mortality rate during adolescence that is related to accidental deaths (e.g. reckless driving). Adolescence is also the age of emergence of major psychopathology that is associated with impairments in motivation and reward-driven behavior, including mood disorders, substance use disorders, and suicide, suggesting that the developmental processes that guide normative adolescent increases in reward-driven behavior may also cause adolescents to be vulnerable to disease. These public health concerns have led to an impetus to understand the neurodevelopmental mechanisms that underlie reward-driven behaviors during adolescence.

1.1 DUAL SYSTEMS MODELS OF ADOLESCENT NEURODEVELOPMENT

Developmental cognitive neuroscience models of adolescent development have hypothesized that the adolescent behavioral profile is the result of a hyperactive affective system paired with immature top-down control of behavior by cognitive control systems (Shulman 2016) (Figure 1). These "dual systems" models emphasize the dopaminergic reward system as playing a central role in affective processing, motivating reward drive and sensation seeking behavior, while prefrontal association cortex plays a role in cognitive control, including goal directed attention and inhibitory control of impulsivity. The dual systems models predict that these systems follow different developmental trajectories such that there is an imbalance in their functional roles occurring during adolescence. Specifically, this developmental imbalance is driven by a hyperactive dopaminergic affective system that has a greater relative influence on behavior relative to the top-down

frontostriatal inhibitory system, leading to heightened sensation seeking during adolescence. Multiple variations of the dual systems model have been proposed and these models have been thoroughly reviewed by Shulman et al. (2016). To summarize, these models vary in terms of the precise developmental trajectories of these brain systems that give rise to a developmental imbalance—a peak vs. curvilinear increase in the affective system and a linear increase vs. curvilinear increase in the cognitive control system (Figure 1). At the intersection of these two systems is the striatum. The striatum is a central hub of the dopaminergic reward system and also receives dense top-down projections from the prefrontal cortex. Thus, the development of the striatum and its connectivity with prefrontal cortex has been a central focus of the dual systems models of adolescent development. In the following sections, we review human and animal studies of striatal development that have motivated the dual systems theoretical models of adolescent development.

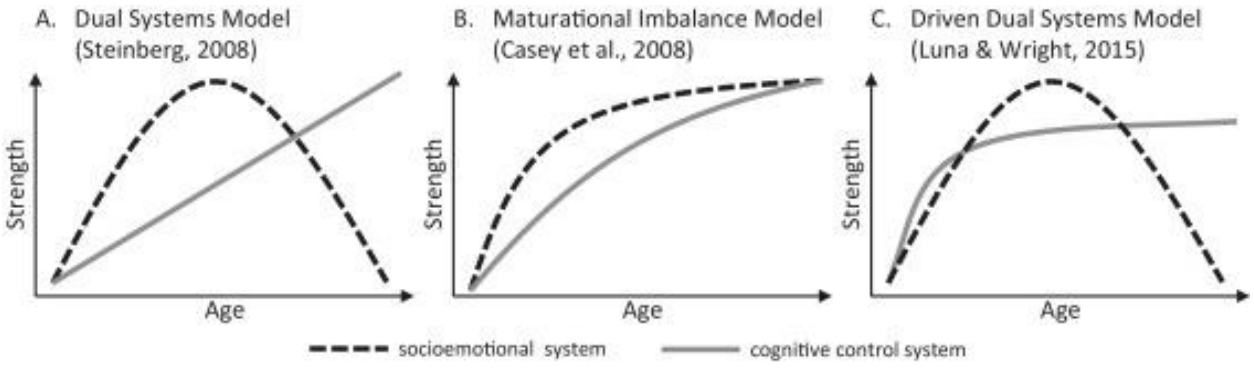

Figure 1. Dual systems models of adolescent neurodevelopment.

1.2 THE STRIATUM

The striatum, including the caudate, putamen, and nucleus accumbens/ventral striatum (VS), is the primary input nucleus to the basal ganglia and is central to core motivational circuitry that has been carefully delineated in both animal models (Wise 2002; Haber and Knutson 2010) and in adult human neuroimaging studies (Breiter and Rosen 1999; Delgado et al. 2000; McClure et al. 2004; Patel et al. 2013). The striatum functions to bias action selection based on both incentives associated with changing environmental cues and internal goals (Humphries et al. 2006; Houk et al. 2007; Harsay et al. 2011; de Wit et al. 2012). The VS in particular is involved in many aspects of motivation, including detection of incentives and reward prediction (O'Doherty 2004; Knutson and Cooper 2005; Cohen et al. 2010). The role of VS in these functions is facilitated by its rich dopamine (DA) innervation. DA is a neurotransmitter that is strongly implicated in reward-driven behavior and learning via neuromodulation of the mesolimbic and mesocortical circuits. Specifically, DA activity supports reward processing and reinforcement by signaling the reward expectancy and value of action outcomes (Clarke et al., 2014; Dreher et al., 2009; Frank, 2005; Hariri, 2009; Luciana et al., 2012; Schultz et al., 1997). Of particular relevance for adolescent sensation and novelty seeking behavior, DA also biases behavior toward exploration and novelty-seeking in both humans (Zald et al., 2008) and animal models (Koob et al., 1978; Le Moal and Simon, 1991) as well as computational simulations (Humphries et al., 2012). The VS is a hub of the mesocorticolimbic DA pathway, receiving dopaminergic inputs from the ventral tegmental area (VTA). In addition to rich connectivity with the midbrain DA circuitry, the striatum receives dense projections from the cerebral cortex, including cortical brain systems involved in affective and cognitive control processes (Alexander et al. 1986; Haber and Knutson 2010; Choi et al. 2012). The striatum has long been thought to integrate cortical information within closed, parallel circuits,

but more recently human (Verstynen et al. 2012; Verstynen 2014; Jarbo and Verstynen 2015) and non-human primate (Averbeck et al. 2014; Choi et al. 2016) studies have shown that areas of the striatum receive convergent projections from functionally disparate cortical regions. These convergent zones are thought to serve as functional hubs that directly integrate and synchronize information to drive basal ganglia action outputs (Haber 2003; Averbeck et al. 2014; Haber 2014). Convergent projections from limbic and cognitive control cortical systems into the striatum then represent an important neuroanatomical substrate for the integration of affective and executive information to influence behavior. Thus, the striatum is an ideal target for investigating both the development of affect processing (including VS development and the development of affective corticostriatal inputs) and developmental shifts in the relative influence of cortical brain systems on behavior.

1.3 THE DEVELOPMENT OF THE STRIATUM IN ADOLESCENCE

1.3.1 Dopamine

Human and animal studies investigating the development of the striatal dopamine system suggest a unique neurobiology during adolescence (Spear 2000; Luciana and Collins 2012). The vast majority of these studies have focused on animal models, particularly rodents, and these studies have been extensively reviewed elsewhere (for Reviews see: (Luciana et al., 2012; Padmanabhan and Luna, 2014; Sturman and Moghaddam, 2011; Telzer, 2016; Wahlstrom et al., 2010)). The multifaceted and complex nature of the dopamine system has similarly led to a complex picture of the development of this system during adolescence, with different indices of DA development (e.g.

receptor concentrations, DA innervation, activity) showing different developmental trajectories (plateaus vs. peaks) (Figure 2). This complexity has likely contributed to the different developmental trajectories of the affective system posited by variations in the dual systems models of development. We will synthesize these developmental studies of the adolescent striatal dopamine system here.

Striatal DA concentration increases throughout adolescence until it plateaus into adulthood in the rat (Giorgi et al. 1987). A similar pattern is evident for the DA transporter in the striatum (Tarazi et al. 1998a; Moll et al. 2000). However, striatal dopamine synthesis (Andersen, Dumont, et al. 1997) as well as D1 and D2 receptor concentrations in the caudate and putamen show distinct peaks during adolescence (Gelbard et al. 1989; Teicher et al. 1995; Andersen, Rutstein, et al. 1997; Tarazi et al. 1998b). Across all age groups, D1 receptor density is greater than D2 receptor density (Gelbard et al. 1989; Andersen, Rutstein, et al. 1997). Interestingly, the adult-like medial-to-lateral gradient of striatal D2 receptors is established during mid-adolescence, suggesting that the spatial organization of D2 receptors, in addition to the quantity, is maturing during adolescence (Teicher et al. 1995).

Studies of the activity of VTA neurons that project to the ventral striatum also provide a complex developmental picture. One study using a rat model found that adolescent VTA neurons fired faster during non-burst activity and had longer burst firing patterns than adult animals both in-vivo and in-slice (McCutcheon et al. 2009). An important caveat to this study is that these recordings were in anesthetized animals (or post-mortem) and thus were not in response to reward stimulation (and not recorded in a natural brain state). Further, reductions in basal firing between adolescent and adult rodents in this study were likely related to the maturation of VTA inhibitory tone, which was greater in adult animals, rather than changes to DA neurons *per se*. A more recent

study recorded VTA activity in awake, behaving rats while they performed a cued reward task. This study found that adolescent animals had a diminished VTA response to both reward anticipation and reward receipt, despite a similar cue-evoked response, suggesting reduced dopaminergic activity in adolescent animals (Kim et al. 2016).

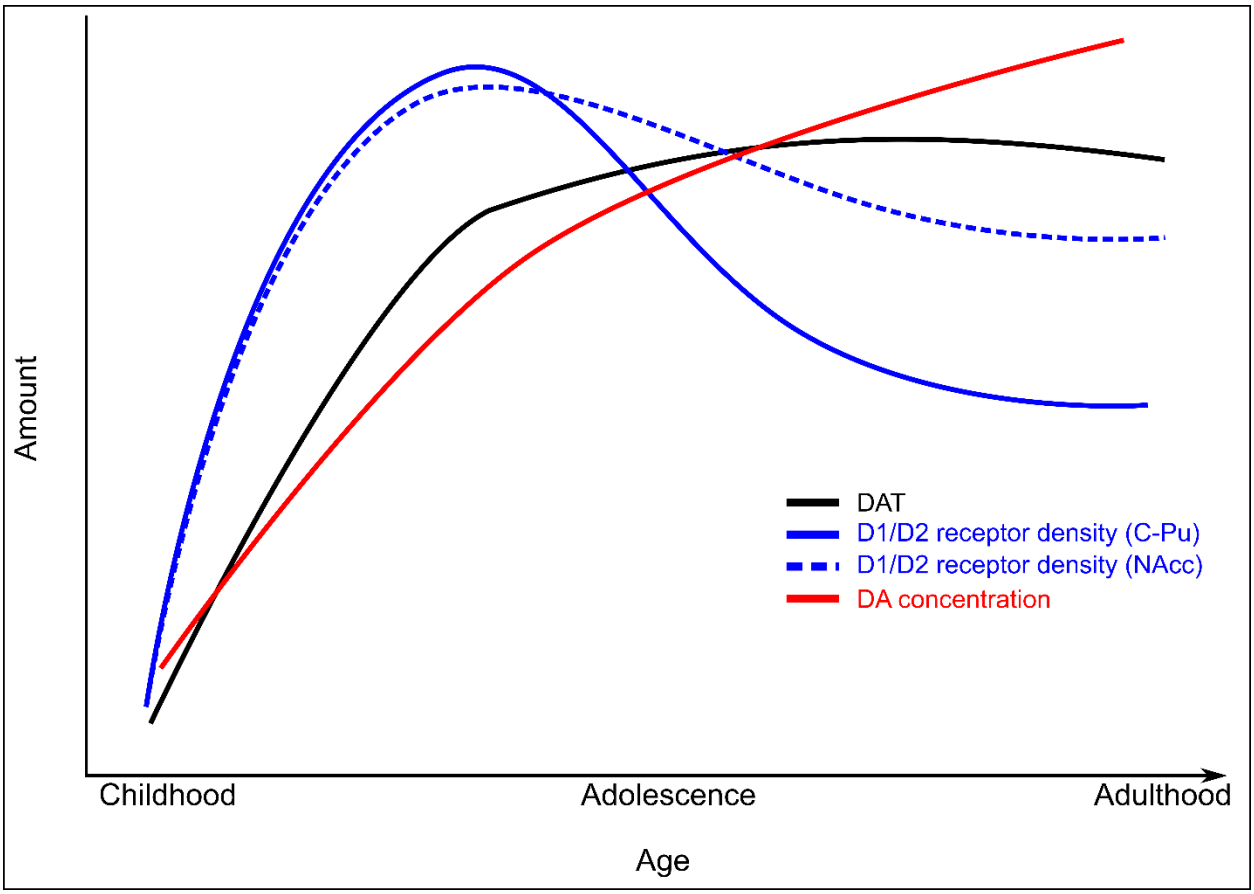

Figure 2. Schematic of rodent studies of striatal dopamine development.

Schematic representation of developmental trajectories of various aspects of striatal neurobiology. Striatal DA concentration (Giorgi et al. 1987) and DAT (Tarazi et al. 1998a; Moll et al. 2000) increases throughout adolescence until it plateaus into adulthood. Distinct peaks in D1 and D2 receptor concentrations occur in the caudate and putamen (Gelbard et al. 1989; Teicher et al. 1995; Andersen, Rutstein, et al. 1997; Tarazi et al. 1998b). This peak is less pronounced in the nucleus accumbens (Tarazi 2000, Teicher 1995).

1.3.2 Limitations in the ability to study DA system development in vivo during adolescence

These observations from animal models have led to the hypothesis that similar developmental processes are unfolding in the adolescent human, informing the inverted "U" trajectories of the affective system proposed by dual systems models (Shulman et al. 2016). However, due to limitations in methodology available for assessing DA neurobiology *in vivo* in humans (Wahlstrom et al. 2010), direct evidence of DA neurobiology development in the adolescent human is scant: One post-mortem study found that striatal DA concentration increases from childhood to adolescence when it either plateaus or decreases(Haycock et al. 2003). Post-mortem studies are difficult to conduct and modern in-vivo DA imaging techniques like positron emission tomography (PET) have limited applicability to pediatric populations. As a result, the field of human developmental neuroscience has tried to investigate the development of the striatal DA system using indirect indices of striatal maturation, including functional and structural morphometry magnetic resonance imaging (MRI). We next review recent findings using these techniques.

1.3.3 Structure

Cross-sectional (Sowell et al. 1999, 2002; Koikkalainen et al. 2007; Ostby et al. 2009; Tamnes et al. 2009) and longitudinal (Dennison et al. 2013; Tamnes et al. 2013; Mills et al. 2014; Raznahan et al. 2014) studies of the development of striatal structural morphometry generally indicate decreasing striatal volume throughout adolescence and young-adulthood, particularly in the rostral-ventral striatum (Koikkalainen et al. 2007; Raznahan et al. 2014), though one study found age-related increases in left nucleus accumbens volume (Dennison et al. 2013). Studies comparing

the development of VS and PFC structural morphometry find that both structures continue to develop into adulthood (Sowell et al. 2002; Mills et al. 2014; Raznahan et al. 2014), and that striatal volume change correlates with volume changes in other nodes of the motivation/limbic circuit, including anterior cingulate cortex and orbitofrontal cortex (Walhovd et al. 2014). However, the molecular mechanisms that drive these changes and the extent they relate to DA neurobiology are unknown.

1.3.4 Function

Human fMRI studies of adolescence have focused on reward responses in the striatum. Many studies have indicated that adolescents exhibit increased activation of putamen and nucleus accumbens in response to rewarding stimuli or in anticipation of the receipt of a reward relative to children and adults (Abdolmaleky et al. 2006, Ernst et al. 2005, Galvan et al. 2006, 2007; Geier et al. 2010, Padmanabhan 2011, Van Leijenhorst 2010). However, this finding has not been consistent as some have shown reduced striatal responses (Bjork et al. 2004, Eshel et al. 2007, lamm 2014) and some have found no differences (Krain 2006, telsovich 2014). These inconsistencies may be resolved, in part, if these studies are separated into those investigating striatal responses to reward *anticipation* as opposed to reward *receipt (*Shulman 2016). Whereas adolescents consistently show greater responses for reward receipt (Van Leijenhorst 2010, Galvan McGlennen 2013, Hoogendam 2013), results for reward anticipation are mixed (Bjork 2007, Teslovich 2014, Geier 2010, Padmanabhan 2011). These results collectively indicate that peaks in striatal DA from animal models are most closely reflected in human studies by striatal responses to reward receipt. However, there may not be direct correspondence between reward-related fMRI activation and DA release in the striatum (Lohrenz et al. 2016), making it difficult to interpret

these findings. Nevertheless, increased reward response in the nucleus accumbens has been associated with a propensity to engage in risky behavior (Galvan et al. 2007), suggesting these functional neuroimaging studies may bear on real-world adolescent behavior.

1.3.5 Iron accumulation

Adolescence is also a period of rapid striatal tissue-iron (ferritin) accumulation (Hallgren and Sourander 1958; Aquino et al. 2009; Wang, Shaffer, et al. 2012). Ferritin, which is distinct from blood (heme) iron, is primarily stored in oligodendrocytes where it supports myelin synthesis and ATP production (Connor and Menzies 1996; Moos 2002; Todorich et al. 2009), and is also found in midbrain and striatal neurons (Drayer et al. 1986). In the striatum, animal models of iron deficiency (Erikson et al. 2000) and disease models of restless leg syndrome (Connor et al. 2009a) and ADHD (Adisetiyo et al. 2014) indicate that tissue-iron is highly related to the dopamine system (Beard and Connor 2003). Animal studies have linked tissue-iron with D2 receptor expression (Beard and Connor 2003; Jellen et al. 2013), dopamine transporter levels and function (Erikson et al. 2000; Wiesinger et al. 2007), and dopamine neuron excitability (Jellen et al. 2013). Iron is also a necessary cofactor in tyrosine hydroxylase, the rate limiting step in dopamine synthesis (Ramsey et al. 1996). Thus, ferritin accumulation during adolescence may support age-related changes in the structure and function of striatal DA circuitry. Importantly, tissue iron is paramagnetic and can consequently be measured non-invasively using MRI, potentially providing a non-invasive window into developmental changes in dopamine circuitry during adolescence. Studies one and two of this dissertation investigate the development of tissue-iron concentration across the striatum during adolescence and evaluate tissue-iron as a non-invasive indirect indicator of striatal dopamine neurobiology.

1.3.6 Connectivity

Concurrent with developmental changes in striatal structural morphometry and reward responses are dynamic changes to pathways linking the striatum to prefrontal cortex. Animal and post-mortem human work provide evidence of increased myelination of cortical to subcortical axons and changes in axonal caliber during adolescence (Yakovlev et al. 1967; Benes et al. 1994). Human DWI studies of the development of structural striatal connectivity provide evidence of decreased radial diffusivity, thought to reflect myelination, of frontostriatal pathways from childhood to adulthood, leading to developmental improvements in inhibitory control (Liston et al. 2006; Asato et al. 2010; Simmonds et al. 2014a) and decreases in impulsivity (Peper et al. 2013). However, these studies typically also find reductions in axial diffusivity along the primary fiber direction, suggesting there may be a more complicated pattern of development. Functional connectivity studies show a pattern of increases and decreases in frontostriatal connectivity that tend to be determined by the functional differences in the respective cortical and striatal targets. Functional connectivity between the ventral striatum and prefrontal areas associated with cognitive control (e.g. lateral PFC) tend to show age-related increases in connectivity strength while connections with prefrontal areas associated with more affective or limbic functions (e.g. ventral medial and orbitofrontal PFC, insula, cingulate) show age related decreases (Porter et al. 2015; van Duijvenvoorde et al. 2016). Similarly, a study that compared cortical connections to associative striatum (e.g. caudate) with cortical connections with affective striatum (e.g. VS) found that associative connections tended to increase with age while affective connections tended to decrease (Porter et al. 2015). Another study looking at the development of task-related functional connectivity found that striatal connections with lateral PFC also increased with age and correlated with improvements in proactive inhibition (Vink et al. 2014). Together these results suggest a

complex pattern of frontostriatal development whereby affective and cognitive control pathways follow differing developmental trajectories. However developmental changes in the specific functional integration of systems involved in limbic and cognitive control functions, and their association with reward-driven behavior, have not been probed directly. The third aim of this dissertation investigates this question.

1.4 SUMMARY AND CURRENT STUDIES

Adolescent sensation seeking is thought to be related to the pronounced development of the mesolimbic DA reward system, with particular emphasis on the striatum. Multiple aspects of DA neurodevelopment have been mapped out in rodent models of adolescence, including DA receptor density, concentration, transporter, and midbrain activity, each following a developmental trajectory that highlights adolescence as a unique period of development (peak, plateau, inflection point; Figure 2). These studies have led to the hypothesis that similar neurodevelopmental processes are occurring in the human. However, limitations on the available techniques to assess DA *in vivo* in the human adolescent have made this difficult. As such, human developmental neuroscience has relied on indices of striatal structural and functional development, which, while valuable, have little known direct relationships to DA. The first two studies in this dissertation address this limitation by proposing new techniques to assess aspects of striatal neuroanatomy that have known links to the DA system. Study one uses a novel MR measure, normalized T2*-weighted imaging (nT2*), sensitive to iron concentration, to measure age-related differences in striatal neuroanatomy during adolescence. Results indicate age-related differences in DA circuitry. Study two follows up on the findings of study one by using a quantitative measure of brain iron

concentration to assess developmental trajectories of iron accumulation and evaluate tissue iron as an indirect measure DA neurobiology. These studies jointly address the hypothesis that the striatal DA system continues to mature during adolescence in the human and propose tissue iron as an indirect indicator of striatal DA that can be measured *in vivo* in human subjects of all ages.

The primary hypothesis of the dual systems model of adolescence is that there is a developmental imbalance between the influence of affective reward systems and cognitive control systems of behavior such that during adolescence the affective system is predominant. Corticostriatal circuitry is an ideal system to test this hypothesis as the striatum is an integration hub for different cortical systems, including those involved in affective processing and cognitive control. Though previous work has characterized developmental increases and decreases in cognitive and affective corticostriatal connectivity (respectively), no work has addressed developmental changes in the integration of these two systems at the level of the striatum and their relation to behavior. The final study of this dissertation addresses this hypothesis by identifying areas of the striatum that integrate corticostriatal projections for brain areas involved affect and cognitive control and investigating age-related differences in the balance of these inputs.

2.0 IN VIVO EVIDENCE OF NEUROPHYSIOLOGICAL MATURATION OF THE HUMAN ADOLESCENT STRIATUM

This chapter is adapted from (Larsen and Luna 2015).

2.1 INTRODUCTION

Adolescent behavior is characterized by increases in sensation-seeking that can lead to maladaptive risk-taking, resulting in increased likelihood of death or serious injury (Eaton et al. 2006). Thus, there is an impetus to understand the neurodevelopmental changes in the motivational system that may contribute to this behavioral profile. The striatum is of particular interest in this context because of its involvement in motivation and reward processing as well as learning, motor control, and cognition (Haber & Knutson 2010, McClure et al. 2003, Middleton & Strick 2000, Vo et al. 2011).

Rodent and non-human primate models provide evidence indicating continued striatal synaptogenesis in early adolescence, peaks in dopamine receptor expression and dopamine projections from the striatum to prefrontal cortex, and synaptic pruning in late adolescence (Crews et al. 2007, Kalsbeek et al. 1988, Rosenberg & Lewis 1995, Tarazi et al. 1998, Teicher et al. 1995). This line of evidence has led to the hypothesis that similar neurophysiological changes are occurring in adolescent humans (Casey et al. 2008, Spear 2000). Initial functional magnetic resonance imaging (fMRI) studies have found compelling evidence suggesting peak sensitivity of the adolescent striatum to reward stimuli relative to adults and children (Ernst et al. 2005, Galvan

et al. 2006, 2007; Geier et al. 2010, Leijenhorst et al. 2010, Padmanabhan et al. 2011), though this finding has not been consistent (Bjork et al. 2004; Eshel et al. 2007) and likely depends on the reward context investigated (Crone and Dahl 2012; Hoogendam et al. 2013) For example, recent work has suggested that striatal reactivity to reward anticipation increases into adulthood while reactivity to reward receipt decreases (Hoogendam et al. 2013). Currently there is a lack of in vivo measures with which to assess age-related differences in human striatal neurophysiology which limits our ability to understand neural mechanisms underlying differences in adolescent striatal function. Understanding the development of striatal neurophysiology is of particular significance given that abnormal striatal neurophysiology and function are implicated in a range of neuropsychological disorders that emerge during childhood and adolescence (Bradshaw & Sheppard 2000, Chambers et al. 2003). An improved understanding of normative neurophysiological maturation of the striatum can thus inform models of normal and abnormal adolescent behavior.

Tissue-iron concentration is predominant in the striatum (Haacke et al. 2005, Schenck 2003) and has been found to support dopamine D2 receptor and dopamine transporter (DAT) densities in studies of iron deficiency, ADHD, and restless leg syndrome, which are related to abnormalities in DA processing, (Erikson et al. 2000; Wiesinger et al. 2007; Connor et al. 2009; Adisetiyo et al. 2014), as well as the function and regulation of dopamine neurons (Beard 2003, Jellen et al. 2013). As such, differences in striatal tissue iron concentration, which can be measured using MRI, can potentially serve as an indicator of dopaminergic differences in adolescence. Tissue-iron is paramagnetic and thus strongly influences the T2*-weighted MRI signal (Langkammer et al. 2010, 2012; Schenck 2003), which can be non-invasively collected in vivo throughout the lifespan (Aquino et al. 2009, Haacke et al. 2005, Wang et al. 2012). The influence

of iron on the T2* signal has been used to quantify iron in a variety of MR measures, including susceptibility weighted imaging (SWI) (Haacke et al. 2004), R2* (Haacke et al. 2010), and R2' (Sedlacik et al. 2014). In this study, we make use of a large of T2*-weighted echo-planar imaging (EPI) dataset, most akin to SWI. Initial studies have used similar data in conjunction with multivariate pattern analysis to investigate the striatal processes underlying learning (Vo et al. 2011).

Here we use T2*-weighted EPI (T2*) to characterize age-related differences in the neurophysiology of the human adolescent striatum in vivo using a multivariate pattern analysis approach. Specifically we use spatial patterns of striatal T2* to generate highly significant age predictions from both task-related and resting state T2*-weighted EPI (fMRI) acquisitions, demonstrating the strong and robust relationship between this measure and development. Furthermore, we identify the ventral striatum, a central hub of dopamine reward pathways hypothesized to underlie adolescent risk-taking (Blum et al. 2000, Casey et al. 2008, Spear 2000), as a critical component of adolescent striatal maturation. This work highlights the dynamic nature of normative adolescent striatal development, informing models of the maturation of motivational systems during adolescence.

2.2 MATERIALS AND METHODS

2.2.1 Sample

One hundred sixty adolescents and young adults participated in this study (ages 10-25, M = 16.56, SD = 3.62). Eighteen participants were excluded due to excess head movement (described below),

yielding a final sample of 142 (ages 10-25, M = 16.41, SD = 3.71, 71 male). A subset of these were also included in a replication analysis using resting-state data (described below). All subjects had medical histories that revealed no neurological disease, brain injury, and no history of personal or first-degree relative with major psychiatric illness. All experimental procedures in this study complied with the Code of Ethics of the World Medical Association (1964 Declaration of Helsinki) and the Institutional Review Board at the University of Pittsburgh. Participants were paid for their participation in the study. These data were initially collected for a project investigating reward processing and resting state functional connectivity and subsets of this dataset were included in previously published studies of resting state network development (Hwang et al. 2013) and incentive processing (Paulsen et al. 2014).

2.2.2 Imaging procedure

Imaging data were collected using a 3.0 Tesla Trio (Siemens) scanner at the Magnetic Resonance Research Center (MRRC), Presbyterian University Hospital, Pittsburgh, PA. The acquisition parameters were: TR = 1.5 sec; TE = 25 ms; flip angle = 70 degrees; single shot; full k-space; 64 x 64 acquisition matrix with FOV = 20 x 20 cm. Twenty-nine 4 mm-thick axial slices with no gap were collected, aligned to the anterior and posterior commissure (AC-PC line), generating 3.125 x 3.125 x 4 mm voxels, which covered the entire cortex and most of the cerebellum. We collected four runs of 302 TRs during the antisaccade task (4 x 302 = 1208) and one run of 200 TRs during the resting-state scan. A three-dimensional volume magnetization prepared rapid acquisition gradient echo (MPRAGE) pulse sequence with 192 slices (1 mm slice thickness) was used to acquire the structural images in the sagittal plane.

T2*-weighted data were collected as part of a separate study investigating reward processing. Briefly, subjects participated in a reward modulated antisaccade task, in which they were instructed to make saccades to the mirror locations of peripherally presented stimuli. At the start of each trial, subjects were presented with either a reward, loss, or neutral cue that indicated the possibility of reward dependent on performance. Performance was evaluated using eye-tracking and participants received auditory feedback for correct and incorrect trials.

2.2.3 Resting-state Dataset

One hundred subjects also participated in a resting state scan. Eleven were excluded due to motion artifacts and thus 89 subjects were included in this analysis (ages 10-25, M = 16.2, SD = 3.77; 43 male). We collected a 5-min (200 volumes) resting-state scan for each subject using the same scan parameters listed above. During the resting-state scan, participants were asked to close their eyes, relax, but not fall asleep.

2.2.4 Preprocessing of T2*-weighted Data

All preprocessing was done using FMRIB Software Library (FSL; Smith et al. 2004) and the Analysis of Functional Neuro Images (AFNI) software package (Cox 1996). Initial preprocessing steps are similar to those used in conventional fMRI. T2*-weighted data was initially de-spiked and slice time corrected to account for sequential acquisition. To address motion, we used rotational and translational head motion estimates to calculate root mean square (RMS) movement measures, and participants with relative RMS greater than a stringent threshold of 0.3mm for more than 15% of volumes in a run were excluded from further analysis. For the remaining subjects, we

applied motion correction by aligning each volume in the time series to the volume obtained in the middle of the acquisition. Each participant's T2*-weighted data was linearly registered to the MPRAGE using FSL's FLIRT utility and then the MPRAGE image was nonlinearly registered into MNI (Montreal Neurological Institute) space using FSL's FNIRT utility. The concatenation of the linear registration from EPI to MPRAGE and the nonlinear registration from MPRAGE into MNI space was then applied to all EPI images for each participant. Volumes were high-pass filtered at .008hz . Data were not smoothed so as not to perturb voxel-wise patterns for the subsequent MVPA analysis. Smoothing can potentially bias the performance of linear support vector machines (Misaki et al. 2013). Resting-state and task-related data were processed separately using identical procedures.

2.2.4.1 Normalization and averaging

Commonly, T2*-weighted EPI data are analyzed across time, quantifying small fluctuations in the T2*-weighted signal related to the blood-oxygen-level dependent (BOLD) response. We wish to emphasize that in this study, we are not interested in these small BOLD fluctuations. Rather, we are interested in the properties of the T2*-weighted signal which do not change with time and are reflective of persistent neurophysiological properties of brain tissue. Thus, the preprocessing stream diverges from that of conventional BOLD analysis at this point. Procedures for processing our T2*-weighted images closely followed Vo et al. (2011). Each volume was first normalized to its own mean, and the normalized signal was then averaged, voxel-wise, across all four runs (1208 volumes) of the task acquisition. This process resulted in one normalized T2*-weighted image for each participant. Resting-state data were analyzed separately and were averaged across all 200 volumes from the five minute acquisition. The normalization step is necessary because the T2*-weighted signal alone is sensitive to potential differences between MRI scans--either within

subjects across time or between subjects--that can lead to shifts in T2*-weighted signal intensity. Normalization thus allows for comparison of T2* values across participants. Though T2* signal could be calculated from a single volume, we averaged across volumes to enhance the signal to noise ratio.

2.2.5 Identification of striatal regions

We anatomically identified the putamen, caudate, and nucleus accumbens according to brain atlases included in the AFNI software package. Region masks were made more conservative by removing any voxels likely to contain cerebrospinal fluid (CSF). CSF was parcellated using FSL's FAST segmentation, and voxels that had an average subject-wise probability greater than .15 of being CSF were removed from anatomically defined regions.

2.2.6 Univariate analysis

We first applied a traditional univariate analysis to assess mean level developmental differences in striatal T2*. For each subject, we computed the spatial mean T2*-weighted signal intensity across voxels within an anatomically defined region and analyzed the relationship between spatial means and chronological age. Specifically, we regressed age on mean T2* values using simple regression and computed the Pearson correlation between the fitted values of age and the true ages of subjects within each region of interest.

2.2.7 Multivariate pattern analysis

It is well established that the striatum and its subregions (caudate, putamen) are not spatially homologous in function, connectivity, or neurobiology (Middleton and Strick 2000; Martinez et al. 2003; Postuma and Dagher 2006; Cohen et al. 2009). Further, the structural development of the striatum progresses in a spatially non-uniform fashion (Raznahan et al. 2014). Therefore, the development of underlying striatal neurophysiology, including tissue-iron concentration, is likely also non-uniform. Thus, we hypothesized that age-related differences in striatal T2* would be better captured by a more sensitive, multivariate approach. To analyze the relationship between fine-grained patterns of T2* intensity and age, we applied multivariate linear support vector machine regression (SVR) in MATLAB (The MathWorks, Inc., Natick, Massachusetts, USA) using LIBSVM (Chang, Chih-Chung & Lin, Chih-Jen 2011). Support vector regression has become a popular analysis tool in neuroimaging studies due to its ability to handle high-dimensional datasets and generate accurate predictions (Misaki et al. 2010). The multivariate approach allows for the assessment of changes in voxel-wise patterns of T2* in the striatum that relate to age. Importantly, this analysis has advantages over conventional averaged region of interest univariate analyses in that it is sensitive to potential spatial heterogeneity of developmental T2* trajectories across the striatum that are not captured by a mass spatial average. Of particular relevance to this study, SVR was previously used by Vo et al. (Vo et al. 2011) to predict learning success from spatial patterns of striatal T2*, and by Dosenbach et al. (2010) to predict age from patterns of resting-state functional connectivity. Support vector machines have been described in detail from both a practical (Luts et al. 2010, Pereira et al. 2009) and detailed mathematical point of view (Burges, Christopher J.C. 1998, Chih-Wei et al. 2003, Vapnik 1999), and will only be described briefly here.

Linear support vector regression is an extension of support vector classification that allows for the association of feature patterns with a real-valued variable, thus allowing for real-valued predictions. Samples (data points) with real-valued labels are represented in a high-dimensional space with dimensions equal to the amount of features of a variable of interest. SVR defines a regression line through the high-dimensional feature space that optimally models the functional relationship between the features of a variable, x (e.g. voxel-wise T2* values in a region of interest), and the real-valued labels of a variable, y (e.g. the age of a subject). Samples are penalized in proportion to their distance from the regression line. We applied epsilon insensitive SVR which defines a tube around the regression line with width controlled by the parameter, epsilon, inside of which samples incur no penalty. The trade-off between the degree to which samples that fall outside the epsilon insensitive tube are penalized and the flatness of the regression line is controlled by the constant, C. As the value of C increases, the regression line is allowed to be less flat, which can increase the generalizability of the model.

We trained and validated our SVR model across subjects (one set of voxel-wise T2* values and one age label per subject) using leave-one-subject-out (LOSO) cross-validation. LOSO is an iterative process in which one subject's data is used for validation while the other n-1 subjects are used for training. An age prediction is generated for the left out sample based on voxel-wise T2* values alone, and the process is repeated until every subject has been used for validation. This results in one age prediction for each subject, and the performance of the SVR model can be determined by the correlation between true subject ages and those predicted by the model. The parameter C was optimized for each fold of LOSO cross-validation using nested LOSO cross-validation. We used the default value of epsilon from the LIBSVM toolbox of 0.001. The SVR analysis was repeated for resting-state T2* data. All p-values were confirmed via random

permutation significance tests (1000 iterations). We chose the LOSO rather than other methods of cross-validation in order to maximize the amount of training data used in each cross-validation iteration, and though our sample size is large, the number of subjects in the sample was often less than the number of features included in the SVR model.

2.2.7.1 Partial volume correction

To ensure that multivariate age predictions were not simply reflecting potential systematic differences in T2* arising from partial volume effects, we used FSL's FAST tissue segmentation tool to create probability masks of white and gray matter from participants' T1-weighted images. We then regressed gray matter probabilities out of the T2* measure across subjects for each voxel and repeated the SVR analysis using the corrected data. In addition to controlling for systematic differences in partial voluming, this process orthogonalized age-related differences in T2* values with respect to potential differences in striatal volume and nonlinear spatial normalization.

2.2.7.2 Pattern characterization

To characterize the spatial patterns of striatal T2* and their trajectory with age, we estimated the developmental trajectory of T2* by regressing age on T2* signal using linear, quadratic, and inverse regression models for each striatal voxel used in the SVR analysis. To quantify the relative contribution of components (voxels) of the spatial patterns of T2*, we computed the absolute value of the average feature weight for each striatal voxel used in the SVR analysis across all folds of LOSO cross-validation.

2.2.8 Searchlight analysis

To explore the relationship between T2* intensity and age beyond our a priori striatal regions, we performed a whole-brain searchlight analysis (Kriegeskorte et al., 2006). To conduct the analysis, we defined a spherical template with a diameter of 5 voxels (81 voxels total), centered the template on each brain voxel in turn, and performed the SVR analysis described above on the 81 voxels in the template. Only voxels included in a conjunction brain mask were included in this analysis. The correlation between true and predicted age at each template location was stored at the center voxel. By repeating this process for each voxel, we obtained a whole-brain mask of correlations. The locations of voxel clusters were estimated using atlases included in AFNI.

2.3 RESULTS

2.3.1 Univariate analysis

The spatial mean of T2* across all voxels in the striatum was not significantly related to age (r = 0.02), with the model accounting for on 0.0004% of variance in the sample. When we segmented the striatum into the caudate, putamen, and nucleus accumbens and repeated the analysis, we found that the information carried in mean T2* was sufficient to generate significant age predictions in the caudate ($r = 0.286$, $p < 0.001$) and putamen ($r = 0.182$, $p < 0.05$), and was particularly predictive in the nucleus accumbens ($r = 0.506$, $p < 10\text{-}9$, Figure 3A, white bars). However, functional and neurobiological subdivisions of the striatum exist at a finer scale than can be captured by spatial mean level analysis (Martinez et al. 2003; Postuma and Dagher 2006; Cohen et al. 2009).

Therefore, we hypothesized that developmental differences in striatal T2* would be better captured using a more sensitive, multivariate approach.

2.3.2 Multivariate pattern analysis

Multivariate patterns of T2* signal produced highly significant age predictions in all striatal regions (Figure 3A, black bars), indicating a strong relationship between this measure and adolescent development. The greatest correlation between predicted age and true participant age was observed in the whole striatum (combined caudate, putamen, and nucleus accumbens), where T2* patterns accounted for 63% of variance in participant age (r = .79, p < 10-30; permutation test: p < .001, Figure 3B).

Striatal gray matter volume varies with age over adolescence (Raznahan et al. 2014, Sowell et al. 1999). To ensure that multivariate age predictions were not reflecting systematic partial volume differences arising from changing striatal volume or artifacts of spatial normalization, we repeated the SVR analysis controlling for voxel-wise differences in gray-matter volume. We found no significant difference in model performance using volume controlled data (Figure 15;0).

The T2* signal reflects persistent neurophysiological tissue properties (Vo et al. 2011) and should be insensitive to task or context effects. Nevertheless, we replicated the analysis for subjects who had participated in a resting state study during the same scan session. We found no significant difference in our ability to predict age from patterns of T2* using task-related and resting state data (Fig. 1B, gray bars). Furthermore, we computed the voxel-wise correlation between spatial patterns of resting state and task-related T2* in the striatum for each participant and observed a median Pearson correlation of 0.97, indicating that patterns are consistent between task and rest.

Thus, here forward we limit our focus to T2* data collected during task, which is averaged over more volumes (1208 vs 200) and has a greater sample size (142 vs 89).

As we predicted, spatial patterns predicted age more accurately for nearly every striatal region of interest. The improvement was particularly striking in whole striatum where the amount of explained variance in participant age increased from close to 0% using spatial means to 63% using spatial patterns. This contrast strongly indicates that the striatum undergoes a complex pattern of neurophysiological development reflected throughout striatal voxels over adolescence. To better elucidate the nature this developmental pattern, we characterized developmental trajectories of T2* across the striatum.

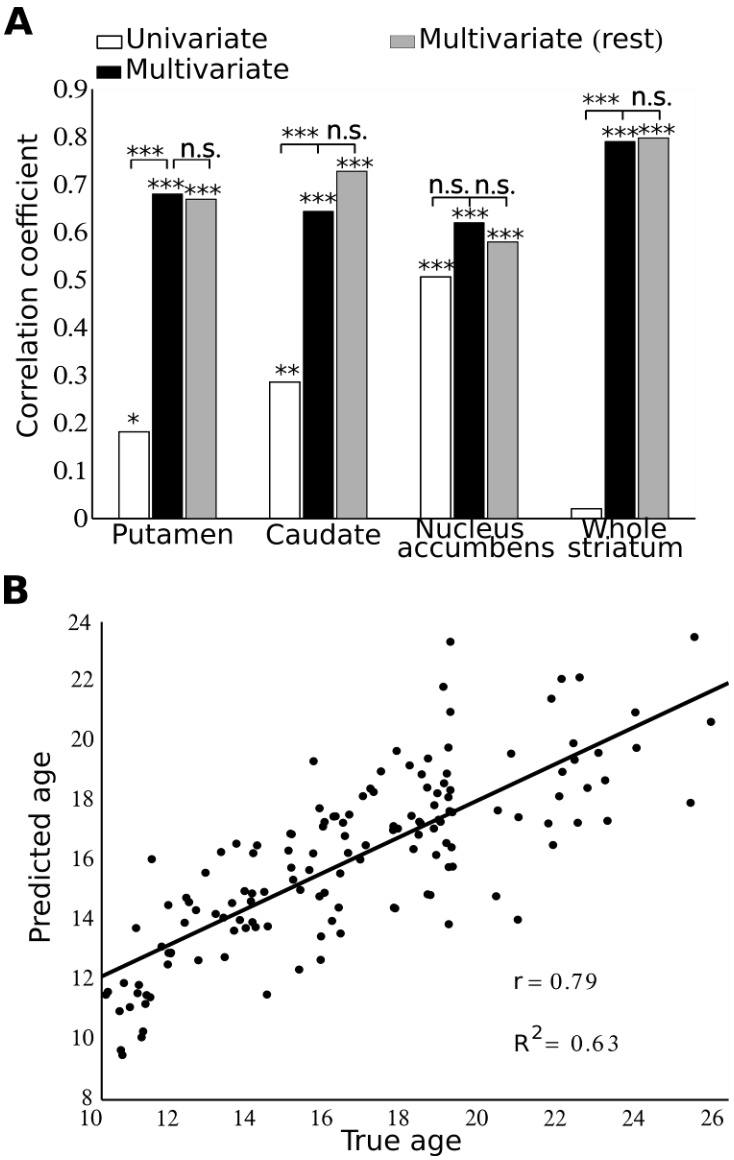

Figure 3. Correlations between true age and predicted age using T2* from univariate and multivariate models in striatal ROIs.

A. Bar graphs comparing correlations between true and predicted age using three models: univariate analysis (white bars) and multivariate pattern analysis of both task (black bars) and rest (gray bars) data. Multivariate analysis yields significantly greater correlation than univariate analysis in the putamen, caudate, and whole striatum. There is no difference between task-related and resting-state results. (*p<0.05, **p<0.01, ***p<0.001 permutation tests). B. True vs. predicted age from the whole striatum using multivariate pattern analysis of T2* in 142 adolescents and young adults. Predicted age accounts for 63% of the sample variance.

2.3.3 Pattern characterization

A key advantage of SVR is the ability to quantify the features that contribute to the multivariate predictor. To make use of this quantitative information, we extracted the feature weights assigned to each voxel from the SVR analysis. A feature weight can be thought of as an index of the importance of a feature (voxel) in generating the multivariate age prediction. To determine the components of the spatial pattern of striatal T2* intensities that had the greatest relative contribution to the multivariate predictor, we quantified absolute feature weights to identify the striatal voxels with the greatest relative weight. A cluster of voxels in the ventral striatum, at the junction of the caudate, putamen, and nucleus accumbens were most influential, followed by a cluster in dorsal caudate (Figure 4. Characterizing multivariate patterns of striatal maturation.Figure 4A). The ventral striatal cluster had a negative linear association with age (R^2 = 0.361, p < 10-14; Figure 4B solid line), and the dorsal caudate cluster had an increasing inverse association with age (R^2 = 0.078, p < 0.001; Figure 4B dashed line).

Though these clusters had the greatest relative weighting, it is important to keep in mind that the age prediction is a function of the multivariate relationship amongst all voxels included in the model. Therefore, we estimated the developmental trajectory of T2* signal for each voxel used in the SVR analysis using simple linear, quadratic, and inverse regression models known to characterize developmental change during this period (Luna et al. 2004) in order to comprehensively visualize maturational patterns. The majority of voxels were linearly related with age, with a subset being best fit by quadratic and inverse relationships. To illustrate this distribution, we categorized voxels based on the best fitting model – positive and negative linear, quadratic, and inverse relationships – and overlaid them on a standard anatomical image, creating a developmental T2* mask of the striatum (Figure 4D).

Descriptively, developmental T2* trajectories largely fell along a ventral to dorsal gradient, ranging from highly negative relationships in ventral portions of the striatum known to have predominantly limbic cortical connections to positive relationships in dorsal portions known to have predominantly executive and motor cortical connections (Alexander et al. 1986, Cohen et al. 2009), that was symmetric across hemispheres (Figure 4C; recall increased tissue iron concentration decreases the T2* signal). Negative quadratic (inverted "U") and increasing inverse relationships were observed in dorsal portions of the putamen, caudate, and nucleus accumbens, with negative quadratic relationships (inverted "U" shaped) clustered more in the right hemisphere and increasing inverse relationships clustered more on the left. Negative quadratic relationships reached average maxima over adolescence at age 18.4 in the caudate and 17.4 in the putamen. Positive quadratic ("U" shaped) and decreasing inverse relationships were observed bilaterally in the ventral putamen, with decreasing inverse relationships occurring in rostroventral putamen and positive quadratic relationships occurring in the caudoventral putamen reaching minima at age 20. The observed heterogeneity in developmental trajectories across striatal voxels likely explains the greater performance of our multivariate model over the univariate model in capturing age-related differences.

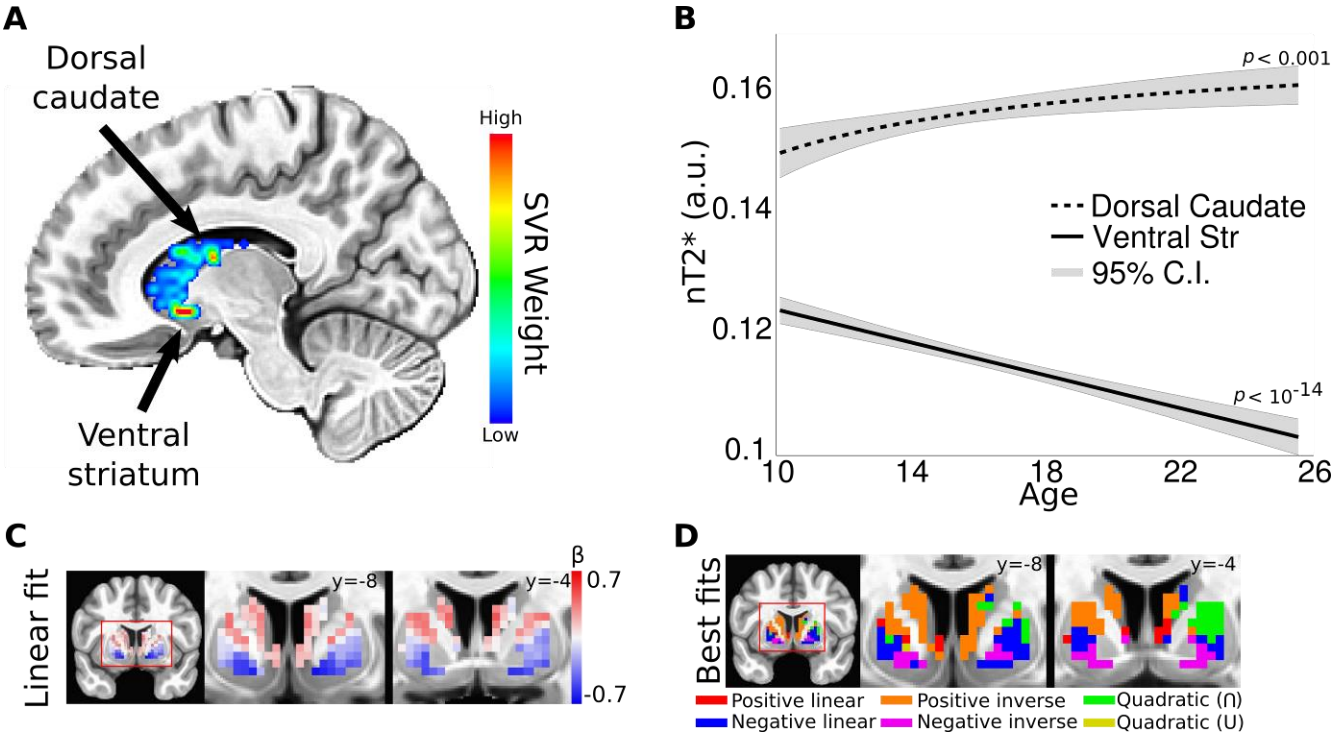

Figure 4. Characterizing multivariate patterns of striatal maturation.

A. Quantification of absolute feature weights for all striatal voxels included in the multivariate SVR model. Higher weights indicate greater relative contributions to the multivariate predictor. The highest weighted voxels were clustered in the ventral striatum and dorsal caudate. B. Average developmental T2* trajectories and 95% confidence intervals for voxels from peak clusters in (B) plotted as a function of age. Panels C-D illustrate the maturational trajectories of individual voxels included in the multivariate SVR analysis. C. Standardized beta estimates from voxel-wise simple linear regressions of age on T2*. Maturational trajectories fell along a dorsal-ventral gradient, with voxel T2* values generally increasing with age dorsally, to generally decreasing ventrally. This relationship is symmetric across hemispheres. D. Striatal voxels from (C) color-coded according to best fitting model (linear: red/blue, inverse: orange/magenta, quadratic: green/yellow).

2.3.4 Whole-brain analysis

To investigate possible associations between spatial T2* patterns and development across the brain and to confirm the specificity of striatal contributions, we performed an exploratory searchlight analysis (Kriegeskorte et al. 2006). The searchlight revealed that age was predicted most significantly in the striatum and midbrain, including the red nucleus, substantia nigra, and other parts of the basal ganglia (Figure 5). Other regions that generated highly significant age predictions include perigenual anterior cingulate cortex, Brodmann Area 10, medial pre-frontal cortex, anterior superior frontal gyrus, insula, pre- and post-central gyrus, anterior thalamus, and the dentate nucleus of the cerebellum. Significant correlations were also observed in the corpus callosum and fronto-parietal white matter structures. Many of these regions (e.g. basal ganglia, midbrain, dentate nucleus, frontal white matter) are among the most iron-rich areas of the brain (Connor & Menzies 1996, Drayer et al. 1986, Haacke et al. 2005, 2007; Langkammer et al. 2010), and part of the mesolimbic/mesocortical and nigrostriatal dopamine pathways (e.g. midbrain, striatum, prefrontal cortex (Beaulieu & Gainetdinov 2011, Haber & Knutson 2010, Puglisi-Allegra & Ventura 2012). The greatest correlations were observed at the juncture of the nucleus accumbens, ventromedial putamen, and ventromedial caudate (peak voxel: MNI -8, 5, -11), indicating that T2* has a particularly strong relationship with adolescent development in this part of the brain, which is strongly associated with dopaminergic reward pathways and the limbic system (Galvan et al. 2006, 2007; McGinty et al. 2013, Puglisi-Allegra & Ventura 2012).

The T2*-weighted signal, particularly when collected in-plane as in EPI, is susceptible to signal dropout due to susceptibility artifacts near the base of the brain (e.g. orbitofrontal cortex and inferotemporal cortex), thus raising the possibility that age-related differences in T2* could arise from susceptibility artifacts in these brain areas. This should not have a large effect given

that the gross morphometry of the brain is established by younger ages than our age group (Caviness et al. 1996). Moreover, 1) our most significant age effects occur in brain areas that are known to be high in iron concentration (e.g. basal ganglia and midbrain) and inset from areas with pronounced signal dropout and 2) that brain areas most prone to susceptibility artifacts (e.g. oribitofrontal cortex and inferotemporal cortex; Figure 16A&B) do not show significant age effects (Figure 16C).

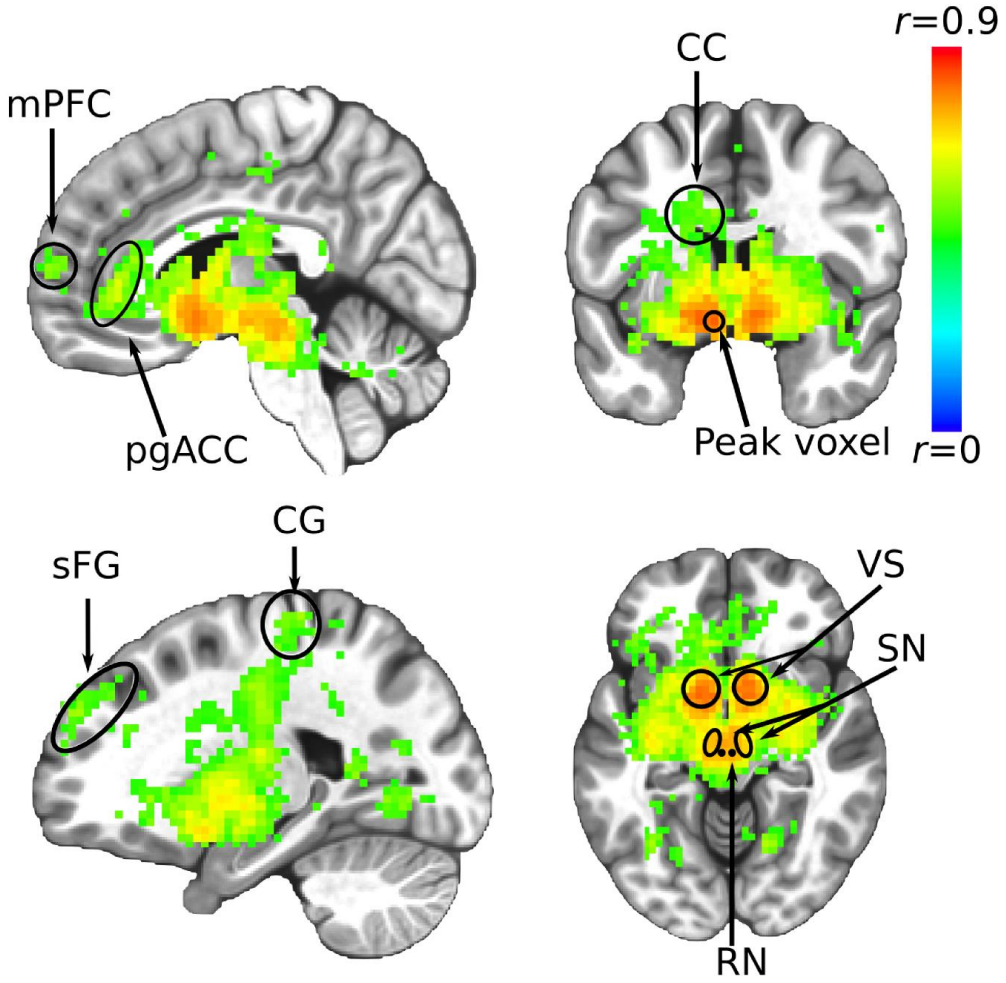

Figure 5. Whole-brain searchlight results highlighting regions with strong associations between T2* and adolescent development.

Colors represent the correlation between true age and predicted age from the SVR searchlight analysis centered at that voxel. Only voxels with correlations between true and predicted age that are significant at $p < 0.001$, Bonferroni corrected (i.e. 0.001/number of brain voxels) are displayed. The peak voxel is located in the ventral striatum (MNI coordinates: -8,5,-11). mPFC: medial pre-frontal cortex, pgAC: perigenual anterior cingulate, CC: corpus callosum, sFG: superior frontal gyrus, CG: central gyrus, VS: ventral striatum (including nucleus accumbens), SN: substantia nigra, RN: red nucleus.

2.3.5 Discussion

The present study used spatial patterns of striatal task-related and resting-state normalized T2*-weighted images to generate highly significant age predictions in a large cross-sectional sample of adolescents and young adults, providing in-vivo evidence of neurophysiological development of the human striatum over adolescence. Spatial patterns of T2* were predictive of adolescent age in the striatum as a whole as well as in striatal sub-regions, caudate, putamen, and nucleus accumbens from as little as five minutes of resting-state fMRI, demonstrating a strong association between T2* and adolescent development throughout the striatum.

2.3.5.1 The T2* signal

Critical for a full interpretation of these findings is an understanding of the neurophysiological components that contribute to the T2* signal. T2* is most strongly related to transverse (spin-spin) relaxation time, magnetic susceptibility of tissue, and magnetic field homogeneity. Thus, tissue-iron (non-heme) concentration and myelin concentration are the tissue types that contribute most strongly to the T2* signal (Aquino et al. 2009, Daugherty & Raz 2013, Langkammer et al. 2012, Schenck 2003). Both tissue-iron and myelin have long transverse relaxation times, thus causing a hypo-intense T2* signal (Aoki et al. 1989, Chavhan et al. 2009, He & Yablonskiy 2009). However, myelin is diamagnetic and tissue-iron is paramagnetic, so tissue-iron has a greater contribution to T2* (greater hypo-intensity) as a consequence of its magnetic susceptibility and effect on magnetic field inhomogeneity (Langkammer et al. 2010, Schenck 2003). Therefore, though tissue-iron and myelin both contribute to T2*, the signal should be most strongly influenced by tissue-iron concentration, particularly in the iron-rich striatum (Haacke et al. 2010, Langkammer et al. 2010). This notion is supported by the searchlight analysis

(Fig. 3) that shows the strongest associations with T2* and age occurring in iron-rich areas of the brain (basal ganglia, midbrain) rather than areas with less tissue-iron, e.g. cortex and posterior white matter tracts. Thus developmental differences in striatal neurophysiology as measured with T2* appear to be primarily driven by developmental differences in tissue-iron concentration during adolescence.

It is important to note that although iron is also contained in hemoglobin, the contribution of heme-iron to T2* is negligible compared to that of tissue-iron (Langkammer et al. 2010, Vymazal et al. 1996). The contribution of hemoglobin to magnetic susceptibility only occurs in deoxy-hemoglobin and is greatest at low oxygen saturation (Pauling 1977), but the paramagnetism of tissue-iron is many times greater than even completely deoxygenated hemoglobin (Vymazal et al. 1996). This small effect of heme-iron is not expected to contribute to the developmental effects observed in this study as its influence on T2* signal should not vary systematically with age in our sample. The vascular system is largely stable during adolescence, with pial vessel coverage and capillary formation (Harris et al. 2011) and total cerebral blood flow volume to the internal carotid artery (the primary blood supply to the striatum) being established by early childhood (Schöning & Hartig 1996).

2.3.5.2 Tissue-iron and the brain

The sensitivity of T2* to tissue-iron is particularly relevant in the context of adolescent development. Iron is transported across the blood-brain barrier via the protein transferrin and stored in cell bodies as ferritin (Aquino et al. 2009, Daugherty & Raz 2013, Drayer et al. 1986). The basal ganglia and midbrain are the regions of the brain with the greatest ferritin concentration (Haacke et al. 2005, Schenck 2003). Cells with the greatest ferritin concentration are oligodendrocytes found in both white and grey matter (Haacke et al. 2005). Ferritin can also be

found in neurons, particularly those in the basal ganglia (Drayer et al. 1986, Moos 2002). Within these cells iron contributes to a host of critical neurophysiological processes. In oligodendrocytes, iron is necessary for myelin synthesis and is required for ATP production necessary to sustain the high oxidative metabolism of these cells (Connor & Menzies 1996, Moos 2002, Todorich et al. 2009). In the basal ganglia, animal models of iron deficiency (Erikson et al. 2000) and disease models of restless leg syndrome (Connor et al. 2009) and ADHD (Adisetiyo et al. 2014) indicate that tissue-iron is highly related to the dopamine system (Beard & Connor 2003). In particular, striatal tissue-iron supports D2 receptor expression (Beard 2003, Jellen et al. 2013), dopamine transmitter function (Erikson et al. 2000; Wiesinger et al. 2007; Adisetiyo et al. 2014), and dopamine neuron excitability (Jellen et al. 2013). As the striatal dopamine system has been shown to develop during adolescence in animal models (Kalsbeek et al. 1988, Rosenberg & Lewis 1995, Teicher et al. 1995) and has been hypothesized to underlie characteristic behavior and brain function in the adolescent human (Casey et al. 2008, Padmanabhan & Luna, Spear 2000), the T2* signal has unique relevance to the study of adolescent striatal development. Furthermore, postmortem (Hallgren & Sourander 1958) and MRI (Aquino et al. 2009, Wang et al. 2012) studies exploring lifespan differences in tissue-iron have shown general increases in iron concentration in the striatum through middle age and suggest the rate of iron accumulation is greatest in the first two decades of life, indicating a decreased rate of change in accumulation following adolescence.

2.3.5.3 T2* and the adolescent brain

The developmental trajectory of T2* signal varied systematically across dorsal and ventral aspects of the striatum. Ventral portions of the striatum, which have predominantly limbic cortical connections (Cohen et al. 2009), showed strong negative relationships with age while dorsal portions, which have predominantly executive and motor cortical connections showed weaker

positive relationships with age suggesting that through adolescence and young adulthood limbic and executive striatal systems may have different relative neurophysiological contributions to behavior. Results are in agreement with findings indicating that the striatum has a spatially heterogeneous pattern of development, i.e. the striatal nuclei do not develop in a globally uniform way (Raznahan et al. 2014). The strong negative relationships in ventral striatum indicate consistent increases in tissue-iron concentration with inverse fits suggesting the rate of increase is greatest early in adolescence. Given the association of tissue-iron with both dopamine function and myelination, these increases may support the maturation and proliferation of the dopamine system and myelination of cortico-striatal connections observed in animal models of adolescent development (e.g. increasing dopamine projections to the primate prefrontal cortex; Rosenberg & Lewis 1995), supporting the maturation of motivational circuitry.

The developmental trajectory of striatal T2* is unique over adolescence in portions of the caudate and putamen. In these areas, voxel values of T2* varied non-linearly with age, in some cases peaking over adolescence between ages 17 and 18. Of particular interest are positive quadratic relationships ("U" shaped) in the ventral putamen that indicate peak tissue-iron concentration in this region over adolescence, possibly relating peaks in dopamine D2 receptor expression observed in the rodent (Teicher et al. 1995) and hypothesized to occur in the human (Casey et al. 2008). Overall, these nonlinear developmental trajectories suggest a period of striatal neurophysiological maturation that may contribute to observed peaks in sensation seeking and risk-taking behavior and striatal reward sensitivity during this stage of development (Padmanabhan et al. 2011, Spear 2000), while linear relationships may reflect continued motivational system development through young adulthood (Arnett 1999; Hoogendam et al. 2013). Given findings in animal models indicating adolescent peaks in dopamine receptor expression and human fMRI

studies suggesting peak ventral striatal reactivity under certain incentive contexts, we were surprised to observe linear or inverse associations of T2* with age in portions of striatum. It is possible that increases in adolescent BOLD response to reward may be sensitive to additional aspects of DA function to which tissue-iron is not directly related, such as DA release quantity or probability, which may have different developmental trajectories. The observed pattern of effects likely also reflects the indirect nature of the relationship between tissue-iron and dopamine receptor density and DAT function as well as its role in many other neurophysiological processes (e.g. myelination and ATP production) that do not decrease in adulthood. Speculatively, it may be that individual differences in T2* and basal ganglia tissue-iron concentration relate to individual differences in indices of the structure and function of the dopamine system. Clearly, further research is needed to directly characterize this relationship, particularly in normative populations.

Quantitatively, the voxel-wise distribution of feature weights from the multivariate support vector regression indicate that neurophysiological maturation of the striatum is most strongly influenced by the continued maturation of the ventral striatum, including the nucleus accumbens and ventromedial portions of the caudate and putamen, into adulthood. During adolescence, the ventral striatum exhibits peak functional reactivity to reward stimuli under certain incentive contexts and is associated with risk-taking behavior during this period (Ernst et al. 2005, Galvan et al. 2006, 2007; Geier et al. 2010, Padmanabhan et al. 2011). Furthermore, this region is highly dopamine innervated and is a central component of the frontostriatal dopamine reward pathways (Knutson & Cooper 2005, McGinty et al. 2013, Puglisi-Allegra & Ventura 2012) hypothesized to underlie sensation seeking and risk-taking behavior (Blum et al. 2000, Spear 2000). Speculatively, increases in tissue-iron concentration in this region may thus be mechanistically related to adolescent behavior and striatal reward reactivity through its association with dopamine receptor

expression, transporter function, and excitability (Erikson et al. 2000, Jellen et al. 2013, Wiesinger et al. 2007) and myelination (Connor and Menzies 1996; Moos 2002; Todorich et al. 2009) within cortico-ventral striatal pathways.

An exploratory whole-brain analysis revealed that the strongest associations between T2* and age occur in ventromedial subcortical and midbrain regions known to be the most dopamine and iron-rich areas of the brain (Drayer et al. 1986, Haacke et al. 2005, Langkammer et al. 2010) with rates of iron accumulation fluctuating across the lifespan (Aquino et al. 2009, Haacke et al. 2010, Hallgren & Sourander 1958). In the cortex, significant associations were observed in frontal limbic areas that fall along the mesolimbic and mesocortical dopamine pathways as well as frontal executive and motor regions. It should be noted that the interpretation of precise neurophysiological properties underlying of the T2* signal outside of the iron-rich striatum is somewhat less straightforward. For example, the degree to which cortical T2* reflects tissue-iron concentration per se is less clear as myelination should have a larger relative contribution to the signal in areas that contain lower levels of tissue-iron (e.g. cortex, white matter). For this reason, it may be advisable for future researchers to focus T2* analyses to brain areas known to have high concentrations of tissue-iron (e.g. the basal ganglia and midbrain). Nevertheless, this collection of cortical and subcortical brain regions are consistent with our striatal findings in that they are structurally and functionally connected within the dopamine system and have been shown to be sensitive to adolescent development (Casey et al. 2008, Cohen et al. 2009, Galvan et al. 2006, Geier et al. 2010, Giedd et al. 1999, Hwang et al. 2010, Lehéricy et al. 2004, Martino et al. 2008, Sowell et al. 1999). As such, these results provide evidence in support of the hypothesis that neurophysiological development of the frontostriatal dopamine circuit in humans occurs over adolescence (Casey et al. 2008, Spear 2000).

2.3.5.4 Limitations and future directions

Our findings, along with those of Vo et al. (2011), suggest that T2*-weighted EPI data may be a useful tool for the investigation of striatal neurophysiology. An advantage of this method is that this measure can be derived from existing fMRI datasets, whether they be resting-state or task-related. As mentioned above, we recommend focusing future analyses on the basal ganglia and other brain areas known to have relatively high concentrations of tissue-iron as the interpretability of the neurophysiological mechanisms contributing to T2* is greatest in these areas. Additionally, we recommend brain areas such as ventral orbitofrontal cortex and portions of inferotemporal cortex that are prone to susceptibility artifacts be avoided for T2*-weighted EPI analyses. We wish to note that investigators interested in specifically quantifying tissue-iron concentrations could also apply quantitative MR sequences, such as R2' or R2*, that have been shown to be linearly related to tissue-iron content (Yao et al. 2009; Sedlacik et al. 2014) to assess this tissue property more precisely. An important direction for future work is to directly characterize the association between tissue-iron concentration in the basal ganglia and indices of dopamine system function in normative populations, expanding on work done in RLS, ADHD, and iron-deficient populations and leading to greater functional interpretability and significance of T2* and related measures. Of course, an enhanced understanding of this relationship has powerful implications for human developmental studies in which more invasive imaging techniques capable of assessing the neurobiology of the dopamine system are not available. Finally, though this study was performed using a large cross-sectional dataset that covered a wide age-range, future work should employ a longitudinal design in order to better asses age-related changes in T2*, per se.

2.3.6 Conclusion

Our results provide in vivo evidence of continued neurophysiological maturation of striatal regions throughout human adolescence. Our findings and the nature of the T2* signal suggest that age related differences in striatal neurophysiology are most strongly influenced by differences in tissue-iron concentration (Aoki et al. 1989, Chavhan et al. 2009, Daugherty & Raz 2013, He & Yablonskiy 2009, Langkammer et al. 2010, Schenck 2003). Given the contribution of this tissue property to brain function, including dopamine function, and the role of the striatum in learning, motivation, and reward processing, protracted maturation of the striatum as indexed by T2* may strongly contribute to known developmental changes in behavior and brain function through adolescence.

3.0 THE DEVELOPMENT OF STRIATAL TISSUE IRON AND ITS ASSOCIATION WITH STRIATAL DOPAMINE NEUROBIOLOGY

3.1 INTRODUCTION

In chapter two we used a novel MR measure, normalized T2*-weighted imaging (nT2*), to detect evidence of striatal tissue maturation during adolescence. The nature of the T2*-weighted signal suggests that nT2* strongly reflects the magnetic field inhomogeneity induced by macromolecular paramagnetic iron concentration. Thus, the age-related differences we observed in chapter two suggest pronounced iron accumulation in ventral striatum, a region associated with reward and limbic function, and a less-pronounced developmental decreases in dorsal striatum, more strongly linked to cognitive and sensorimotor processes. This pattern of results suggests qualitative differences in the maturational processes occurring across the striatum. However, the direct relationship of nT2* to tissue iron has not been quantified, and nT2* can also be influenced by other tissue properties that influence T2* relaxation, such as myelin (Bender and Klose 2010). In this chapter, we build on these findings by characterizing the development of striatal iron concentration using a validated, quantitative MR index of tissue iron concentration, and by determining the relationship between tissue iron and a critical component of striatal neurobiology, dopamine.

Iron crosses the blood-brain barrier via the protein transferrin and is transported to neurons, oligodendrocytes, and astrocytes where it is either used or stored as ferritin (Connor and Menzies 1996; Rouault 2013). In these cells, iron is essential for many fundamental brain processes including cellular respiration, myelination, and neurotransmitter synthesis (Connor and Menzies

1996; Rouault 2013; Ward et al. 2014). Tissue iron is heterogeneously distributed, and the brain areas with the greatest iron concentration are the basal ganglia and midbrain. The reason for pronounced iron accumulation in these brain areas and mechanism by which this heterogeneous iron distribution develops are unknow; however, these brain areas are among the most DA rich areas of the brain, and iron has been linked to multiple aspects DA neuroanatomy and neurophysiology. Neurological disorders that affect the mesolimbic and nigrostriatal DA systems, such as Parkinson's disease, Huntington's disease, ADHD, and restless legs syndrome (RLS), are also associated with atypical iron concentration (Allen and Earley 2007; Adisetiyo et al. 2014; Ward et al. 2014; Khan et al. 2017; Piao et al. 2017; Zucca et al. 2017). In these disorders, reduced iron concentration has been linked to reduced DAT function and reduced D2 receptor density (Connor et al. 2009b; Earley et al. 2011, 2014). In patients with Parkinson's disease that also have symptoms of RLS, CSF iron levels are reduced relative to patients without RLS symptoms, and CSF iron levels are correlated with CSF DA levels (Piao et al. 2017). Patients with ADHD have reduced iron levels relative to healthy controls, and iron levels can be returned to typical levels after treatment with psychostimulant medication (a DA agonist), suggesting that pharmacological up-regulation of the DA system leads to increased iron concentration (Adisetiyo et al. 2014). Similarly, cocaine (also a DA agonist) addiction leads to increased basal ganglia iron concentration that scales with the duration of use (Ersche et al. 2017). Animal models of iron deficiency (ID) have revealed similar relationships between iron and dopamine as are observed in neurological disorders. Rodents fed iron deficient diets have reduced striatal iron concentration as well as reduced DAT function, D2 receptor density, and intracellular DA concentration relative to control animals (Erikson et al. 2000, 2001, Beard et al. 2002, 2003). ID also reduces the expression of genes that control the excitability of midbrain DA neurons (Jellen et al. 2013). Importantly,

infusion of physiologic levels of iron into either the ventral midbrain or striatum is capable of restoring iron concentrations of ID animals to normative levels and correspondingly increase levels of striatal DA (Unger et al. 2014), and dietary iron repletion can restore striatal D2 receptor density (Unger et al. 2008). Effects of ID on DAT levels and D2 receptor density can be replicated in in-vitro studies of iron chelation and repletion (Wiesinger et al. 2007; Unger et al. 2008).

Inside dopamine neurons, iron is a necessary co-factor for tyrosine hydroxylase, the rate-limiting step of DA synthesis (Ramsey et al. 1996; Zucca et al. 2017), and iron accumulates in dopaminergic vesicles (Ortega et al. 2007). Further, DA-containing cells exposed to iron in-vitro increase in intracellular iron concentration and this effect is blocked when DA synthesis is inhibited (Ortega et al. 2007). Intracellular ferritin stores are also commonly bound by neuromelanin, a pigment that encapsulates excess cytosolic DA that is not packaged in vesicles, suggesting iron co-localizes with vesicular and cytosolic DA within DA neurons (Zucca et al. 2017).

The co-localization of iron and dopamine on the macroscopic and microscopic level, and the association between iron concentration and multiple aspects of striatal DA neurobiology suggest that iron may be a useful indirect marker of striatal DA neurobiology. Currently, techniques available to measure indices of striatal DA neurobiology are limited to positron emission tomography (PET). PET utilizes positron-emitting radiotracers that are tailored to target specific targets (e.g. receptors for specific neurotransmitters) in the brain to measure the concentrations of those targets in tissue. Though useful, PET is an invasive technique that requires intravenous injection of the radiotracer and exposure to a small dose of radioactivity. For these reasons, PET imaging is not suitable for all populations, including children and adolescents. For researchers interested in measuring aspects of the DA system in pediatric populations, there is no

currently available alternative. Importantly, tissue iron is paramagnetic and can consequently be measured non-invasively using MRI, potentially providing a non-invasive window into developmental changes in dopamine circuitry during adolescence. A number of MR acquisitions have been created to quantitatively measure iron concentration in the brain, including T2 and T2* relaxation and quantitative susceptibility mapping (Haacke et al. 2005, 2010). One such measure is R2', the reversible transverse relaxation rate (1/T2' = 1/T2* - 1/T2) (Yablonskiy 1998). R2' is linearly related to postmortem tissue iron concentration (Sedlacik et al. 2014) and has been used to quantify striatal tissue iron in patients with Parkinson's disease (Graham et al. 2000). Similar measurements (e.g. R2*) have also been used to characterize the development of tissue iron across the lifespan (Aquino et al. 2009).

In this chapter we use R2' to assess age-related differences in tissue-iron concentration across sub-regions of the striatum in a developmental sample of adolescents and young-adults. In the adult cohort, we also collect two PET indices of DA, [^{11}C]dihydrotetrabenazine (DTBZ) and [^{11}C]raclopride (RAC). DTBZ binds to the vesicular monoamine transporter type 2 (VMAT2), which packages intracellular DA into vesicles and transports them to the synapse, and is used as an indicator of presynaptic terminal density (Vander Borght et al. 1995; Frey et al. 2001; Kilbourn 2014). RAC binds to D2 receptors and can be used as an indicator of striatal D2 receptor concentration (Volkow et al. 1996; Ginovart 2005; Elsinga et al. 2006). Considering links between basal ganglia tissue iron concentration and both D2 receptor concentration and synthesis, as well as its co-localization with dopamine vesicles, the R2' index of iron concentration may be linked to either or both DTBZ and RAC in the adult striatum.

3.2 MATERIALS AND METHODS

3.2.1 Sample

One hundred forty adolescents and young adults were included in the sample (ages 12-30; *M* = 19.87, *SD* = 5.01). The adult portion of the sample (*N* = 80; ages 18-30 years, *M* = 23.39, *SD* = 3.57) also participated in simultaneous PET imaging in addition to iron imaging (R2') in order to assess indices of striatal DA neurobiology and compare them to tissue-iron concentration. All participants reported no history of psychiatric or neurological disorder, and all participants provided informed consent to participate.

3.2.2 R2'

R2' represents the reversible transverse relaxation rate (1/T2') and is calculated as the difference between the effective (R2*; 1/T2*) and irreversible (R2; 1/T2) relaxation rates. This measure has been shown to be linearly related to tissue-iron concentration (Sedlacik et al. 2014)(Fig 3). In this study, we collected R2' using mTSE with the following parameters: effective echo times 12, 86, and 160ms; TR = 6580 ms; 12ms spacing between spin refocusing pulses; FoV = 240X240 mm2; 27 3mm transverse slices; 1mm slice gap. R2* was calculated using mGRE with parameters: echo times 3, 8, 13, 18, and 23ms; TR = 724 ms; flip angle, 25°; FoV = 240X240mm^2. Both R2 and R2* maps were estimated using a regularized iterative algorithm to better control for noise amplification in the estimation process. Finally, using the estimated R2 and R2* maps, we estimated R2' at the voxel level as follows: R2' = R2* - R2. All R2, R2*, and R2' images were individually assessed for quality, and participants that had visible artifacts—including motion,

shimming, registration, or susceptibility (n = 38)—in any image were removed from all analyses (n = 38).

3.2.3 PET

Tissue-iron has been suggested to be related to multiple aspects of DA neurobiology, including D2 receptor density, dopamine transporter, synthesis, and energy production required for DA function. As such, we collected two PET indices of striatal DA neurobiology, DTBZ and RAC. DTBZ binds to VMAT2 that transports monoamine neurotransmitters to presynaptic vesicles. DTBZ binding is a stable measure of presynaptic neuronal integrity in humans since over 95% of striatal VMAT2 binding sites are dopaminergic. In contrast, RAC binds to D2/D3 receptors throughout striatum, providing an index of D2/D3 receptor density. We acquired DTBZ using a bolus+infusion (B+I) paradigm (Martinez et al. 2003) collected over a 60 minute acquisition. Similarly, RAC is acquired using a B+I paradigm collected over a 90 minute acquisition. For both acquisitions, PET attenuation correction is performed using a combined segmentation- and atlas-based approach. Binding potential (BPND) is estimated voxel-wise using Ichise's Multilinear Reference Tissue Model (MRTM) (Ichise et al. 1998, 2003) based on the resulting time activity curves, using pericalcarine sulcus as a reference region.

3.2.4 Statistical approach

We used regression models to assess the developmental trajectories of R2' across the striatum. We tested linear, quadratic, and age^{-1} functional forms of age and performed model selection using AIC. Regression analyses were performed at the region of interest (ROI) level as well as voxel-

wise level across the striatum. Striatal ROIs included nucleus accumbens, putamen, and caudate. The caudate was further sub-divided into anterior and posterior aspects using the Oxford-GSK-Imanova structural atlas (Tziortzi et al. 2011). As iron deposition tends to monotonically increase throughout the first half of life and D2 receptor density is hypothesized to peak during adolescence, to test for relationships between R2' and PET measures, we investigated the extent that individual differences (residualized with respect to age and sex) in R2' and PET measures were related. We regressed the best fitting functional form of age and its interaction with sex out of both measures and tested for a correlation amongst the residuals. These analyses were conducted at the ROI and voxelwise levels. Outlier detection for all regression models was performed using Cook's distance with a threshold of Cook's distance greater than five times the mean of the Cook's distance distribution. For all voxel-wise regression analyses, multiple comparison correction was performed using family-wise error correction implemented in AFNI (Cox 1996). It is not possible to quantify within-scan motion in R2' data, however motion is highly rank-order correlated across subjects for within-session MR acquisitions (Savalia et al. 2017). To control for potential between-subjects effects of motion in regression analyses, we estimated motion on an fMRI scan that occurred during the RAC acquisition (data not reported in this study) and used it as a covariate.

3.3 RESULTS

3.3.1 Development of R2'

R2' significantly increased with age in all striatal ROIs (Figure 6B; Table 1). Voxelwise analyses supported this finding and indicated that the most pronounced and protracted age-related increases occurred in the ventromedial aspect of the striatum (including VS). Voxelwise age effects followed a rostroventral to caudodorsal gradient such that the degree of age-related increases were diminished and no longer significant in the dorsocaudal aspects of the striatum (e.g. posterior caudate Figure 7).

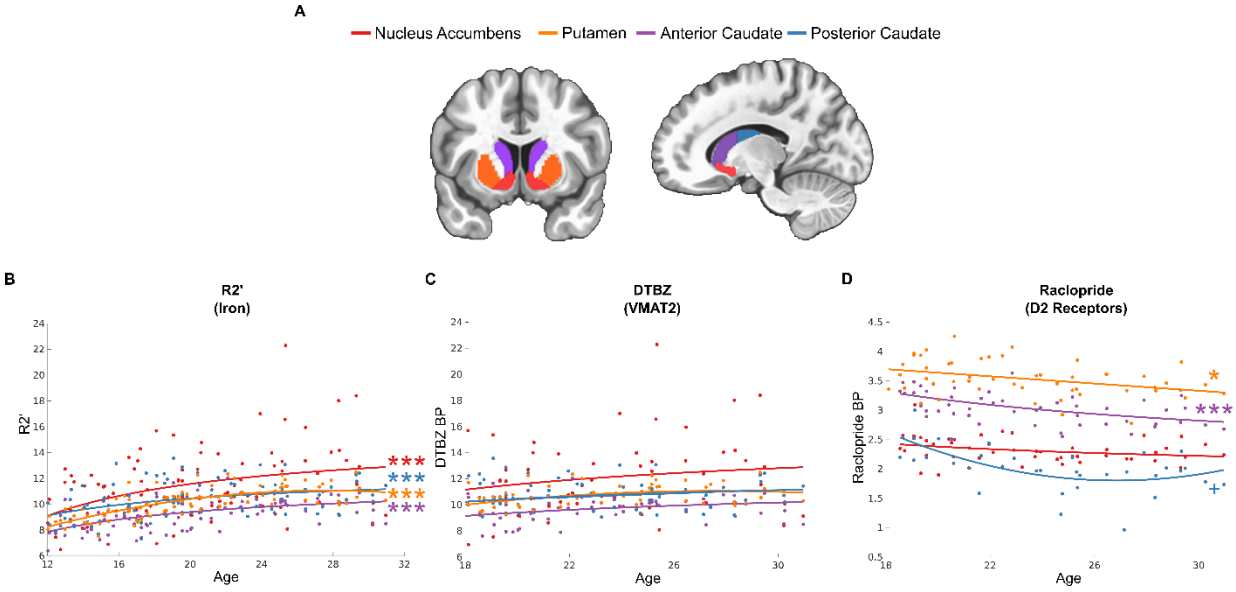

Figure 6. Age-related differences in R2', DTBZ, and Raclopride in striatal sub-regions.

A. Regions of interest for analyses in B-D. B. R2', and index of iron concentration increased with age in all areas. The putamen was best fit by a quadratic age function, indicating a peak or asymptote during adulthood. C. DTBZ, an index of VMAT2, did not significantly differ with age in any striatal regions. D. Raclopride, and index of D2 receptor concentration, significantly decreased with age in the putamen and anterior caudate.

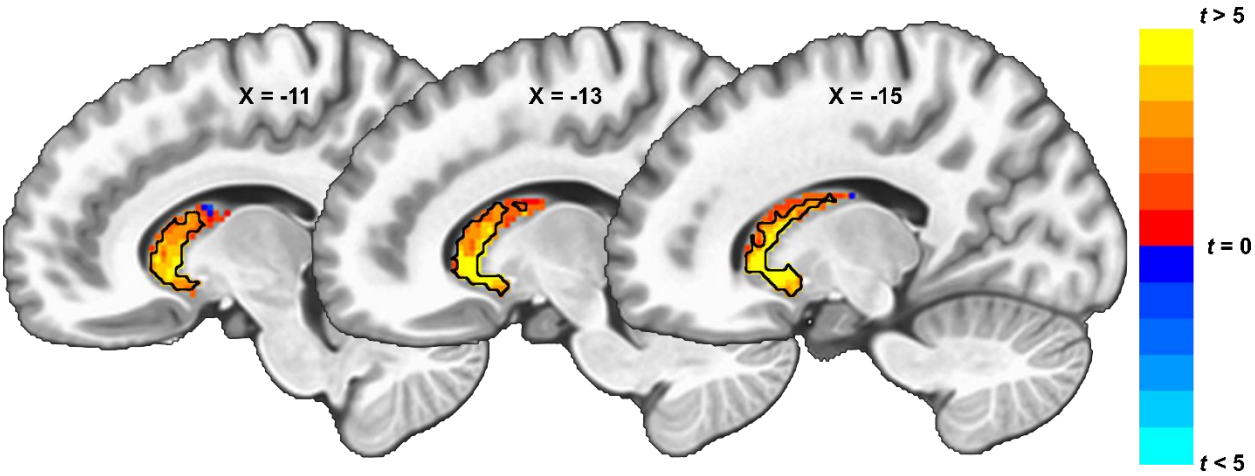

Figure 7. Age-related differences in R2' across the striatum.
R2' significantly increased with age following an age^{-1} function. Voxels with significant age effects, controlling for sex and trait motion, are outlined in black. Age effects followed a ventromedial to dorsolateral gradient, with greatest changes occurring in near VS and decreasing until posteriodorsal caudate where they are no longer significant and begin to change sign (decreasing with age, blue voxels). Color bar represents *t* statistics for the age^{-1} term in the multiple regression (note: colors are flipped for interpretability).

3.3.2 Development of RAC and DTBZ

In the adult sample, RAC binding potential generally decreased with age throughout the striatum with most pronounced age-related decreases in the putamen Figure 6**Error! Reference source not found.**D). Voxelwise analyses did not reveal any significant effects of age on RAC binding potential after family-wise error correction. However, the spatial pattern of age effects followed a similar ventral to dorsal gradient as observed in the R2' analyses (Figure 18). DTBZ did not significantly differ by age (Figure 6C). Again, though non-significant, the spatial pattern and direction of age effects followed a similar ventral to dorsal gradient as observed in the RAC R2' analyses (Figure 17).

Table 1. Age-related differences in R2', RAC, and DTBZ.

Measure	ROI	Variable	Estimate	*SE*	*t*	*p*
R2'						
	Nucleus Accumbens					
		Age^{-1}	-65.1845	18.6435	-3.4963	**.000695**
		Sex	0.02685	0.49263	0.05	.9566
		Trait motion	6.51989	2.41516	2.70	**.00069**
	Putamen					
		Age	0.6217	0.1313	4.73	**.000007**
		Age^2	-0.0113	0.0031	-3.60	.000482
		Sex	-0.4190	0.1500	-2.79	.006212
		Trait motion	0.9491	0.6337	1.50	.137224
	Anterior Caudate					
		Age^{-1}	-43.7808	7.1230	-6.15	**.00000001**
		Sex	-0.3068	0.1906	-1.61	.110571
		Trait motion	1.0669	0.8158	1.31	.193797
	Posterior Caudate					
		Age^{-1}	-35.5954	8.9574	-3.97	**.000129**
		Sex	-0.1236	0.2379	-0.52	.604518
		Trait motion	0.4781	1.0063	0.48	.635678
Raclopride						
	Nucleus Accumbens					
		Age	9.0864	4.4470	2.04	.046314
		Sex	0.0135	0.0577	0.23	.816264
		Trait motion	-0.3803	0.2665	-1.43	.159719
	Putamen					
		Age	-0.0297	0.0105	-2.82	**.006764**
		Sex	0.0321	0.0763	0.42	.675959
		Trait motion	0.1955	0.3596	0.54	.588998
	Anterior Caudate					
		Age^{-1}	22.0732	4.6567	4.74	**.000018**
		Sex	-0.0301	0.0605	-0.50	.621514
		Trait motion	0.3140	0.2807	1.12	.268550
	Posterior Caudate					
		Age	-0.5527	0.2158	-2.56	.015040
		Age^2	0.0103	0.0044	2.34	.025371
		Sex	0.1153	0.1054	1.09	.281534
		Trait motion	0.4157	0.4706	0.88	.383333
DTBZ						
	Nucleus Accumbens					

	Age	0.0067	0.0080	0.84	.406211
	Sex	-0.0776	0.0562	-1.38	.173019
	Trait motion	-0.7600	0.4014	-1.89	.063868
Putamen					
	Age	0.0063	0.0132	0.48	.634553
	Sex	-0.1112	0.0925	-1.20	.234616
	Trait motion	-0.4317	0.6606	-0.65	.516318
Anterior Caudate					
	Age^{-1}	5.1826	7.1340	0.73	.470814
	Sex	-0.1098	0.0901	-1.22	.228666
	Trait motion	-0.2977	0.6447	-0.46	.646201
Posterior Caudate					
	Age^{-1}	3.6660	5.3517	0.69	.496378
	Sex	-0.1065	0.0676	-1.58	.121136
	Trait motion	-0.3073	0.4836	-0.64	.527958

*Bold font indicates significant after multiple comparison correction.

3.3.3 Associations between R2' and PET

There were no significant associations between R2' and RAC at the ROI level. Voxel-wise analyses indicated a significant positive association between R2' and RAC, residualized with respect to age, in the left rostral caudate, controlling for age and sex (Figure 9).

R2' and DTBZ, residualized with respect to age, were significantly positively associated in the nucleus accumbens at the ROI level (Figure 8). Voxelwise analyses reflected this pattern, with significant associations between R2' and DTBZ occurring in the right VS (Figure 10).

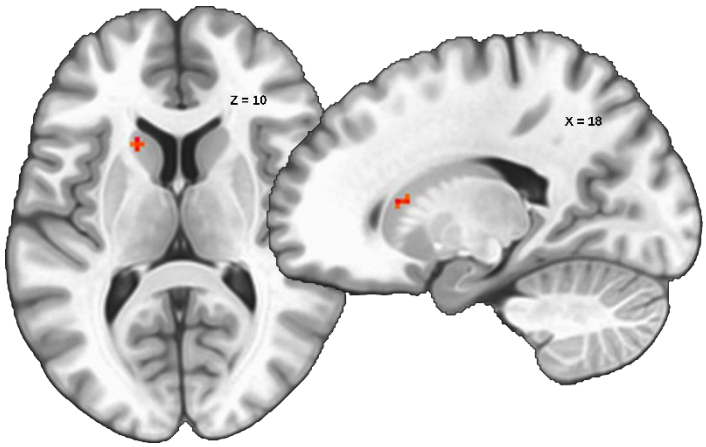

Figure 9. Voxelwise results for R2' and RAC.

R2’ and RAC were positively associated in the left anterior caudate after controlling for age, sex, and trait motion.

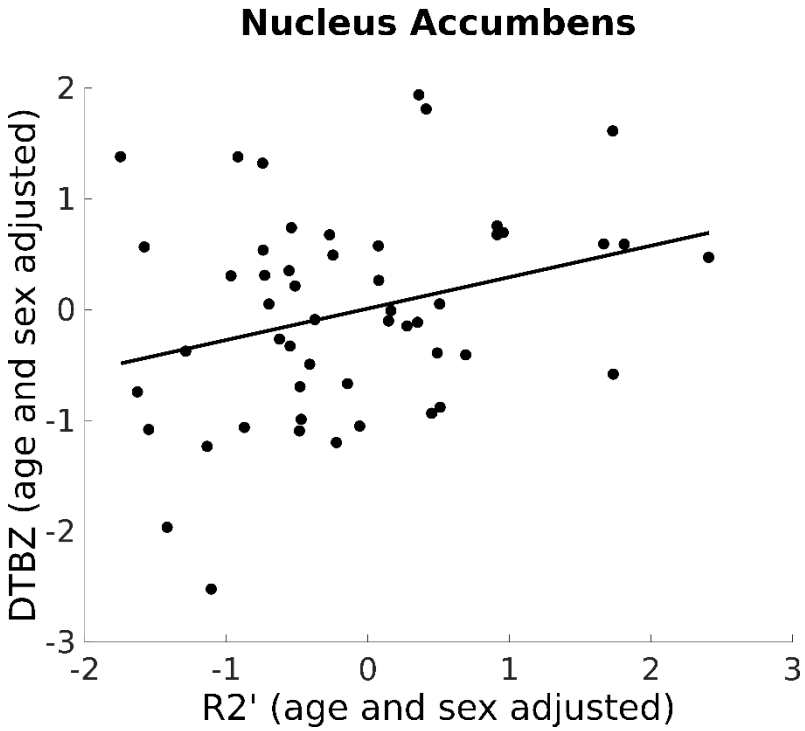

Figure 8. R2’ is positively related to DTBZ in the nucleus accumbens.

Age and sex have been regressed out of both measures. Axes reflect R2’ and DTBZ after the adjustment for age and sex (standardized residuals).

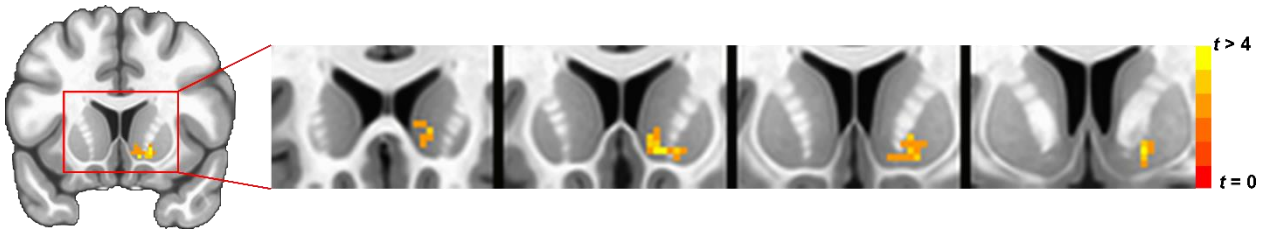

Figure 10. Voxelwise results for R2' and DTBZ.

R2’ and DTBZ were significantly positively associated in the right ventral striatum after controlling for age, sex, trait motion, and family-wise error.

3.4 DISCUSSION

3.4.1 Developmental findings

3.4.1.1 Tissue Iron

R2’ significantly increased throughout most of the striatum, including nucleus accumbens, caudate, and putamen, replicating prior work indicating age-related increases in tissue-iron concentration throughout the first two decades of life (Hallgren and Sourander 1958; Aquino et al. 2009; Wang, Shaffer, et al. 2012) as well as our findings from chapter two (Larsen and Luna 2015). Further, the spatial pattern of age-related increases in R2’ tended to follow a ventral-rostral to dorsal-caudal gradient such that the greatest age effects occurred in the ventral-rostral striatum and became non-significant in the most dorsal-caudal aspects of the striatum, also replicating the gradient of age-related differences we observed in chapter two (Larsen and Luna 2015) (Figure 4). As VS is primarily associated with reward processing and limbic function, our results support the hypothesis of dual systems models that the limbic/affective circuitry continues to mature during adolescence. The relatively less pronounced age-related differences in dorsal striatum (Figure 7)

suggest that associative and sensorimotor striatal circuitry may mature earlier than limbic striatum, supporting the "driven dual systems" version of the dual systems model that hypothesizes protracted affective system development in parallel with more stable cognitive control system development (Luna and Wright 2016).

3.4.1.2 RAC and DTBZ

Rodent models of adolescence have consistently indicated a peak in D1 and D2 receptor concentrations in the striatum during adolescence (Gelbard et al. 1989; Teicher et al. 1995; Andersen, Rutstein, et al. 1997; Tarazi et al. 1998b). To investigate age-related differences in D2 receptor density in our adult sample, we used RAC, which binds to striatal D2 receptors and provides an estimate of receptor concentration. Our RAC findings indicated developmental decreases in D2 receptor concentration in the putamen and caudate in late adolescence and early adulthood (ages 18-30), supporting findings from animal models indicating age-related decreases in D2 receptor concentration from adolescence to adulthood. Studies extending into childhood however are needed to determine if this decline follows a peak in D2 receptor density during adolescence. The positive association between RAC and R2' in the caudate paired with the pronounced age-related increases in R2' in anterior caudate during early adolescence may reflect, in part, developmental increases in receptor concentration. Counter to our hypothesis, we did not observe age-related decreases in the nucleus accumbens, and voxelwise relationships, though not significant, suggest the relationship may become positive in VS. Interestingly, rodent studies that look at D2 receptor concentrations in the nucleus accumbens separately from the corpus striatum (caudate-putamen) suggest that accumbens receptor concentrations have either a less pronounced peak or plateau during late adolescence (Tarazi and Baldessarini 2000). As such, the pattern of results observed in this study largely reflect rodent models of striatal D2 receptor development.

Rodent models also indicate monotonic increases in DA levels and DAT levels during adolescence that begin to plateau in adulthood. DTBZ provides an index of VMAT2, which packages and transports vesicular DA and is concentrated in presynaptic DA terminals in the striatum. As such, VMAT2 should be correlated with overall striatal DA concentration; however, it does not account for extracellular or cytosolic DA. The lack of developmental differences in DTBZ may indicate that peak levels of DA concentration have already been reached by adolescence. Speculatively, given the positive association between DTBZ and R2' in the VS, the pronounced age-related increases in R2' in VS during early adolescence may reflect, in part, increases in vesicular DA concentration.

Overall, findings the developmental findings presented here indicate a combination of process that have stabilized by adulthood (ages 18-30) and those that continue to develop during adulthood. The lack of observed age-related differences in DTBZ across all striatal ROIs suggests that presynaptic striatal vesicular DA may stabilize prior to adulthood. Similarly, the RAC analyses suggest that VS D2 receptor concentration is stabile prior to adulthood. In contrast, the observed decreases in RAC in the caudate and putamen indicate that D2 receptor concentration continues to decline into early adulthood. Tissue-iron significantly increases from early adolescence to adulthood (ages 12-30) for all striatal ROIs; however, age trajectories suggest that the increase begins to plateau earlier in the posterior caudate and putamen relative to the VS and anterior caudate.

3.4.2 Striatal tissue iron concentration is associated with VMAT2 in ventral striatum

VMAT2 functions to transport vesicular DA to the synapse for release and thus serves as an indicator of presynaptic vesicular DA concentration. Considering the role of iron in DA synthesis,

the association between iron levels and DAT function, and the tendency for co-localization of iron with vesicular DA at the microscopic level, we hypothesized that striatal tissue-iron concentration, as estimated using R2', would be associated with VMAT2, as estimated using DTBZ. The results of this study provide support for this hypothesis in the VS, with the relationship being particularly strong in the right hemisphere. This study provides the first evidence of a relationship between tissue iron and DA *in vivo* in the human. Importantly, this relationship was estimated after controlling for age and age*sex interactions in both measures, suggesting it is not likely to be driven by age (or age*sex) covariance.

While the relationship of R2' and DTBZ in the VS is striking and in support of our hypothesis, it is somewhat surprising that the relationship was not significant across other areas of the striatum. This is likely due to a number of factors. First, though R2' and DTBZ are among the best methods currently available for estimating striatal tissue iron and VMAT2 *in vivo* in the human, they have spatial resolution on the level of millimeters which may be several orders of magnitude greater than the spatial resolution of co-localization of iron and DA, reducing the spatial signal-to-noise ratio and thus the ability to detect relationships. In support of this explanation, we observed significant relationships in the areas of the striatum that have relative high R2' signal. Another factor is likely the high degree of complexity of striatal DA neurobiology (e.g. complex interrelationships between DA synthesis, transporters, receptors, release properties, storage, etc) (Gainetdinov et al. 1998; Qi et al. 2008; Beaulieu and Gainetdinov 2011; Leviel 2011). This is compounded by the fact that many properties of DA function and neurobiology vary along spatial gradients in the striatum (Fusa et al. 2002). Functionally, ventromedial anterior aspects of the striatum are involved in limbic processes and dorsolateral posterior aspects are primarily involved in sensorimotor processes, and areas in between are associated with associated processes. This

gradation is mirrored by sources of DA innervation, with ventromedial striatum being most heavily innervated by VTA DA neurons and dorsolateral aspects of the striatum being more heavily innervated by nigrostriatal pathways (Alexander et al. 1986; Haber 2003; Haber and Knutson 2010). This ventromedial to dorsolateral gradient is characteristic of other neurophysiological and neuroanatomical features of the DA system as well. The rostral ventromedial striatum has less DAT uptake, less DA release, and a higher ratio of VMAT2/uptake than caudal dorsolateral striatum (Leroux-Nicollet and Costentin 1994; Wu et al. 2001; Cragg et al. 2002; Calipari et al. 2012). A similar gradient exists even within the nucleus accumbens, where D1 and D2 receptor concentrations increase from ventromedial to dorsolateral (Bardo and Hammer 1991). Two studies that investigated the effect of a rodent gene knockout model for iron regulation found that impaired iron regulation mechanisms led to reduced DAT, tyrosine hydroxylase, and VMAT2 in VS, but has little to no effect in dorsal striatum, indicating iron levels may have particular significance for the regulation of DA neurobiology in VS (Salvatore et al. 2005; Salvatore and Pruett 2012). These factors may jointly explain the relatively localized relationship between tissue iron and DTBZ observed in the ventral striatum.

3.4.3 Tissue iron as an indirect indicator of striatal neurobiology: Limitations and future directions

We have demonstrated a significant positive relationship between tissue iron concentration, as measured using R2', and both VMAT2 and D2 receptor concentration, measure with DTBZ and RAC. These results may have important implications for researchers interested in assessing processes related to striatal DA in populations unsuitable for PET imaging. While the results of this study are promising for this purpose, there are a few important caveats. First, we have found

significant associations specifically in the VS for VMAT2 and anterior caudate for D2 receptors. Therefore, tissue iron may only be interpreted as reflecting these aspects of DA neurobiology in these areas, and future studies replicating these findings are needed before such interpretations can be made with confidence. Second, as iron concentration and DA change with age over early development (as well as aging), we corrected for age in both measures before assessing the relationships between them. Future researchers should take similar cautions in interpreting findings related to tissue iron in developmental samples. Between-subject comparisons made in same-age cohorts may be an ideal application of this technique. Lastly, we have only assessed two indices of DA neurobiology in this study, DTBZ and RAC. It is possible that iron may be more or less sensitive to other measures of DA. Given the relationships observed between iron and DAT in disease models and models of iron deficiency (Erikson et al. 2000; Beard et al. 2003; Wiesinger et al. 2007; Unger et al. 2014). Future work can test this hypothesis using readily available PET ligands for the quantification of striatal DAT (Stehouwer and Goodman 2009; Rami-Mark et al. 2013).

As iron accumulates at a decreasing rate over the second decade of life, and there is not a mechanism in place to clear iron from the basal ganglia (Moos and Rosengren Nielsen 2006; Boserup et al. 2011), it is possible that the *rate* of change in striatal tissue iron concentration is more strongly associated with age-related changes in DA measures. Future studies using longitudinal data can address this hypothesis and inform relationships between tissue iron and DA more fully.

4.0 DEVELOPMENTAL CHANGES IN THE INTEGRATION OF AFFECTIVE AND COGNITIVE CORTICOSTRIATAL PATHWAYS IS ASSOCIATED WITH REWARD-DRIVEN BEHAVIOR

This chapter is adapted from (Larsen et al. n.d.)

4.1 INTRODUCTION

Adolescence is a unique stage of development characterized, in part, by increases in reward-driven behavior that, while adaptive in nature, can lead to maladaptive risk-taking that undermines survival (Shulman et al. 2016). Developmental cognitive neuroscience models propose that this adolescent predisposition is driven by a unique balance between the influence of systems supporting affective processes, including socioemotional and reward processing (i.e., limbic systems), and systems supporting cognitive control on behavior, with affective systems having a greater relative influence on behavior in adolescence than in adulthood (Shulman et al. 2016). These influential models have been generated in large part from human neuroimaging observations that suggest unique maturational trajectories for brain areas commonly ascribed to cognitive control (e.g. prefrontal and related circuitry) and incentive processing (e.g. ventral striatum and cortical limbic circuitry). *Structural* MRI studies indicate protracted maturation of brain regions involved in in reward-processing and cognitive control (e.g. prefrontal cortex, striatum) from adolescence to adulthood into adulthood with unique timelines (Giedd et al. 1999; Sowell et al. 1999; Gogtay et al. 2004; Mills et al. 2014). Relatedly, *functional* magnetic resonance imaging

(fMRI) studies suggest differential task-related activation of brain regions involved in in both systems from adolescence to adulthood (Geier and Luna 2009; van Leijenhorst et al. 2010; Bari and Robbins 2013). Evidence for age-related changes in the functional integration of these systems is more limited. Graph theoretical analyses of large-scale structural and functional network organization indicate developmental enhancements in the global integration of systems and networks including subcortical and frontal systems (Dennis et al. 2013; Hwang et al. 2013; Baker et al. 2015; Marek et al. 2015); however developmental changes in the specific functional integration of systems involved in limbic and cognitive control functions, and their association with reward-driven behavior, have not been probed directly. This limits our ability to understand the interactive dynamics underlying the relative contributions of these systems to behavior.

An ideal target for investigating developmental shifts in the influence of cortical brain systems on behavior is corticostriatal circuitry. The striatum is the primary input nucleus to the basal ganglia and functions to bias action selection (Humphries et al. 2006; Houk et al. 2007; Kimchi and Laubach 2009). It is neuroanatomically well-positioned for this function, receiving dense projections from the cerebral cortex, including cortical brain systems involved in affective and cognitive control processes (Alexander et al. 1986; Choi et al. 2012). The striatum has long been thought to integrate cortical information within closed, parallel circuits, but more recently human (Verstynen et al. 2012; Verstynen 2014; Jarbo and Verstynen 2015) and non-human primate (Averbeck et al. 2014; Choi et al. 2016) studies have shown that areas of the striatum receive convergent projections from functionally disparate cortical regions. These convergent zones are thought to serve as functional hubs that directly integrate and synchronize information to drive basal ganglia action outputs (Haber 2003; Averbeck et al. 2014; Haber 2014). Convergent projections from limbic and cognitive control-related cortical systems into the striatum then

represent an important neuroanatomical substrate for the integration of affective and executive information to influence behavior. Further, the striatum has been shown to structurally develop into adulthood (Sowell et al. 1999; Raznahan et al. 2014; Larsen and Luna 2015) and play a critical role in increasing global network integration during adolescence (Marek et al. 2015). The development of convergent corticostriatal inputs from limbic and cognitive control-related systems may thus be an important developmental mechanism for the changing relative influence of cognitive control and limbic functional brain systems on adolescent behavior.

Here we analyze diffusion MRI data to characterize the relative integrity of convergent corticostriatal projections from cortical systems functionally involved in affect processing (i.e., limbic networks) and cognitive control (i.e., frontal-parietal and attention networks) (Yeo et al. 2011) and determine the nature of these convergent inputs changes across development. Specifically, we hypothesized that projections from predominantly affective cortical systems into striatal convergent zones would have greater relative integrity than projections from predominantly cognitive control-related cortical systems early in adolescence, with the affective influence decreasing into adulthood, and the nature of this convergence relationship would be associated with individual differences to reward-driven behavior.

4.2 MATERIALS AND METHODS

4.2.1 Sample

A total of 115 adolescents and young-adults between the ages of 10 and 28 participated in this study (M = 18.43, SD = 4.67; 62 males). Eighteen participants were excluded due to either excess

head motion during the diffusion MRI (dMRI) scan, low temporal signal-to-noise ratio (tSNR), or visible distortion or artifact in the raw diffusion images (details described below). All participants were recruited from the community and reported no history of neurological disease or brain injury and no personal history or first-degree relative with major psychiatric illness. A description of the sample can be found in Table 2. All experimental procedures in this study complied with the Code of Ethics of the World Medical Association (1964 Declaration of Helsinki) and the Institutional Review Board at the University of Pittsburgh. Participants gave informed consent and were paid for their participation in the study. Aspects of this data have been previously reported in studies of resting state network development (Hwang et al. 2013) and incentive processing (Paulsen et al. 2014).

Table 2 Sample Demographics

Variable	Mean (SD) or Count	Range
Age	18.43 (4.67)	10 – 28
Sex	62M/53F	
Race	79 W; 17 B; 10 A; 9 O	
Mother education	5.75 (1.15)	3 – 7
Father education	5.58 (1.13)	3 -7
IQ	114.6 (12.7)	76 – 138

Note. M = male, F = female; W = white, B = black, A = Asian, O = other (multiple endorsements = 7, not endorsed = 2); Education levels are: 1 = Less than 7th grade, 2 = Junior high school, 3 = Partial high school, 4 = Completed high school or equivalent, 5 = Some college, 6 = Completed college, 7 = Completed post-graduate training. Four participants did not indicate mother's education and five participants did not indicate father's education.

4.2.2 dMRI acquisition

Imaging data were collected using a 3.0 Tesla Trio (Siemens) scanner at the Magnetic Resonance Research Center (MRRC), Presbyterian University Hospital, Pittsburgh, PA. The images were acquired with a total of 60 diffusion sampling directions (TR = 6.4s, TE = 0.89s, field of view = 255x255mm, 52 slices) and a single-shell b-value of 850 s/mm2. Two b = 0 images were collected. The in-plane resolution was 2.5 mm. The slice thickness was 2.5 mm. Participants viewed a movie of their choosing for the duration of the acquisition.

4.2.3 dMRI preprocessing

Eddy current and motion correction were performed using the "eddy" function (Andersson and Sotiropoulos 2016) from the FMRIB Software Library (FSL; (Jenkinson et al. 2012)). Participants with motion estimates that exceeded 2.5 standard deviations above the sample mean were excluded

from further analyses. Motion metrics (and means after exclusion and cutoffs) were the following: mean volume-by-volume translation (M = 0.35mm, cutoff = 0.85mm) and rotation (M = 0.35mm, cutoff = 0.95mm) and percentage of slices with signal dropout (e.g. (Benner et al. 2011; Yendiki et al. 2014)) (M = 0.41%, cutoff = 3.5%). For the remaining participants, these metrics were used as continuous covariates in all subsequent statistical analyses. Participants were also excluded if their tSNR exceeded 2.5 standard deviations below the sample mean (M = 8.08, cutoff = 6.5). Notably, this tSNR cutoff is nearly identical to the cutoff reported by Roalf and colleagues (Roalf et al. 2016) to optimally separate poor data from good quality data (6.47). There was no significant relationship between age and any of the motion metrics. There was a main effect of sex for percentage of slices with signal dropout such that females had a greater percentage than males, though both groups averaged less than one slice with signal dropout (Males = 0.2%, Females = 0.6%, t = -4.1, p < .001). There was a significant negative association between age and tSNR, which was driven by an age by sex interaction such that age was negative associated with tSNR in males but not females (age*sex parameter estimate = 0.-0.06, SE = 0.18, p < .01; see Figure 19). Due to the significant association between age and tSNR, age regression models were performed with and without tSNR as a covariate. After eddy current and motion correction, the diffusion data were reconstructed and warped to standard space using q-space diffeomorphic reconstruction (Yeh and Tseng 2011) with a diffusion sampling length ratio of 1.25 using DSI Studio software (http://dsi-studio.labsolver.org). The output resolution was 2 mm.

4.2.4 Region of interest identification

Cortical brain systems were identified according to the seven-network cortical atlas created by (Yeo et al. 2011) (Figure 11). This atlas was chosen because it contained a cortical

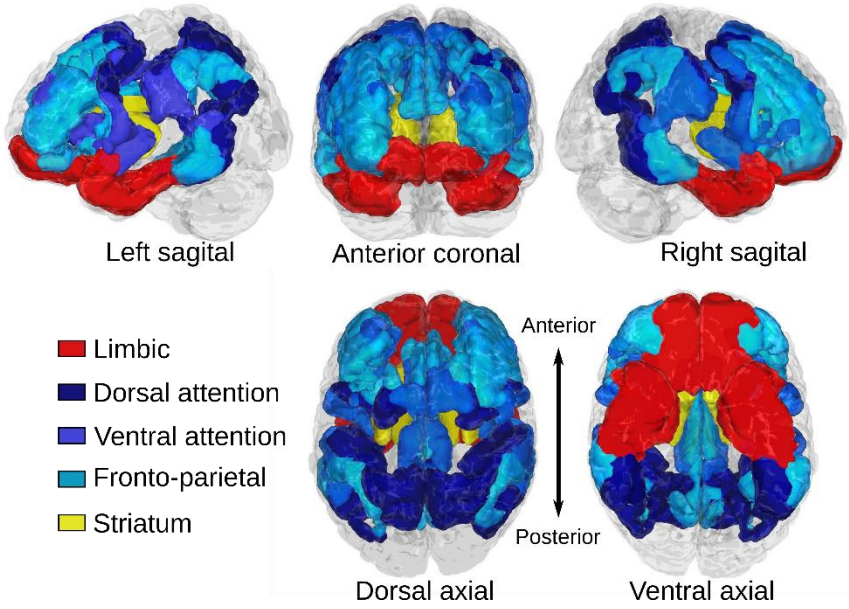

Figure 11. Regions of interest for corticostriatal tractography.

Cortical regions of interest relating to cognitive control function are colored in blue hues and include dorsal attention, ventral attention, and fronto-parietal systems. The cortical limbic system is colored in red. The striatum is colored yellow. Cortical regions were defined according to (Yeo et al. 2011).

limbic system as well as cognitive control-related systems, and has been previously been used in studies of corticostriatal functional connectivity (Choi et al. 2012). We considered the fronto-parietal, dorsal attention, and ventral attention systems as systems related to aspects of cognitive control, and we considered the cortical limbic system to be involved reward processing and motivation (Figure 11). The striatum was defined according to the Harvard-Oxford subcortical atlas distributed with FSL. Each ROI was split by left/right hemisphere. Gross identification and labeling of white matter fiber pathways was performed according to the *MRI Atlas of Human White Matter* (Mori et al. 2005).

4.2.5 Deterministic fiber tracking

To identify corticostriatal pathways, we applied a deterministic fiber tracking algorithm (Yeh et al. 2013) to each participant's reconstructed diffusion data using DSI Studio. Fiber tractography was performed for each cortical region of interest and the striatum, separately for each hemisphere. Whole brain seeding was used and fiber streamlines were identified that passed through the cortical ROI and terminated ("END" mask in DSI Studio) in the striatum. The anisotropy threshold was set at 0.06. The angular threshold was 75 degrees. The step size was 1 mm. The fiber trajectories were smoothed by averaging the propagation direction with 80% of the previous direction. A total of five million seeds were placed to ensure comprehensive detection of corticostriatal fibers across participants, and a connectivity map was calculated from the resulting tracts. We elected to use deterministic rather than probabilistic fiber tracking because our goal was to localize white matter targets to later quantify the connectivity value. Probabilistic fiber tracking provides a connectivity estimate that is solely based on computational simulation of the possible connections and a probability threshold is needed localize pathways. This connectivity definition is not necessarily related to axonal characteristics (Jbabdi and Johansen-Berg 2011) and interpretation of the results can be challenging. In our deterministic approach, connectivity is defined by the quantitative anisotropy value derived from diffusion MRI signals, which are more closely related to axonal characteristics. As such, deterministic fiber tracking is a better fit for this application.

4.2.6 Analyses

4.2.6.1 Convergent zones

We first sought to determine the location of areas of the striatum that receive convergent corticostriatal inputs from limbic and cognitive control-related brain systems. To determine striatal fiber streamline endpoint locations for each cortical ROI, fiber streamline endpoint counts for striatal voxels were smoothed with a 4mm kernel and thresholded at one percent of total striatal endpoints for each participant in order to estimate a more conservative endpoint map. The resulting maps were then binarized to form fiber tract endpoint masks. Individual participant striatal convergent zones were calculated as the intersections of the limbic projection field mask with the fronto-parietal, dorsal attention, and ventral attention projection field masks (i.e. three total convergent zones; limbic/fronto-parietal, limbic/dorsal attention, and limbic/ventral attention). Voxel-wise convergence probability masks were then generated from the entire sample. To determine where the convergence probability exceeded chance levels, we performed spatial permutation tests, randomly permuting the voxel indices of the pathway endpoint masks for all participants and calculating a null convergence probability distribution for each striatal voxel. Convergent zones were determined as clusters of voxels where the observed convergence probability for the sample significantly exceeded the null distribution with an alpha of 0.05, FDR corrected. To determine if the size or shape of convergent zones differed as a function of age, we performed voxel-wise logistic regression on the thresholded, binarized convergence maps across participants to test whether the likelihood of convergence differed by age across striatal voxels. Voxel-wise tests were multiple comparison corrected at a FDR alpha of 0.05.

4.2.6.2 Convergence ratio

After identifying convergent zones, we quantified the integrity of fiber streamlines connecting each convergent zone to its corresponding limbic and cognitive cortical ROIs. To determine pathways linking each convergent zone to its respective set of cortical ROIs, deterministic fiber tractography was performed between the cortical ROIs and the convergent zones we identified using the above procedure. We performed deterministic tractography on the CMU60 high resolution diffusion template included with DSI studio using the same tracking parameters mentioned above. White matter regions of interest were then created from the tracked fiber streamlines. These white matter ROIs were used to extract corresponding mean estimates (i.e. mean across voxels in the white matter ROI mask) of pathway integrity (see below: *Quantitative anisotropy*) along pathways for each participant. This process resulted in measures of connection integrity for each pair of corticostriatal convergent fiber projections. Quantitative anisotropy (QA; (Yeh et al. 2010, 2013)) was used as the primary measure of fiber integrity because it is more robust to partial volume effects and crossing fibers than the commonly used fractional anisotropy (FA). To compute the relative weighting of convergent projections from limbic and cognitive-control related cortical ROIs we calculated the limbic/cognitive control convergence ratio, defined as:

Equation 1

$$\frac{Limbic\ QA - Cognitive\ control\ QA}{Limbic\ QA + Cognitive\ Control\ QA}$$

The convergence ratio thus varies between -1 and 1 such that a positive value indicates greater relative weighting of limbic projections and a negative value indicates greater weighting toward cognitive control projections.

4.2.6.3 Quantitative anisotropy

We assessed fiber integrity with QA because this measure has been shown to be more robust to the influence of crossing fibers, which are common along corticostriatal tracts, and partial volume effects on estimates of diffusion anisotropy along the principle fiber direction than other indices, such as fractional anisotropy (FA) (Yeh et al. 2013; Zhang et al. 2013; Lim et al. 2015; Shen et al. 2015). This is because QA is calculated from a spin distribution function, estimated with q-space diffeomorphic reconstruction, that allows for the modeling of diffusion along multiple vectors. Diffusion modeled along fiber orientations that are inconsistent with the primary fiber orientation (e.g. crossing or branching fibers) do not bias the calculation of quantitative anisotropy along the primary fiber direction (Yeh et al. 2013). Other indices, such as FA, can paradoxically increase overall when the anisotropy of an individual off-axis fiber population decreases (Pierpaoli et al. 2001). Further, our QA based fiber tracking approach was evaluated in the 2015 ISMRM tractography challenge (http://www.tractometer.org/ismrm_2015_challenge/) as ID#03. The valid connection of the QA-based fiber tracking achieved the highest valid connections score (93%) among all 96 methods evaluated. In this study, we further improved the tracking results using a region of interest, and thus we could expect that the percentage valid connections should be greater than 90%. Although we still cannot assert that our tracking results are 100% accurate, the quality achieved should be among the best considering the state-of-the-art approach.

4.2.6.4 Regression analyses

All regression analyses were performed using MATLAB 2016a (The Mathworks, Inc., Natick, MA, United States). To determine age-related differences in the relative weighting of limbic and cognitive control-related convergent connections we regressed the convergence ratio on age and sex, covarying our three motion metrics and whole-brain (global) averaged QA using simple linear

regression. To determine age-related differences in QA for tracks that influence the convergence ratio, we regressed QA on age and sex, covarying motion and global QA, separately for each tract. For all regression analyses, functional forms of age that have been previously shown to characterize age-related change during this period (Luna et al. 2004)—linear, inverse (1/age), and quadratic—were separately tested and model selection was performed among these functional forms using AIC. Cook's distance was used to detect influence outliers based on the default MATLAB threshold of greater than three times the mean cook's distance of the sample. Multiple comparison correction of *p*-values was done using the Bonferroni correction. Age-by-sex interactions were further included in the initial regression models. In the case of non-significant interaction effects, results were reported from regression models that included main effects only. The age variable was centered when interaction terms were included in the model.

4.2.7 Behavioral assessment

As part of the original study protocol, participants performed an incentivized antisaccade task, which is used to assess incentive modulated inhibitory control behavior. These data were collected in a separate visit that occurred 1 – 77 days (median = 17.5) prior to the diffusion MRI scan. The design of the task has been described in detail elsewhere (Paulsen et al. 2014). Here we report on the initial cross-sectional sample of the longitudinal sample reported on previously (Paulsen et al. 2014). We used these data for a follow-up analysis assessing the relationship between affective/cognitive control convergence ratios and incentive-modulated inhibitory control (which relies on both affective and cognitive control processes). In the task, participants received a cue indicating whether correct performance on the upcoming trial would result in an increase in points (reward trials), the prevention of a loss of points (loss trials), or not influence point totals (neutral

trials). Participants were informed that their point total and the end of the experiment would lead to a monetary reward of up to $25. Participants selected whether they would prefer this reward to be in the form of cash or a gift card of their choosing. Participants also indicated their subjective valuation of the $25 reward using a 7-point Likert scale. All participants were provided this additional compensation at the end of the study. Following the incentive cue, a fixation-cross appeared on the computer screen for 1.5s followed by a yellow dot that flashed in the periphery. To perform the trial correctly, participants had to make a saccade (monitored with eye-tracking) to the side of the screen opposite the stimulus. The influence of reward incentives on inhibitory control performance was calculated as the difference in accuracy (commission errors only) for reward and neutral trials (loss trials were not included in analyses for this study). For behavioral analyses, this difference was regressed on age, controlling for sex. For brain-behavior analyses, this difference was regressed on the convergence ratio and age, covarying sex, motion metrics and global QA. For convergent zones in which the convergence ratio was significantly related to both age and behavior, we tested for mediation (i.e. convergence ratio as a mediator of age-related differences in behavior). Mediation models were statistically evaluated using bias-corrected bootstrap significance values over 5000 bootstraps and were implemented using the M3 Mediation Toolbox (https://canlabweb.colorado.edu/wiki/doku.php/help/mediation/m3_mediation_fmri_toolbox (Wager et al. 2008). For all regression and mediation models including behavioral data, participants were excluded that were missing eye tracking data for greater than one third of total trials in either condition (N = 8) or that performed at ceiling for both conditions (N = 14).

4.3 RESULTS

4.3.1 Convergence of corticostriatal pathways

Convergent corticostriatal projections were identified between the cortical limbic system and the fronto-parietal and ventral attention systems in the rostral striatum but not the dorsal attention system (Figure 12).

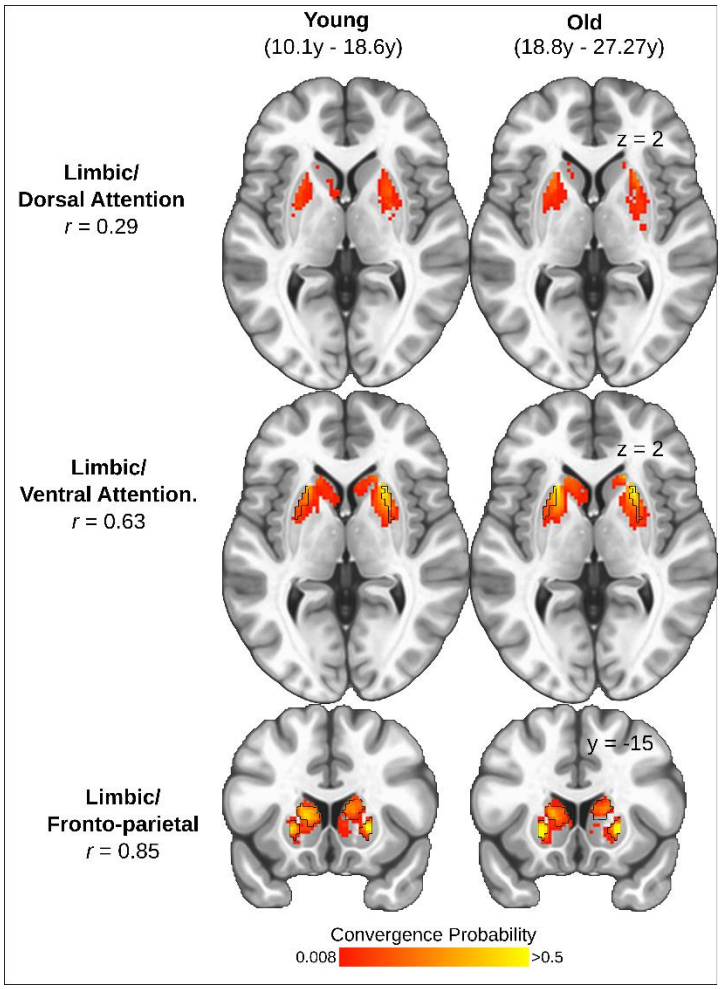

Figure 12. Spatially consistent convergent zones in adolescents and adults.

The sample was split at the median age (18.6y) and the striatal convergence probabilities for each pair of cortical ROIs were calculated for each group. The convergence probability maps between young (left column) and old (right column) participants and spatial correlations are presented for all convergence pairs (Top: limbic/dorsal attention $r = 0.29$; Middle: limbic/ventral attention $r = 0.63$; Bottom: limbic/fronto-parietal $r = 0.85$). Black outlines indicate the identified locations of the convergent zones used to conduct all subsequent analyses (as estimated from the entire sample). We did not observe a significant convergent zone for the limbic and dorsal attention systems.

Zones of convergent corticostriatal projections between the *fronto-parietal* system, supporting on-line aspects of cognitive control (Dosenbach et al. 2007), and the cortical limbic system, supporting affective processes (reward and socioemotional processing), were observed bilaterally in clusters that extend from the head of the caudate to the anterior putamen (peak coordinates: -22,18,0 and 22,18,0 for left and right hemispheres respectively) (Figure 13A). The convergent zones encompassed 46.5% and 56% of the estimated limbic and fronto-parietal corticostriatal projection areas respectively (Figure 13A). These areas largely overlapped with areas of the striatum previously identified in a functional connectivity parcellation of the striatum to have primary functional connections with the limbic and fronto-parietal systems ((Choi et al. 2012) Figure 20A; 0). White matter tracts connecting each convergent zone to the fronto-parietal system included anterior aspects of the inferior and superior fronto-occipital fasciculi and posterior aspects of the superior fronto-occipital fasciculus. The inferior fronto-occipital and uncinate fasciculi connected each convergent zone to the cortical limbic system (Figure 13B).

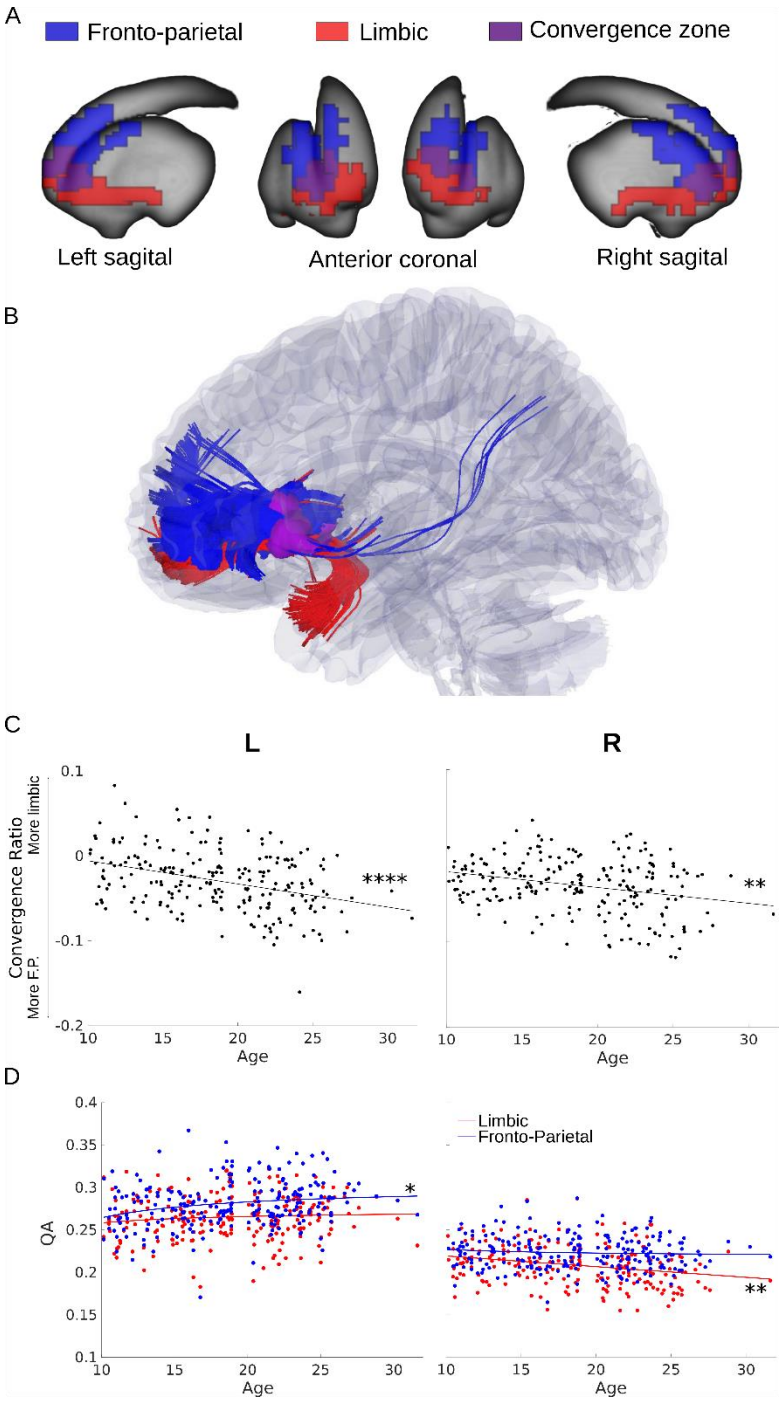

Figure 13. Limbic/Fronto-parietal convergence assessed using quantitative anisotropy.

A. Limbic (red) and fronto-parietal (blue) corticostriatal fiber tracking striatal endpoints overlaid on the surface of the striatum. The convergent zone is colored in purple. B. Fiber tracts connecting the limbic (red) and fronto-parietal (blue) cortical regions of interest to the striatal convergent zone from (A). C. The convergence ratio significantly decreased with age throughout adolescence in both hemispheres (Table 1). D. The individual maturational trajectories of limbic and fronto-parietal projections to the convergent zone. +p<.05 uncorrected; *p<.05, **p<.01, ****p<.0001 Bonferroni corrected.

Corticostriatal projections from the *ventral attention system*, supporting sustained aspects of cognitive control and salience-based attention (Dosenbach et al. 2006, 2007), and limbic systems converged bilaterally in the anterior putamen (peak coordinates: -26,10,0 and 26,12,2 for left and right hemispheres respectively)(Figure 14A). The convergent zones encompassed 10% and 6% of the limbic and ventral attention corticostriatal projection areas respectively Figure 14A). These areas largely overlapped with or were nearby to areas of the striatum previously identified in a functional connectivity parcellation of the striatum to have primary functional connections with the ventral attention and limbic systems ((Choi et al. 2012) Figure 20B). White matter tracts connecting these convergent zones to the ventral attention system originated in the insular and middle frontal cortices. The inferior fronto-occipital and uncinate fasciculi connected each convergent zone to the cortical limbic system (Figure 14B).

We did not detect a convergent zone for the dorsal attention system and the cortical limbic system. Though converging projections were detected in a small number of subjects, the probability of convergence did not exceed 7% for our sample (Figure 12A). As such, subsequent analyses focus on limbic/fronto-parietal and limbic/ventral attention convergent zones.

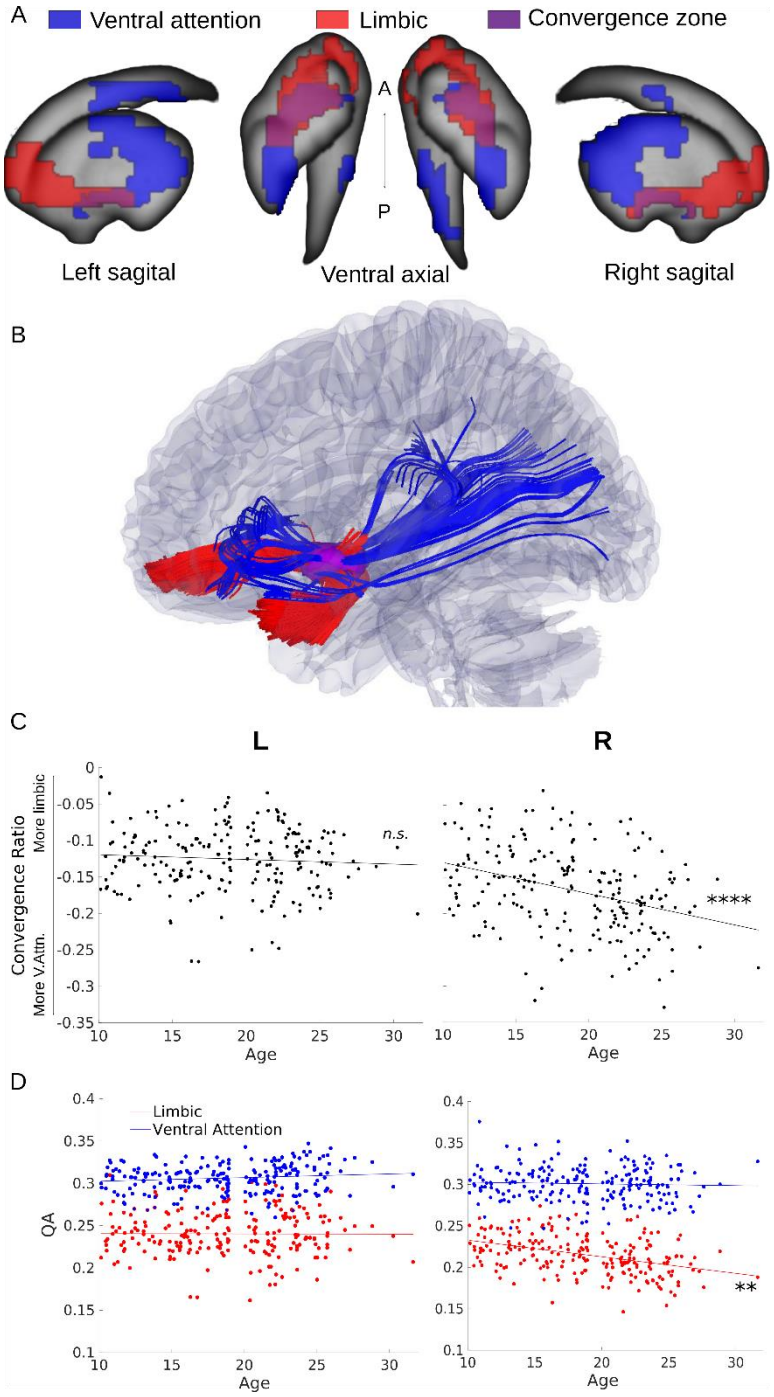

Figure 14. Limbic/ventral attention convergence assessed using quantitative anisotropy

A. Limbic (red) and ventral attention (blue) corticostriatal fiber tracking striatal endpoints overlaid on the surface of the striatum. The convergent zone is colored in purple. B. Fiber tracts connecting the limbic (red) and ventral attention (blue) cortical regions of interest to the striatal convergent zone from (A). C. The convergence bias significantly decreased with age throughout adolescence in the right hemisphere only (Table 3). D. The individual maturational trajectories of limbic and ventral attention projections to the convergent zone.
+p<.05 uncorrected; *p<.05, **p<.01, ****p<.0001 Bonferroni corrected.

4.3.2 Maturation of convergent corticostriatal inputs

We first sought to examine whether the location or shape of the convergent zones differs with age. Voxel-wise logistic regression models indicated no striatal voxels significantly differed in the probability of being a convergent endpoint for any of the affective/cognitive convergence pairs as a function of age. This suggests that the spatial extent of the convergent zones does not expand or contract as a function of age and suggests the macro-level circuit architecture is in place by this stage of development. To further illustrate this, we split our sample at the median age (18.6y), independently calculated convergence probabilities for both groups, and calculated the spatial correlation of convergence probabilities across striatal voxels. The probability maps between groups were highly correlated for the limbic/fronto-parietal (r = 0.85) and limbic/ventral attention (r = 0.63) convergent zones (Figure 12), further indicating that convergent zones are spatially consistent across age-groups. Notably, despite the overall low observed convergence probability in the limbic/dorsal attention convergent zone, there was still a spatial correlation between old and young groups (r = 0.29).

We next quantified the relative integrity of the converging corticostriatal pathways that link affective and cognitive control-related cortical systems to the identified striatal convergent zones, the *convergence ratio* (see Convergence ratio), and examined its association with age in our sample. The limbic/fronto-parietal convergence ratio linearly decreases in both hemispheres throughout adolescence (Figure 13C, Table 3), indicating that the relative weighting of limbic projections decreases throughout adolescence and into adulthood. This developmental change towards greater relative fronto-parietal weighting appears to be driven by a trend-level inverse linear age-related decrease in limbic QA in the left hemisphere (1/Age coefficient = 0.27, *SE* = 0.12, $p < .05$ uncorrected) while fronto-parietal QA remained stable (coefficient = 0.006, *SE* =

0.004, *n.s.*) (Figure 13D, left panel) and a greater age-related decrease in limbic QA (coefficient = -0.003, *SE* = 0.0003, $p < .01$ corrected) than fronto-parietal QA (coefficient = -0.001, *SE* = 0.0004, $p < .05$ Bonferroni corrected)(Figure 13D, right panel). These developmental effects were not meaningfully changed by including tSNR as a covariate.

The limbic/ventral attention convergence ratio also linearly decreases with age, though the effect is only significant in the left hemisphere (Figure 14C, Table 3). The age-related decrease in the left hemisphere convergence ratio appeared to be driven by a trend-level inverse linear age-related decrease in limbic QA (1/Age coefficient = 0.45, *SE* = 0.2, $p < .05$ uncorrected) while ventral attention QA remained stable (coefficient = -0.0009, *SE* = 0.0005, *n.s.*) (Figure 14D, left panel). The inclusion of tSNR as a covariate reduced the significance of the left hemisphere age coefficient to a trend-level effect, however tSNR itself was not a significant predictor of the convergence ratio, ruling out tSNR as a mediator of the relationship between age and the convergence ratio.

Convergent zone	Variable	Coefficient	SE	*t*	*p*
Limbic/Fronto-parietal					
Left					
	Age	-0.0029	0.0006	-4.82	**<.00001******
	Sex	0.0111	0.0060	1.85	.067
	Motion				
	Translation	0.0115	0.0201	0.57	.568
	Rotation	-0.0279	0.0188	-1.48	.142
	Slice	-0.0735	0.5003	-0.15	.884
	Global QA	-0.0751	0.0428	-1.75	.083
Right					
	Age	-0.0035	0.0005	-6.93	**<.00001******
	Sex	0.0100	0.0049	2.03	.046^{+}
	Motion				
	Translation	0.0243	0.0165	1.47	.144
	Rotation	-0.0457	0.0153	-2.99	**.004***
	Slice	-0.0132	0.4340	-0.03	.976
	Global QA	-0.0372	0.0339	-1.10	.276
Limbic/Ventral Attention					
Left					
	Age	-0.0041	0.0012	-3.31	**.001****
	Sex	0.0328	0.0123	2.67	**.009***
	Motion				
	Translation	0.0744	0.0385	1.93	.057
	Rotation	-0.1214	0.0385	-3.15	**.002****
	Slice	0.4232	1.0407	0.41	.685
	Global QA	-0.1426	0.0770	-1.85	.067
Right					
	1/Age	0.3626	0.2385	1.52	.132
	Sex	-0.0119	0.0083	-1.44	.154
	Motion				
	Translation	0.0014	0.0276	0.05	.960
	Rotation	0.0357	0.0267	1.34	.185
	Slice	-0.1321	0.7251	-0.18	.856
	Global QA	0.0069	0.0524	0.13	.895

Note. Bold indicates significant after multiple comparison correction.
+ p<.05; *p<.05, **p<.01, ***p<.001, ****p<.0001 Bonferroni corrected

Table 3 Convergence Ratio Maturation Regression Models

4.3.3 Sex differences in convergence ratios

There was a significant main effect of sex in the left limbic/ventral attention convergent zone and a trend-level effect *(*$p < .05$ uncorrected) in the right limbic/fronto-parietal convergent zone (see Table 3). In both cases, the direction of the effect was such that males had greater (i.e. more limbic) limbic/cognitive control convergence ratios than females. There were no significant age-by-sex interactions.

4.3.4 Convergence ratio and incentive modulated inhibitory control

To determine whether the observed age-related differences in the affective/cognitive control convergence ratios were related to reward-related cognitive control performance, we performed follow-up analyses investigating the relationship between the convergence ratio and performance on an incentive modulated inhibitory control task, the rewarded antisaccade. Though reward incentives did not significantly improve accuracy across the entire sample (Fig 5 A), we found that the right limbic/fronto-parietal and right limbic/ventral attention convergence ratios were positively associated with accuracy improvements under reward incentives (i.e. greater relative limbic weighting is associated with greater performance improvement) (Fig 5 B&C). Considering that accuracy was high overall in both conditions (Fig 5 A), as a follow-up analysis we compared the mean convergence ratios for only the participants who had the greatest difference in performance between conditions to test the hypothesis that those who have the greatest reward-related improvement in accuracy should have a greater (i.e. more limbic) convergence ratio. We

found that participants who had a greater than 5% increase in accuracy in the *reward* condition (i.e. reward accuracy – neutral accuracy > 5%; $N = 5$) had significantly more limbic convergence ratios than those who had a greater than 5% increase in performance in the *neutra*l condition (i.e. reward accuracy – neutral accuracy < -5%; $N = 8$) in the bilateral limbic/fronto-parietal (Left: $t = 2.21$, $p = .0495$; Right: $t = 2.82$, $p = .0155$) and left limbic/ventral attention convergent zone (Left: $t = 2.94$, $p = .0136$; Right: $t = 1.47$, $p = .176$). Previous work using a rewarded antisaccade task (Padmanabhan et al. 2011) has demonstrated that the influence of reward incentives is greatest early in adolescence and diminishes into adulthood. Our findings generally support this pattern, though the effect was only significant at the trend level in this sample (Fig 5 D). Importantly, this effect not likely to be related to age-related differences in the subjective valuation of the reward incentive because we did not observe a significant association between age and the subjective valuations provided by participants ($r = -.05$, $p = .57$). As the right limbic/fronto-parietal convergence ratio is significantly associated with both age (Figure 13C) and performance (Fig 5 B), we sought to determine whether this effect mediated the trend-level association between age and reward-related performance improvements. Mediation analysis indicated that the right limbic/fronto-parietal convergence ratio significantly mediates the association between age and reward-related antisaccade performance (Fig 5 E).

4.4 DISCUSSION

Conceptual models of the neural basis for adolescent heightened reward drive, sensation seeking, and risk-taking suggest a developmental imbalance in the integration of affective and cognitive control systems and their resulting influence on behavior (Shulman et al. 2016); however direct

evidence for developmental differences in the integration of these systems has been lacking. We addressed this by showing how age-related differences in corticostriatal circuitry that integrates information from cortical limbic and control systems correlates with developmental differences in reward-driven behavior. Converging corticostriatal pathways form an infrastructure by which information from functionally distinct cortical systems can be integrated to influence action selection (Haber 2003; Averbeck et al. 2014; Haber 2014; Verstynen 2014). Different cortical systems are selective for different feature representations and sensitive to different task contexts, stimuli, or goal states, in effect prioritizing different types of information (e.g. (Klink et al. 2014)). Whether competitive or complementary, this information must be integrated to select appropriate actions. This is accomplished, in part, by corticostriatal projections that are the inputs to the cortico-basal ganglia-thalamo-cortical pathways that bias action selection either directly (Humphries et al. 2006; Houk et al. 2007; Kimchi and Laubach 2009) or indirectly via action value representations (Frank 2005; Seo et al. 2012). In this way, striatal convergent zones function as one substrate for the integration of information from distinct cortical systems to influence behavior.

The influence of cortical systems on behavior should then vary with the relative connectivity integrity white matter projections to striatal convergent zones. To this end, we found that the relative integrity of convergent cortical affective (limbic) and cognitive control-related (fronto-parietal and ventral attention) pathways into the striatum differs with age, such that the relative integrity of affective pathways reduces throughout adolescence and into adulthood, coinciding with developmental changes in reward-guided decision making. Thus, these findings not only provide support for the notion that limbic systems have greater relative influence on behavior during adolescence than during adulthood (Shulman et al. 2016), they also provide one

neurologically plausible mechanism by which these systems can influence behavior. Indeed, the right hemisphere limbic/fronto-parietal and limbic/ventral attention convergence ratios were positively associated with reward-related improvements in inhibitory control performance (Fig 5).

The striatal convergent zones for the limbic/fronto-parietal and limbic/ventral attention systems identified were observed in the rostral aspects of the dorsal and ventral striatum. The spatial location of these convergent zones fell on or near the borders between areas of the striatum previously identified to be predominantly connected to the limbic and fronto-parietal or ventral attention regions investigated in this study (Supplementary Fig 2), providing a notable consistency between functional (resting-state) and structural (dMRI) indices of corticostriatal connectivity. The cortical limbic system forms a cognitive map that prioritizes inferred economic or hedonic value via the OFC (Kringelbach 2005; Stalnaker et al. 2015), as well as socioemotional information via the temporal pole (Olson et al. 2007). Cortical cognitive control-related systems, on the other hand, prioritize goal-directed control of behavior. The fronto-parietal system is involved in transient aspects of cognitive control, such as control initiation, task-switching, and rule updating (Dosenbach et al. 2007; Cole et al. 2013). The ventral attention system prioritizes context-dependent visuospatial and perceptual salience, playing a functional role in orienting attention (Dosenbach et al. 2006; Fox et al. 2006; Fair et al. 2009). Considering these functional characteristics and the role of cortico-basal ganglia circuitry in influencing action selection (Seo et al. 2012; Wiecki and Frank 2013; Jin et al. 2014; Dunovan and Verstynen 2016), greater relative weighting of convergent cortical limbic projections in relation to projections from these cognitive control systems should bias adolescents to select actions or focus attention on items in the environment that have high inferred reward value even if those items are irrelevant to the present goal-state. This bias may then underlie the behavioral phenotype of greater reward sensitivity, a

propensity for reward-driven behavior, and inconsistent cognitive control, which are hallmarks of adolescent behavior (Somerville and Casey 2010; Luna et al. 2015). Accordingly, we found that the right hemisphere limbic/fronto-parietal convergence ratio mediated age-related reductions in the influence of reward on inhibitory control performance. As has been previously reported (Padmanabhan et al. 2011; Geier and Luna 2012), the known developmental limitations in antisaccade performance during adolescence can be overcome in the presence of reward incentives. As we report here, this effect does not seem to be a function of developmental differences in the subjective value of reward stimuli. Rather, our present results indicate that this developmental phenomenon may be associated with the affective/cognitive-control convergence ratio, particularly at limbic/fronto-parietal striatal convergent zones (Fig 5 E). In this experimental paradigm, where there is synergy between the cognitive demands and reward information, developmental differences in the limbic/cognitive control convergence ratio (i.e. greater relative weighting of limbic projections to limbic/cognitive control convergent zones during early adolescence) may form a neural substrate for the greater facilitation of task performance during rewarded trials for adolescents over adults. In this way, a greater affective/cognitive control convergence ratio may have adaptive qualities in early adolescence, facilitating, in this case, adult-like inhibitory control ability with incentive motivation.

We did not observe a convergent zone for the limbic and dorsal attention systems. This suggests that convergence of affective corticostriatal projections with other functional systems is selective even within the cognitive domain. The absence of a corticostriatal convergent zone is likely due to anatomical and topographical characteristics of the dorsal attention and limbic cortical systems. (Yeo et al. 2011). As a result, it's corticostriatal connections are predominant in the caudal putamen whereas corticostriatal connections from the limbic system are predominant in the

rostroventral striatum (Choi et al. 2012). The dorsal attention system is functionally involved in goal-directed sustaining of attention and is thus associated with sustained aspects of cognitive control (Fox 1995; Dosenbach et al. 2007). This is in contrast to the more transient control functions of the fronto-parietal and, to some extent, ventral attention systems (Dosenbach et al. 2007; Cole et al. 2013; Vossel et al. 2014). Speculatively, limbic system convergence with the fronto-parietal and ventral attention systems but not the dorsal attention system may indicate greater ability for reward information to interact with cognitive control in a transient manner, biasing task-switching and orienting of attention toward reward stimuli or contexts. Further, considering the close interaction between the ventral and dorsal attention systems to respectively orient and sustain attention (Vossel et al. 2014), there may not be a functional imperative for convergence between the limbic and dorsal attention system as the ventral attention system could function as an intermediary. Future work using functional imaging may help to delineate these complex functional interactions.

The development of the affective/cognitive control convergence ratio was predominantly driven by age-related decreases in the mean QA of cortical limbic projections to convergent zones while cognitive control projections generally remained stable, supporting the notion that systems supporting limbic function may be particularly influential in adolescence (Luna et al. 2015). Though developmental decreases in mean QA may appear surprising in consideration of studies assessing diffusion with the tensor model and reporting developmental increases in fractional anisotropy (FA), it is important to note that these same studies typically also report developmental decreases in diffusion along the parallel axis, axial diffusivity, during adolescence (Qiu et al. 2008; Kumar et al. 2012; Simmonds et al. 2014b), which in principle may be a more similar, though less robust (see Materials and methods: *Quantitative anisotropy*), measure to QA. This suggests that

decreases in QA may speculatively reflect a developmental refinement in limbic corticostriatal structural connectivity. Notably, a recent longitudinal study similarly found age-related reductions in the QA of limbic (fronto-amygdalar) white patter pathways during adolescence (Jalbrzikowski et al. 2017). Additionally, a recent study (Baker et al. 2015) found decreased fractional anisotropy of subcortical tracts during late adolescence, which suggests developmental specialization may continue within subcortical systems throughout adolescence. These findings agree with resting state functional connectivity MRI studies that find decreased fronto-striatal functional connectivity with age during adolescence (Supekar et al. 2009; Dosenbach et al. 2010; Padmanabhan et al. 2013; Porter et al. 2015). Considering that myelination may increase or decrease based on neuronal activity (Hines et al. 2015; Mensch et al. 2015), decreased functional connectivity and decreased white matter integrity observed here may be mechanistically interrelated.

We observed some evidence of hemispheric differences in our developmental and brain-behavior analyses. The right hemisphere limbic/ventral attention convergence ratio was not significantly associated with age in our sample, though the direction of the effect was consistent with the left hemisphere. We also observed that both the left hemisphere limbic/fronto-parietal and limbic/ventral attention did not have a significant linear association with incentive modulated inhibitory control performance. However, when we focused our analyses only on participants with the greatest change in performance between conditions, we found that the left hemisphere convergence ratios did differentiate groups such that participants with greatest improvement in performance under reward incentives had a more limbic convergence ratio than those who had the greatest improvement in performance in the neutral condition, suggesting the left hemisphere convergent zones are still behaviorally relevant.

Sex differences impact many aspects of neural function and anatomy (Cahill and Aswad 2015) including white matter development (Wang, Adamson, et al. 2012; Simmonds et al. 2014b). Here we find that males tended to have a greater limbic/cognitive control convergence ratio than females, with no significant age by sex interaction. This pattern of results suggests a greater influence of the cortical limbic system on male behavior relative to that of females regardless of age. This finding is in-line with recent work showing that adolescent males are more sensation seeking and have less impulse control than adolescent females (Shulman et al. 2015), and may play a role in sex differences in the development of striatum-related psychopathologies such as ADHD (Willcutt 2012) and substance abuse (Compton et al. 2007) which have greater incidence in males, and mood disorders, which have greater incidence in females (Cover et al. 2014).

Based on our specific hypotheses pertaining to developmental differences in the integration of affective and cognitive control systems and their influence on behavior throughout adolescence, our current study has selectively focused on the development of convergent corticostriatal projections from affective and cognitive control systems. We wish to acknowledge that convergent zones for other functional brain systems as well as corticostriatal projections from individual brain are also likely to play important functional roles in cognition and behavior and may also display important maturational changes throughout development. Future studies may further interrogate the development of these corticostriatal pathways to complement the findings of this study.

In sum, our findings indicate that early in adolescences the cortical affective system has the greatest relative integrity of projections into corticostriatal hubs that integrate affect and cognitive control information and that this neuroanatomical configuration is related to reward-driven behavior during this period of development. Thus, we propose that cortical projections to striatal convergent zones serve as one important developmental mechanism for the changing

influence of affective and control systems on behavior, whereby the relative influence of affective systems decreases as adolescents make the transition to adulthood. Importantly, the greater influence of affective systems during early adolescence can be adaptive in nature in that it underlies an incentivized increase in cognitive control abilities. Developmental changes in the relative weighting of convergent corticostriatal projections may have implications that extend to abnormal development and behavior. Psychopathologies such as schizophrenia, substance abuse, and mood disorders emerge during adolescence and are associated with striatal abnormalities. As such, corticostriatal convergent zones may be a useful target for future clinical studies.

5.0 **DISCUSSION**

Heightened sensation seeking is one of the most salient features of the adolescent behavioral profile. The contribution of sensation seeking to risk-taking behavior during adolescence has created a public health interest in understanding the neurodevelopmental processes that contribute to sensation seeking behavior during adolescence. Prominent neurodevelopmental models of adolescence hypothesize that adolescent sensation seeking is related to a functional peak in DA reward processing that creates a developmental imbalance in the influence of the DA system on behavior relative to top-down control from cognitive control systems (Shulman 2016). The studies presented here test key components of these models, including 1) that the striatal DA system continues to mature during adolescence and 2) that there is a developmental imbalance in affective vs. cognitive control systems on behavior during adolescence.

Evidence for the development of the striatal DA system during adolescence has been largely based on animal models of development. In particular, rodent studies have provided evidence of continued development of striatal DA receptor density, DA concentration, and DAT. These studies have led to the hypothesis that the same neurodevelopmental processes are unfolding during adolescence in the human; however, this hypothesis has been difficult to test directly due to limitations in techniques available to study DA neurobiology *in vivo* in the human in pediatric populations. The studies included in chapters 2.0 and 3.0 of this dissertation addressed this limitation by investigating tissue-iron concentration, a striatal tissue property that has been linked with multiple aspects of mesostriatal DA neurobiology (Wiesinger et al. 2007; Unger et al. 2008, 2014; Zucca et al. 2017). In chapter 2.0 , we used a novel MR measure sensitive to tissue iron, nT2*, to investigate age-related differences in striatal development. The results indicated that the

spatial pattern of nT2* systematically differs as a function of age, with greatest age-related differences in VS. The direction of the effect suggests greater tissue-iron accumulation with age in the ventral striatum, with less pronounced changes occurring in dorsal striatum. In other words, greater age effects were centered on affective rather than associative/sensorimotor striatum. In chapter 3.0 , we replicated findings these findings using a quantitative measure of tissue iron concentration, R2' (note that nT2* is inversely related to tissue iron concentration whereas R2' is positively associated with tissue iron concentration, thus age-related decreases in nT2* and age-related increases in R2' both indicate age-related increases in striatal tissue iron concentration). We found that the development of R2' roughly followed a ventral-rostral to dorsal-caudal gradient such that the greatest age-related increases in tissue iron were occurring in ventral striatum.

Chapter 3 continued to build on the findings in chapter 2 by including PET indices of striatal neurobiology in the adult portion of the sample. Specifically, we assessed DTBZ and RAC across the striatum as measures of VMAT2 and D2 receptor density, respectively, and related them to R2' estimates of tissue iron concentration. PET measures generally agreed with rodent studies of striatal development. D2 receptor concentration decreased with age in the putamen and anterior caudate and did not significantly decrease in the nucleus accumbens, reflecting the decline in receptors in late adolescence that follows an early adolescent peak in rodent caudate-putamen, and the less pronounced decline in nucleus accumbens (Tarazi 2000, Teicher 1995). DTBZ did not significantly differ by age in the adult sample, perhaps reflecting a plateau in striatal DA levels (as well as DAT levels) during the transition to adulthood (Giorgio 1987). Importantly, we found that tissue R2' was positively associated with DTBZ in the ventral striatum, indicating that tissue iron concentration is associated with VMAT2 in limbic striatum. To our knowledge, this is the first time an association between striatal tissue iron and striatal DA neurobiology has been

demonstrated *in vivo* in the human. Considering the age-related rise in tissue iron during adolescence, it is possible that there is a corresponding increase in presynaptic vesicular DA during adolescence that occurs prior to the plateau observed using DTBZ in the adult sample. This increase would correspond to increases in DA levels observed in the rodent (Giorgio 1987). However, this inference is speculative and should be interpreted with caution until future studies can replicate the association between tissue iron and VMAT2 that we observe in our data.

The studies presented in chapters two and three advance previous work assessing the structural development of the striatum. These prior studies have focused on striatal volume as an indicator of structural development and have generally reported age-related decreases in volume over adolescence, though one study found increased volume in the nucleus accumbens (Dennison et al. 2013). Interestingly, one study that examined changes in surface area across the surface of the striatum (Raznahan et al. 2014) found patterns of expansion and contraction that seem to be somewhat anti-correlated with the pattern of tissue iron accumulation we observe; that is, areas of the striatum that show greatest contraction with age (anterior striatum) tended to have greater age-related increases in iron concentration, while areas showing the greatest expansion with age (posterior dorsal striatum) tended to have non-significant age-related differences in iron concentration. It is not clear how iron should directly affect volume estimates, however iron is inversely related to T1 relaxation time (i.e. linearly related to 1/T1) (Vymazal et al. 1995; Ogg and Steen 1998; Stüber et al. 2014) which is the measure used to calculate volume and surface area, so an anticorrelation between volume and iron is reasonable. For this reason, it is possible that striatal tissue iron may actually bias estimates of striatal volume due to the shortening of T1 relaxation time. Importantly, tissue iron is essential for a variety of neural processes, including oxidative metabolism, myelination, and neurotransmitter synthesis, and have been directly linked to aspects

of DA neurobiology (including the results presented in chapter three), making tissue iron a useful index of striatal development. In contrast, the factors that contribute to MR indices of structural morphometry are unclear. Overall, results from chapters 2 and 3 suggest that VS and anterior caudate iron concentration and caudate and putamen D2 receptor density are continuing to develop into adulthood whereas presynaptic DA concentration across the striatum and iron concentration in the posterior caudate and putamen stabilize at or prior to the transition from adolescence to adulthood (i.e. by age 18).

Chapter 4 tested the hypothesis that the affective system has greater influence on behavior during adolescence by investigating the development of affective and cognitive corticostriatal connectivity. We found that areas of the striatum that receive convergent corticostriatal inputs from affective and cognitive control areas of the cortex ("convergent zones") have greater relative connectivity integrity of affective inputs during adolescence. Whereas inputs from cognitive control systems were relatively stable during adolescence, inputs from affective cortex tended to decrease in integrity as a function of age, leading to a decreasing ratio of affective-to-cognitive control connection integrity at convergent zones (the convergence ratio). Further, the convergence ratio mediated age-related decreases in the impact of reward incentives on oculomotor inhibitory control during adolescence. These results thus support the hypothesis that there is a greater relative influence of affective vs. cognitive control systems on adolescent behavior (at least at the level of corticostriatal circuitry) that relates to elevated reward drive. Prior work has characterized developmental increases and decreases in cognitive and affective corticostriatal functional connectivity, respectively. This study builds on these studies by specifically targeting corticostriatal integration of information from cognitive and affective functional subdivisions of cortex. Corticostriatal integration at striatal convergent zones may be the ideal candidates for

assessing the influence of different cortical systems on behavior as these areas are thought to serve as functional hubs that directly integrate and synthesize information to bias future action selection via basal ganglia action outputs (Averbeck et al. 2014; Haber 2014).

Overall, our findings suggest continued development of affective striatal neurobiology and corticostriatal connectivity in parallel with relative stable cognitive and sensorimotor striatal neurobiology and connectivity during adolescence. Functional sub-divisions of the striatum generally fall along a rostroventral to caudodorsal gradient whereby affective and limbic functions are associated with rostroventral striatum, sesnsorimotor functions reside in caudodorsal striatum, and associative/executive functions fall between (Haber 2014). Tissue-iron, measured with both nT2* and R2', increased at the greatest rate in VS and followed a ventral dorsal gradient whereby the most dorsal (and posterior) aspects of the striatum either did not significantly differ by age (R2'; chapter 3) or followed an opposite developmental trajectory (nT2*; chapter 2). This developmental pattern thus maps on to functional gradients and indicates that the most pronounced development is occurring in affective/limbic striatum. Corticostriatal connectivity to affective/cognitive control convergent zones followed a similar pattern of development; affective connectivity decreased across adolescence while cognitive connectivity remained developmentally stable (Chapter 4). PET measures of DA could only be assessed in a late adolescence to adult cohort, so developmental effects can only be detected over ages 18-30. Though we did not observe age-related differences in VMAT2, D2 receptor density generally decreased with age. Notably, there was a lack of age-related differences in VS D2 receptors. While this may appear to be inconsistent with other findings, the lack of change again suggests unique developmental processes happening in ventral and dorsal striatum and suggests elevated DA neurobiology in VS that stabilizes into adulthood. It is possible that there is a protracted peak in receptor density in the

nucleus accumbens that extends further into adulthood and that the age-related decline occurs outside the age range included in our sample, but future research is needed to test this hypothesis. The overall pattern across all measures most supports the driven dual systems model (Luna and Wright 2016) of the dual systems family of neurodevelopmental models. The driven dual systems model posits that cognitive systems are largely developed by the onset of adolescence and affective systems continue to develop. Our results differ from the driven dual systems model in that the driven dual systems model hypothesizes that the affective system follows an inverted "U" developmental trajectory and our results depict largely linear or monotonic changes (e.g. curvilinear plateau). Importantly, these models are largely theoretical in nature and cannot possibly capture the development of these complex and multifaceted neural systems. This complexity is evident in the studies presented here as development of connectivity, iron accumulation, D2 receptors, and VMAT2 do not have a 1:1 correspondence. This family of developmental processes, combined with others not studied here, likely combine to produce characteristic adolescent behavior.

It is important to note that, while these findings represent a significant step forward into the investigation of the striatal DA system during adolescence, there are important limitations to consider. The striatal DA system is complex and multifaceted; though we have targeted two important aspects of the striatal DA system here, VMAT2 levels and D2/D3 receptor concentration, there are many additional aspects of striatal DA that are critical for striatal function and that we are not capable of measuring using the methods employed here. For example, we did not measure D1-like receptors (D1 and D5). D1-like and D2-like receptors jointly play important roles in striatal function based, at least in part, on their contributions to direct and indirect pathways in the basal ganglia which function to facilitate or inhibit actions, respectively (Surmeier et al.

2007; Gerfen and Surmeier 2011). Thus, increases or decreases in DA levels can have differential functional effects based on different patterns of post-synaptic DA receptor class distributions. Further, DA levels themselves are not a singular construct. Here we have used DTBZ to measure VMAT2 levels as an indicator of presynaptic DA concentration, however VMAT2 levels may vary according to multiple factors, including DA synthesis, DAT levels, and do not reflect unpackaged intracellular DA or extracellular DA concentrations—all factors that likely have important functional and developmental significance. In addition, the source of presynaptic DA neurons—VTA or SN—also has functional significance and cannot be determined in the analyses presented here. Limitations in our ability to assess these critical aspects of striatal DA are related to limitations in techniques available to measure them in vivo in humans. Thus, in order to understand adolescent striatal development more fully, future work must be done that continues to rely on both human and animal models of adolescence and leverages techniques available on multiple scales to begin to characterize these aspects of striatal DA and how they interact across development.

Adolescence is the age of emergence of major psychopathology that is characterized by abnormalities in affective processing. Though we did not assess abnormal populations, these findings may provide a useful normative template from which to compare disease populations and to form hypotheses about potential loci of impairments that correspond to symptoms of these disorder. These studies provide a first step in understanding the differential development of specific DA mesolimbic processing that can inform normative development and can motivate future studies.

APPENDIX A

FIGURES

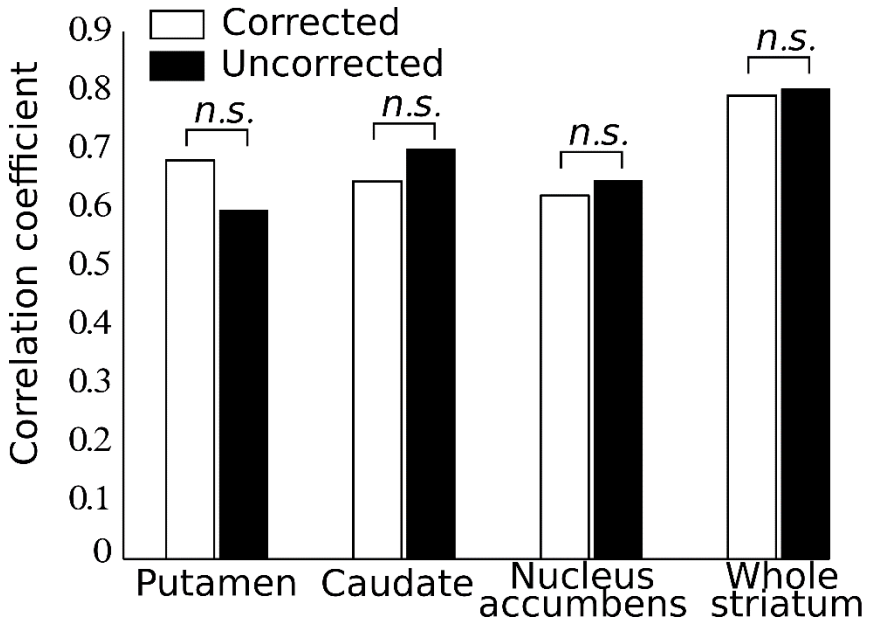

Figure 15 Bar graphs comparing performance of the multivariate support vector regression with and without controlling for potential volume effects.

The bars reflect the correlation between true and predicted age using both techniques. There are no significant differences in performance.

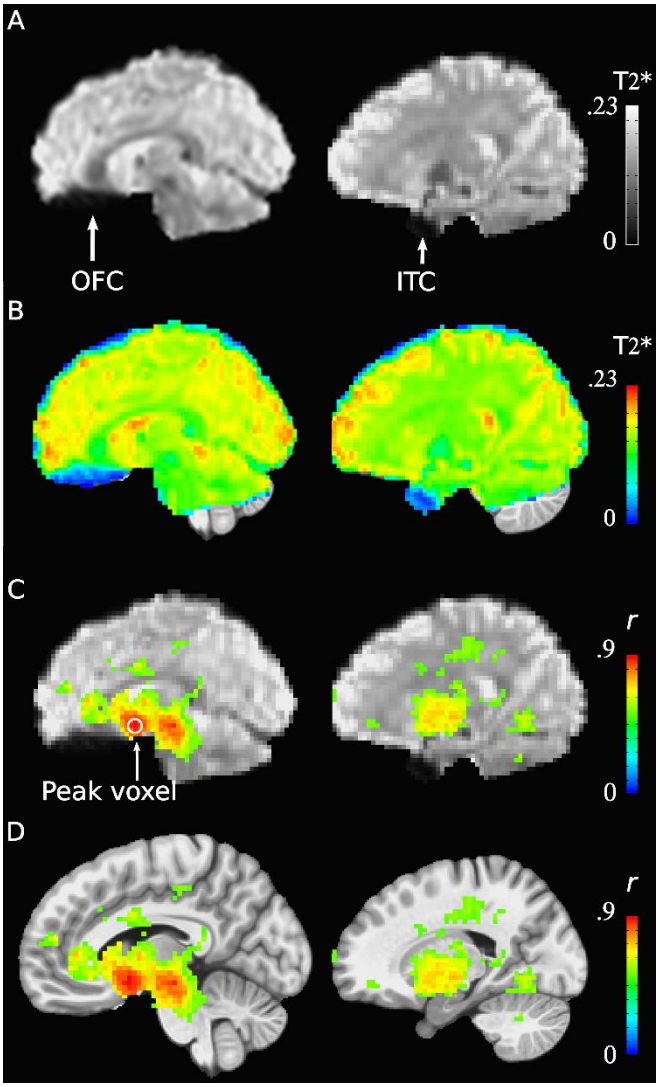

Figure 16. Susceptibility artifacts do not create spurious age effects on T2* images.

A. Representative preprocessed T2*-weighted images (subject age 15.9). Slices highlight signal dropout due to susceptibility artifact in orbitofrontal cortex (OFC, left) and inferotemporal cortex (IFC, right). B. T2*-weighted images from A overlaid on standard anatomical T1 image. C. Whole brain results overlaid on T2*-weighted images with voxel showing peak age effect highlighted. Significant age effects do not occur in areas with greatest susceptibility artifacts. D. Results from C overlaid on the standard T1 anatomical image.

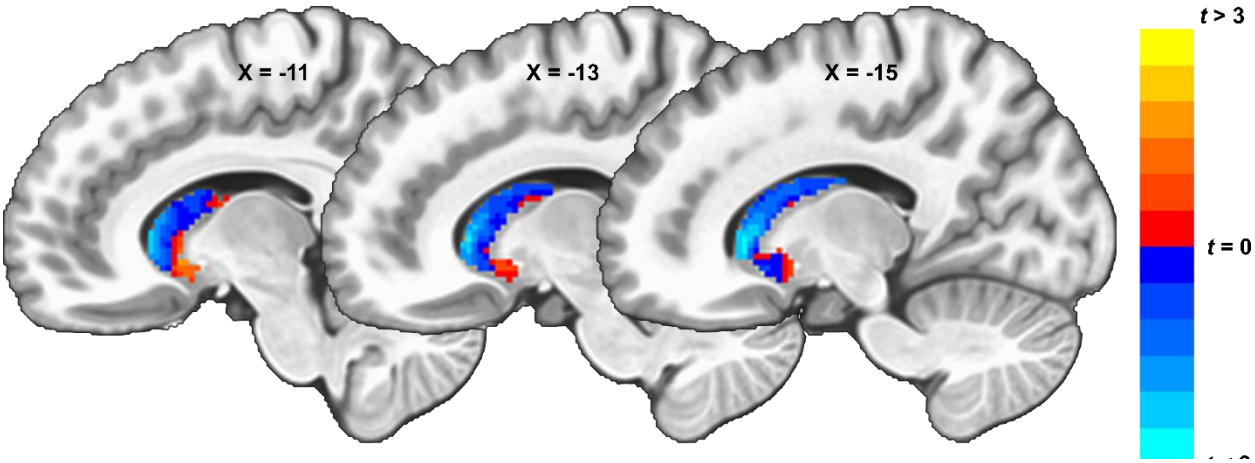

Figure 18. Map of t-statistics for the effect of age on DTBZ (controlling for sex and trait motion).

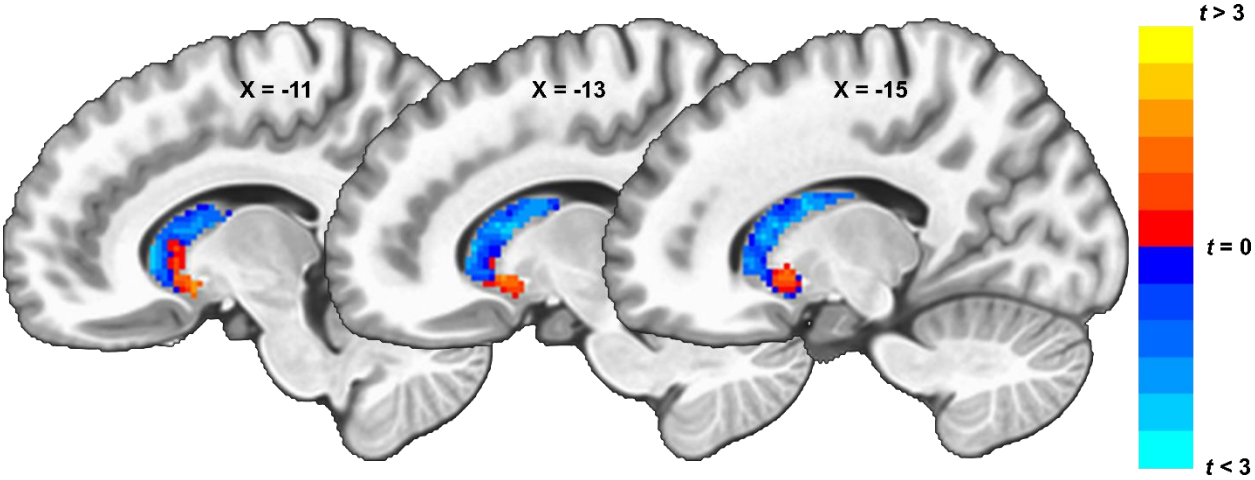

Figure 17. Map of t-statistics for the effect of age on Raclopride (controlling for sex and trait motion).

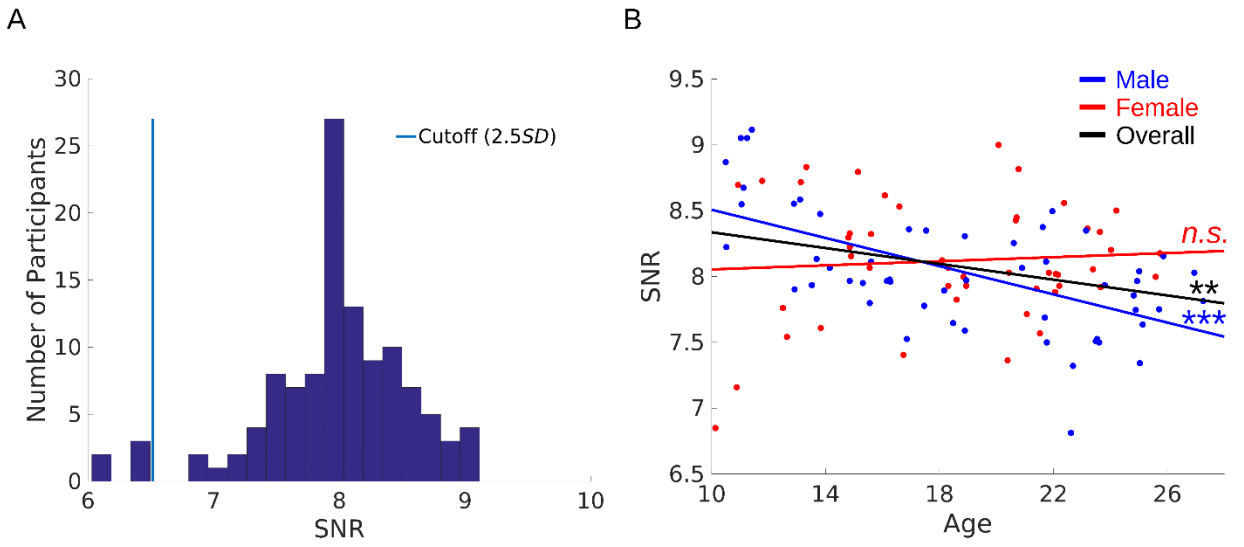

Figure 19 Signal-to-noise-ratio for the sample.

A. Histogram of SNR across the sample including the 2.5 standard deviation cutoff (6.5, blue line) for inclusion in future analyses. B. SNR is negatively associated with age after outlier removal, however this association is driven by and age-by-sex interaction such that SNR decreases with age for males and remains stable in females.

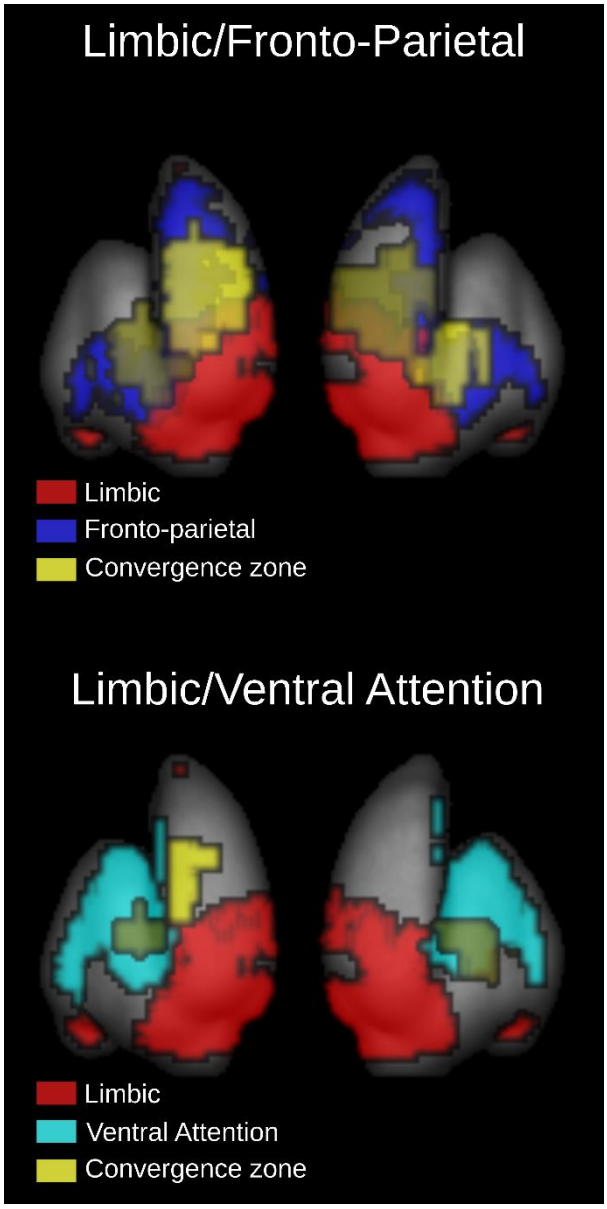

Figure 20 Spatial locations of convergent zones in relation to resting-state functional connectivity parcellation of the striatum.

Convergent zones for the limbic/fronto parietal systems (top) and limbic/ventral attention systems (bottom) are shown in yellow overlaid on striatal regions from Choi and colleagues (2012) that are predominantly functionally connected to the cortical systems used as cortical regions of interest in this study (Red = limbic, Blue = Fronto-parietal (top), Teal = Ventral attention (bottom)). Convergent zones largely lie on or near the boundaries between the striatal areas from the functional connectivity parcellation.

BIBLIOGRAPHY

Adisetiyo V, Jensen JH, Tabesh A, Deardorff RL, Fieremans E, Di Martino A, Gray KM, Castellanos FX, Helpern JA. 2014. Multimodal MR imaging of brain iron in attention deficit hyperactivity disorder: a noninvasive biomarker that responds to psychostimulant treatment? Radiology. 272:524–532.

Adriani W, Chiarotti F, Laviola G. 1998. Elevated novelty seeking and peculiar d-amphetamine sensitization in periadolescent mice compared with adult mice. Behav Neurosci. 112:1152–1166.

Alexander GE, DeLong MR, Strick PL. 1986. Parallel organization of functionally segregated circuits linking basal ganglia and cortex. Annu Rev Neurosci. 9:357–381.

Allen RP, Earley CJ. 2007. The role of iron in restless legs syndrome. Mov Disord Off J Mov Disord Soc. 22 Suppl 18:S440-448.

Andersen SL, Dumont NL, Teicher MH. 1997. Developmental differences in dopamine synthesis inhibition by (+/-)-7-OH-DPAT. Naunyn Schmiedebergs ArchPharmacol. 356:173–181.

Andersen SL, Rutstein M, Benzo JM, Hostetter JC, Teicher MH. 1997. Sex differences in dopamine receptor overproduction and elimination. Neuroreport. 8:1495–1498.

Andersson JLR, Sotiropoulos SN. 2016. An integrated approach to correction for off-resonance effects and subject movement in diffusion MR imaging. NeuroImage. 125:1063–1078.

Aquino D, Bizzi A, Grisoli M, Garavaglia B, Bruzzone MG, Nardocci N, Savoiardo M, Chiapparini L. 2009. Age-related Iron Deposition in the Basal Ganglia: Quantitative Analysis in Healthy Subjects1. Radiology. 252:165–172.

Asato MR, Terwilliger R, Woo J, Luna B. 2010. White matter development in adolescence: a DTI study. Cereb Cortex. 20:2122–2131.

Averbeck BB, Lehman J, Jacobson M, Haber SN. 2014. Estimates of Projection Overlap and Zones of Convergence within Frontal-Striatal Circuits. J Neurosci. 34:9497–9505.

Baker STE, Lubman DI, Yücel M, Allen NB, Whittle S, Fulcher BD, Zalesky A, Fornito A. 2015. Developmental Changes in Brain Network Hub Connectivity in Late Adolescence. J Neurosci. 35:9078–9087.

Bardo MT, Hammer RP. 1991. Autoradiographic localization of dopamine D1 and D2 receptors in rat nucleus accumbens: resistance to differential rearing conditions. Neuroscience. 45:281–290.

Bari A, Robbins TW. 2013. Inhibition and impulsivity: behavioral and neural basis of response control. Prog Neurobiol. 108:44–79.

Beard J, Erikson KM, Jones BC. 2003. Neonatal iron deficiency results in irreversible changes in dopamine function in rats. J Nutr. 133:1174–1179.

Beard JL, Connor JR. 2003. Iron status and neural functioning. Annu Rev Nutr. 23:41–58.

Beard JL, Erikson KM, Jones BC. 2002. Neurobehavioral analysis of developmental iron deficiency in rats. Behav Brain Res. 134:517–524.

Beaulieu J-M, Gainetdinov RR. 2011. The Physiology, Signaling, and Pharmacology of Dopamine Receptors. Pharmacol Rev. 63:182–217.

Bender B, Klose U. 2010. The in vivo influence of white matter fiber orientation towards B0 on T2* in the human brain. NMR Biomed. 23:1071–1076.

Benes FM, Turtle M, Khan Y, Farol P. 1994. Myelination of a key relay zone in the hippocampal formation occurs in the human brain during childhood, adolescence, and adulthood. Arch Gen Psychiatry. 51□ □:477–484.
Benner T, van der Kouwe AJW, Sorensen AG. 2011. Diffusion imaging with prospective motion correction and reacquisition. Magn Reson Med. 66:154–167.
Boserup MW, Lichota J, Haile D, Moos T. 2011. Heterogenous distribution of ferroportin-containing neurons in mouse brain. BioMetals. 24:357–375.
Breiter HC, Rosen BR. 1999. Functional magnetic resonance imaging of brain reward circuitry in the human. Ann N Y Acad Sci. 877□ □:523–547.
Cahill L, Aswad D. 2015. Sex Influences on the Brain: An Issue Whose Time Has Come. Neuron. 88:1084–1085.
Calipari ES, Huggins KN, Mathews TA, Jones SR. 2012. Conserved dorsal-ventral gradient of dopamine release and uptake rate in mice, rats and rhesus macaques. Neurochem Int. 61:986–991.
Choi EY, Tanimura Y, Vage PR, Yates EH, Haber SN. 2016. Convergence of prefrontal and parietal anatomical projections in a connectional hub in the striatum. NeuroImage.
Choi EY, Yeo BTT, Buckner RL. 2012. The organization of the human striatum estimated by intrinsic functional connectivity. J Neurophysiol. 108:2242–2263.
Cohen JR, Asarnow RF, Sabb FW, Bilder RM, Bookheimer SY, Knowlton BJ, Poldrack RA. 2010. A unique adolescent response to reward prediction errors. NatNeurosci. 13:669–671.
Cole MW, Reynolds JR, Power JD, Repovs G, Anticevic A, Braver TS. 2013. Multi-task connectivity reveals flexible hubs for adaptive task control. Nat Neurosci. 16:1348–1355.
Compton WM, Thomas YF, Stinson FS, Grant BF. 2007. Prevalence, correlates, disability, and comorbidity of DSM-IV drug abuse and dependence in the United States: results from the national epidemiologic survey on alcohol and related conditions. Arch Gen Psychiatry. 64:566–576.
Connor JR, Menzies SL. 1996. Relationship of iron to oligodendrocytes and myelination. Glia. 17:83–93.
Connor JR, Wang X-S, Allen RP, Beard JL, Wiesinger JA, Felt BT, Earley CJ. 2009a. Altered dopaminergic profile in the putamen and substantia nigra in restless leg syndrome. Brain. 132:2403–2412.
Connor JR, Wang X-S, Allen RP, Beard JL, Wiesinger JA, Felt BT, Earley CJ. 2009b. Altered dopaminergic profile in the putamen and substantia nigra in restless leg syndrome. Brain. 132:2403–2412.
Cover KK, Maeng LY, Lebrón-Milad K, Milad MR. 2014. Mechanisms of estradiol in fear circuitry: implications for sex differences in psychopathology. Transl Psychiatry. 4:e422.
Cox RW. 1996. AFNI: software for analysis and visualization of functional magnetic resonance neuroimages. Comput Biomed Res. 29:162–173.
Cragg SJ, Hille CJ, Greenfield SA. 2002. Functional domains in dorsal striatum of the nonhuman primate are defined by the dynamic behavior of dopamine. J Neurosci Off J Soc Neurosci. 22:5705–5712.
de Wit S, Watson P, Harsay HA, Cohen MX, van de Vijver I, Ridderinkhof KR. 2012. Corticostriatal connectivity underlies individual differences in the balance between habitual and goal-directed action control. J Neurosci Off J Soc Neurosci. 32:12066–12075.
Delgado MR, Nystrom LE, Fissell C, Noll DC, Fiez JA. 2000. Tracking the hemodynamic responses to reward and punishment in the striatum. J Neurophysiol. 84□ □:3072–3077.

Dennis EL, Jahanshad N, McMahon KL, de Zubicaray GI, Martin NG, Hickie IB, Toga AW, Wright MJ, Thompson PM. 2013. Development of brain structural connectivity between ages 12 and 30: A 4-Tesla diffusion imaging study in 439 adolescents and adults. NeuroImage. 64:671–684.

Dennison M, Whittle S, Yücel M, Vijayakumar N, Kline A, Simmons J, Allen NB. 2013. Mapping subcortical brain maturation during adolescence: evidence of hemisphere- and sex-specific longitudinal changes. Dev Sci. 16:772–791.

Dosenbach NUF, Fair DA, Miezin FM, Cohen AL, Wenger KK, Dosenbach RAT, Fox MD, Snyder AZ, Vincent JL, Raichle ME, Schlaggar BL, Petersen SE. 2007. Distinct brain networks for adaptive and stable task control in humans. Proc Natl Acad Sci U S A. 104:11073–11078.

Dosenbach NUF, Nardos B, Cohen AL, Fair DA, Power JD, Church JA, Nelson SM, Wig GS, Vogel AC, Lessov-Schlaggar CN, Barnes KA, Dubis JW, Feczko E, Coalson RS, Pruett JR, Barch DM, Petersen SE, Schlaggar BL. 2010. Prediction of Individual Brain Maturity Using fMRI. Science. 329:1358–1361.

Dosenbach NUF, Visscher KM, Palmer ED, Miezin FM, Wenger KK, Kang HC, Burgund ED, Grimes AL, Schlaggar BL, Petersen SE. 2006. A core system for the implementation of task sets. Neuron. 50:799–812.

Drayer B, Burger P, Darwin R, Riederer S, Herfkens R, Johnson GA. 1986. MRI of brain iron. AJR Am J Roentgenol. 147:103–110.

Dunovan K, Verstynen T. 2016. Believer-Skeptic Meets Actor-Critic: Rethinking the Role of Basal Ganglia Pathways during Decision-Making and Reinforcement Learning. Decis Neurosci. 106.

Earley CJ, Connor J, Garcia-Borreguero D, Jenner P, Winkelman J, Zee PC, Allen R. 2014. Altered brain iron homeostasis and dopaminergic function in Restless Legs Syndrome (Willis-Ekbom Disease). Sleep Med. 15:1288–1301.

Earley CJ, Kuwabara H, Wong DF, Gamaldo C, Salas R, Brasic J, Ravert HT, Dannals RF, Allen RP. 2011. The Dopamine Transporter is Decreased in the Striatum of Subjects with Restless Legs Syndrome. Sleep. 34:341–347.

Elsinga PH, Hatano K, Ishiwata K. 2006. PET tracers for imaging of the dopaminergic system. Curr Med Chem. 13:2139–2153.

Erikson KM, Jones BC, Beard JL. 2000. Iron deficiency alters dopamine transporter functioning in rat striatum. J Nutr. 130:2831–2837.

Erikson KM, Jones BC, Hess EJ, Zhang Q, Beard JL. 2001. Iron deficiency decreases dopamine D1 and D2 receptors in rat brain. Pharmacol Biochem Behav. 69:409–418.

Ersche KD, Acosta-Cabronero J, Jones PS, Ziauddeen H, van Swelm RPL, Laarakkers CMM, Raha-Chowdhury R, Williams GB. 2017. Disrupted iron regulation in the brain and periphery in cocaine addiction. Transl Psychiatry. 7:e1040.

Fair DA, Cohen AL, Power JD, Dosenbach NUF, Church JA, Miezin FM, Schlaggar BL, Petersen SE. 2009. Functional brain networks develop from a “local to distributed” organization. PLoS Comput Biol. 5:e1000381.

Fox MD, Corbetta M, Snyder AZ, Vincent JL, Raichle ME. 2006. Spontaneous neuronal activity distinguishes human dorsal and ventral attention systems. ProcNatlAcadSciUSA. 103:10046–10051.

Fox PT. 1995. Physiological ROI definition by image subtraction. J Cereb Blood Flow Metab.

Frank MJ. 2005. Dynamic dopamine modulation in the basal ganglia: a neurocomputational account of cognitive deficits in medicated and nonmedicated Parkinsonism. JCogn Neurosci. 17:51–72.

Frey KA, Koeppe RA, Kilbourn MR. 2001. Imaging the vesicular monoamine transporter. Adv Neurol. 86:237–247.

Fusa K, Saigusa T, Koshikawa N, Cools AR. 2002. Tyrosine-induced release of dopamine is under inhibitory control of presynaptic dopamine D2 and, probably, D3 receptors in the dorsal striatum, but not in the nucleus accumbens. Eur J Pharmacol. 448:143–150.

Gainetdinov RR, Jones SR, Fumagalli F, Wightman RM, Caron MG. 1998. Re-evaluation of the role of the dopamine transporter in dopamine system homeostasis. Brain Res Brain Res Rev. 26:148–153.

Geier CF, Luna B. 2009. The maturation of incentive processing and cognitive control. Pharmacol Biochem Behav. 93:212–221.

Geier CF, Luna B. 2012. Developmental effects of incentives on response inhibition. Child Dev. 83:1262–1274.

Gelbard HA, Teicher MH, Faedda G, Baldessarini RJ. 1989. Postnatal development of dopamine D1 and D2 receptor sites in rat striatum. Brain Res Dev Brain Res. 49:123–130.

Gerfen CR, Surmeier DJ. 2011. Modulation of striatal projection systems by dopamine. Annu Rev Neurosci. 34:441–466.

Ginovart N. 2005. Imaging the dopamine system with in vivo [11C]raclopride displacement studies: understanding the true mechanism. Mol Imaging Biol MIB Off Publ Acad Mol Imaging. 7:45–52.

Giorgi O, De Montis G, Porceddu ML, Mele S, Calderini G, Toffano G, Biggio G. 1987. Developmental and age-related changes in D1-dopamine receptors and dopamine content in the rat striatum. Brain Res. 432:283–290.

Graham JM, Paley MNJ, Grünewald RA, Hoggard N, Griffiths PD. 2000. Brain iron deposition in Parkinson's disease imaged using the PRIME magnetic resonance sequence. Brain. 123:2423–2431.

Haacke EM, Cheng NYC, House MJ, Liu Q, Neelavalli J, Ogg RJ, Khan A, Ayaz M, Kirsch W, Obenaus A. 2005. Imaging iron stores in the brain using magnetic resonance imaging. Magn Reson Imaging. 23:1–25.

Haacke EM, Miao Y, Liu M, Habib CA, Katkuri Y, Liu T, Yang Z, Lang Z, Hu J, Wu J. 2010. Correlation of change in R2* and phase with putative iron content in deep gray matter of healthy adults. J Magn Reson Imaging JMRI. 32:561–576.

Haber SN. 2003. The primate basal ganglia: parallel and integrative networks. J Chem Neuroanat, Special Issue on the Human Brain - The Structural Basis for understanding Human Brain function and dysfunction. 26:317–330.

Haber SN. 2014. The place of dopamine in the cortico-basal ganglia circuit. Neuroscience. 282C:248–257.

Haber SN, Knutson B. 2010. The Reward Circuit: Linking Primate Anatomy and Human Imaging. Neuropsychopharmacology. 35:4–26.

Hallgren B, Sourander P. 1958. The effect of age on the non-haemin iron in the human brain. J Neurochem. 3:41–51.

Harden KP, Tucker-Drob EM. 2011. Individual differences in the development of sensation seeking and impulsivity during adolescence: further evidence for a dual systems model. Dev Psychol. 47:739–746.

Harsay HA, Cohen MX, Oosterhof NN, Forstmann BU, Mars RB, Ridderinkhof KR. 2011. Functional connectivity of the striatum links motivation to action control in humans. J Neurosci Off J Soc Neurosci. 31:10701–10711.
Haycock JW, Becker L, Ang L, Furukawa Y, Hornykiewicz O, Kish SJ. 2003. Marked disparity between age-related changes in dopamine and other presynaptic dopaminergic markers in human striatum. J Neurochem. 87:574–585.
Hines JH, Ravanelli AM, Schwindt R, Scott EK, Appel B. 2015. Neuronal activity biases axon selection for myelination in vivo. Nat Neurosci. 18:683–689.
Houk JC, Bastianen C, Fansler D, Fishbach A, Fraser D, Reber PJ, Roy SA, Simo LS. 2007. Action selection and refinement in subcortical loops through basal ganglia and cerebellum. Philos Trans R Soc Lond B Biol Sci. 362:1573–1583.
Humphries MD, Stewart RD, Gurney KN. 2006. A Physiologically Plausible Model of Action Selection and Oscillatory Activity in the Basal Ganglia. J Neurosci. 26:12921–12942.
Hwang K, Hallquist MN, Luna B. 2013. The development of hub architecture in the human functional brain network. Cereb Cortex N Y N 1991. 23:2380–2393.
Ichise M, Ballinger JR, Tanaka F, Moscovitch M, George-Hyslop PHS, Raphael D, Freedman M. 1998. Age-Related Changes in D2 Receptor Binding with Iodine-123-Iodobenzofuran SPECT. J Nucl Med. 39:1511–1518.
Ichise M, Liow J-S, Lu J-Q, Takano A, Model K, Toyama H, Suhara T, Suzuki K, Innis RB, Carson RE. 2003. Linearized reference tissue parametric imaging methods: application to [11C]DASB positron emission tomography studies of the serotonin transporter in human brain. J Cereb Blood Flow Metab Off J Int Soc Cereb Blood Flow Metab. 23:1096–1112.
Jalbrzikowski M, Larsen B, Hallquist MN, Foran W, Calabro F, Luna B. 2017. Development of White Matter Microstructure and Intrinsic Functional Connectivity Between the Amygdala and Ventromedial Prefrontal Cortex: Associations With Anxiety and Depression. Biol Psychiatry. 0.
Jarbo K, Verstynen TD. 2015. Converging structural and functional connectivity of orbitofrontal, dorsolateral prefrontal, and posterior parietal cortex in the human striatum. J Neurosci Off J Soc Neurosci. 35:3865–3878.
Jbabdi S, Johansen-Berg H. 2011. Tractography: where do we go from here? Brain Connect. 1:169–183.
Jellen LC, Lu L, Wang X, Unger EL, Earley CJ, Allen RP, Williams RW, Jones BC. 2013. Iron deficiency alters expression of dopamine-related genes in the ventral midbrain in mice. Neuroscience. 252:13–23.
Jenkinson M, Beckmann CF, Behrens TEJ, Woolrich MW, Smith SM. 2012. FSL. NeuroImage. 62:782–790.
Jin X, Tecuapetla F, Costa RM. 2014. Basal ganglia subcircuits distinctively encode the parsing and concatenation of action sequences. Nat Neurosci. 17:423–430.
Khan FH, Ahlberg CD, Chow CA, Shah DR, Koo BB. 2017. Iron, dopamine, genetics, and hormones in the pathophysiology of restless legs syndrome. J Neurol. 1–8.
Kilbourn MR. 2014. Radioligands for Imaging Vesicular Monoamine Transporters. In: PET and SPECT of Neurobiological Systems. Springer, Berlin, Heidelberg. p. 765–790.
Kim Y, Simon NW, Wood J, Moghaddam B. 2016. Reward Anticipation Is Encoded Differently by Adolescent Ventral Tegmental Area Neurons. Biol Psychiatry, Addiction. 79:878–886.
Kimchi EY, Laubach M. 2009. Dynamic Encoding of Action Selection by the Medial Striatum. J Neurosci. 29:3148–3159.

Klink PC, Jentgens P, Lorteije JAM. 2014. Priority Maps Explain the Roles of Value, Attention, and Salience in Goal-Oriented Behavior. J Neurosci. 34:13867–13869.
Knutson B, Cooper JC. 2005. Functional magnetic resonance imaging of reward prediction. Curr Opin Neurol. 18:411–417.
Koikkalainen J, Hirvonen J, Nyman M, Lötjönen J, Hietala J, Ruotsalainen U. 2007. Shape variability of the human striatum—Effects of age and gender. NeuroImage. 34:85–93.
Kringelbach ML. 2005. The human orbitofrontal cortex: linking reward to hedonic experience. Nat Rev Neurosci. 6:691–702.
Kumar R, Nguyen HD, Macey PM, Woo MA, Harper RM. 2012. Regional brain axial and radial diffusivity changes during development. J Neurosci Res. 90:346–355.
Larsen B, Luna B. 2015. In vivo evidence of neurophysiological maturation of the human adolescent striatum. Dev Cogn Neurosci. 12:74–85.
Larsen B, Verstynen TD, Yeh F-C, Luna B. n.d. Developmental Changes in the Integration of Affective and Cognitive Corticostriatal Pathways are Associated with Reward-Driven Behavior. Cereb Cortex. 1–12.
Leroux-Nicollet I, Costentin J. 1994. Comparison of the subregional distributions of the monoamine vesicular transporter and dopamine uptake complex in the rat striatum and changes during aging. J Neural Transm Gen Sect. 97:93–106.
Leviel V. 2011. Dopamine release mediated by the dopamine transporter, facts and consequences. J Neurochem. 118:475–489.
Lim SY, Tyan Y-S, Chao Y-P, Nien F-Y, Weng J-C. 2015. New Insights into the Developing Rabbit Brain Using Diffusion Tensor Tractography and Generalized q-Sampling MRI. PLoS ONE. 10:e0119932.
Liston C, Watts R, Tottenham N, Davidson MC, Niogi S, Ulug AM, Casey BJ. 2006. Frontostriatal microstructure modulates efficient recruitment of cognitive control. Cereb Cortex N Y N 1991. 16:553–560.
Lohrenz T, Kishida KT, Montague PR. 2016. BOLD and its connection to dopamine release in human striatum: a cross-cohort comparison. Phil Trans R Soc B. 371:20150352.
Luciana M, Collins PF. 2012. Incentive Motivation, Cognitive Control, and the Adolescent Brain: Is It Time for a Paradigm Shift? Child Dev Perspect. 6:392–399.
Luna B, Garver KE, Urban TA, Lazar NA, Sweeney JA. 2004. Maturation of cognitive processes from late childhood to adulthood. Child Dev. 75:1357–1372.
Luna B, Marek S, Larsen B, Tervo-Clemmens B, Chahal R. 2015. An Integrative Model of the Maturation of Cognitive Control. Annu Rev Neurosci. 38:null.
Luna B, Wright C. 2016. Adolescent brain development: Implications for the juvenile criminal justice system. In: Heilbrun K,, DeMatteo D,, Goldstein NES, editors. APA handbook of psychology and juvenile justice. APA handbooks in psychology series. Washington, DC, US: American Psychological Association. p. 91–116.
Marek S, Hwang K, Foran W, Hallquist MN, Luna B. 2015. The Contribution of Network Organization and Integration to the Development of Cognitive Control. PLoS Biol. 13:e1002328.
Martinez D, Slifstein M, Broft A, Mawlawi O, Hwang D-R, Huang Y, Cooper T, Kegeles L, Zarahn E, Abi-Dargham A, Haber SN, Laruelle M. 2003. Imaging human mesolimbic dopamine transmission with positron emission tomography. Part II: amphetamine-induced dopamine release in the functional subdivisions of the striatum. J Cereb Blood Flow Metab Off J Int Soc Cereb Blood Flow Metab. 23:285–300.

McClure SM, York MK, Montague PR. 2004. The neural substrates of reward processing in humans: the modern role of FMRI. Neuroscientist. 10:260–268.
McCrae RR, Costa PT, Terracciano A, Parker WD, Mills CJ, De Fruyt F, Mervielde I. 2002. Personality trait development from age 12 to age 18: longitudinal, cross-sectional, and cross-cultural analyses. J Pers Soc Psychol. 83:1456–1468.
McCutcheon JE, White FJ, Marinelli M. 2009. Individual differences in dopamine cell neuroadaptations following cocaine self-administration. Biol Psychiatry. 66:801–803.
Mensch S, Baraban M, Almeida R, Czopka T, Ausborn J, El Manira A, Lyons DA. 2015. Synaptic vesicle release regulates myelin sheath number of individual oligodendrocytes in vivo. Nat Neurosci. 18:628–630.
Mills KL, Goddings A-L, Clasen LS, Giedd JN, Blakemore S-J. 2014. The Developmental Mismatch in Structural Brain Maturation during Adolescence. Dev Neurosci.
Moll GH, Mehnert C, Wicker M, Bock N, Rothenberger A, Rüther E, Huether G. 2000. Age-associated changes in the densities of presynaptic monoamine transporters in different regions of the rat brain from early juvenile life to late adulthood. Brain Res Dev Brain Res. 119:251–257.
Moos T. 2002. Brain iron homeostasis. Dan Med Bull. 49:279–301.
Moos T, Rosengren Nielsen T. 2006. Ferroportin in the postnatal rat brain: implications for axonal transport and neuronal export of iron. Semin Pediatr Neurol. 13:149–157.
Mori S, Wakana S, Nagae-Poetscher LM, VanZijl PCM. 2005. MRI Atlas of Human White Matter. Amsterdam: Elsevier B. V.
O'Doherty JP. 2004. Reward representations and reward-related learning in the human brain: insights from neuroimaging. Curr Opin Neurobiol. 14:769–776.
Ogg RJ, Steen RG. 1998. Age-related changes in Brain T1 are correlated with iron concentration. Magn Reson Med. 40:749–753.
Olson IR, Plotzker A, Ezzyat Y. 2007. The Enigmatic temporal pole: a review of findings on social and emotional processing. Brain. 130:1718–1731.
Ortega R, Cloetens P, Devès G, Carmona A, Bohic S. 2007. Iron Storage within Dopamine Neurovesicles Revealed by Chemical Nano-Imaging. PLOS ONE. 2:e925.
Ostby Y, Tamnes CK, Fjell AM, Westlye LT, Due-Tønnessen P, Walhovd KB. 2009. Heterogeneity in subcortical brain development: A structural magnetic resonance imaging study of brain maturation from 8 to 30 years. J Neurosci Off J Soc Neurosci. 29:11772–11782.
Padmanabhan A, Geier CF, Ordaz SJ, Teslovich T, Luna B. 2011. Developmental changes in brain function underlying the influence of reward processing on inhibitory control. Dev Cogn Neurosci. 1:517–529.
Padmanabhan A, Lynn A, Foran W, Luna B, O'Hearn K. 2013. Age related changes in striatal resting state functional connectivity in autism. Front Hum Neurosci. 7:814.
Patel KT, Stevens MC, Meda SA, Muska C, Thomas AD, Potenza MN, Pearlson GD. 2013. Robust Changes in Reward Circuitry During Reward Loss in Current and Former Cocaine Users During Performance of a Monetary Incentive Delay Task. Biol Psychiatry.
Paulsen DJ, Hallquist MN, Geier CF, Luna B. 2014. Effects of incentives, age, and behavior on brain activation during inhibitory control: A longitudinal fMRI study. Dev Cogn Neurosci.
Peper JS, Mandl RCW, Braams BR, de Water E, Heijboer AC, Koolschijn PCMP, Crone EA. 2013. Delay discounting and frontostriatal fiber tracts: a combined DTI and MTR study on impulsive choices in healthy young adults. Cereb Cortex N Y N 1991. 23:1695–1702.

Piao Y-S, Lian T-H, Hu Y, Zuo L-J, Guo P, Yu S-Y, Liu L, Jin Z, Zhao H, Li L-X, Yu Q-J, Wang R-D, Chen S-D, Chan P, Wang X-M, Zhang W. 2017. Restless legs syndrome in Parkinson disease: Clinical characteristics, abnormal iron metabolism and altered neurotransmitters. Sci Rep. 7:10547.

Pierpaoli C, Barnett A, Pajevic S, Chen R, Penix LR, Virta A, Basser P. 2001. Water diffusion changes in Wallerian degeneration and their dependence on white matter architecture. NeuroImage. 13:1174–1185.

Porter JN, Roy AK, Benson B, Carlisi C, Collins PF, Leibenluft E, Pine DS, Luciana M, Ernst M. 2015. Age-related changes in the intrinsic functional connectivity of the human ventral vs. dorsal striatum from childhood to middle age. Dev Cogn Neurosci. 11:83–95.

Qi Z, Miller GW, Voit EO. 2008. A Mathematical Model of Presynaptic Dopamine Homeostasis: Implications for Schizophrenia. Pharmacopsychiatry. 41:S89–S98.

Qiu D, Tan L-H, Zhou K, Khong P-L. 2008. Diffusion tensor imaging of normal white matter maturation from late childhood to young adulthood: Voxel-wise evaluation of mean diffusivity, fractional anisotropy, radial and axial diffusivities, and correlation with reading development. NeuroImage. 41:223–232.

Rami-Mark C, Bornatowicz B, Fink C, Otter P, Ungersboeck J, Vraka C, Haeusler D, Nics L, Spreitzer H, Hacker M, Mitterhauser M, Wadsak W. 2013. Synthesis, radiosynthesis and first in vitro evaluation of novel PET-tracers for the dopamine transporter: [(11)C]IPCIT and [(18)F]FE@IPCIT. Bioorg Med Chem. 21:7562–7569.

Ramsey AJ, Hillas PJ, Fitzpatrick PF. 1996. Characterization of the Active Site Iron in Tyrosine Hydroxylase REDOX STATES OF THE IRON. J Biol Chem. 271:24395–24400.

Raznahan A, Shaw PW, Lerch JP, Clasen LS, Greenstein D, Berman R, Pipitone J, Chakravarty MM, Giedd JN. 2014. Longitudinal four-dimensional mapping of subcortical anatomy in human development. Proc Natl Acad Sci. 111:1592–1597.

Roalf DR, Quarmley M, Elliott MA, Satterthwaite TD, Vandekar SN, Ruparel K, Gennatas ED, Calkins ME, Moore TM, Hopson R, Prabhakaran K, Jackson CT, Verma R, Hakonarson H, Gur RC, Gur RE. 2016. The impact of quality assurance assessment on diffusion tensor imaging outcomes in a large-scale population-based cohort. NeuroImage. 125:903–919.

Rouault TA. 2013. Iron metabolism in the CNS: implications for neurodegenerative diseases. Nat Rev Neurosci. 14:551–564.

Salvatore MF, Fisher B, Surgener SP, Gerhardt GA, Rouault T. 2005. Neurochemical investigations of dopamine neuronal systems in iron-regulatory protein 2 (IRP-2) knockout mice. Mol Brain Res. 139:341–347.

Salvatore MF, Pruett BS. 2012. Dichotomy of Tyrosine Hydroxylase and Dopamine Regulation between Somatodendritic and Terminal Field Areas of Nigrostriatal and Mesoaccumbens Pathways. PLOS ONE. 7:e29867.

Savalia NK, Agres PF, Chan MY, Feczko EJ, Kennedy KM, Wig GS. 2017. Motion-related artifacts in structural brain images revealed with independent estimates of in-scanner head motion. Hum Brain Mapp. 38:472–492.

Sedlacik J, Boelmans K, Löbel U, Holst B, Siemonsen S, Fiehler J. 2014. Reversible, irreversible and effective transverse relaxation rates in normal aging brain at 3 T. NeuroImage. 84:1032–1041.

Seo M, Lee E, Averbeck BB. 2012. Action selection and action value in frontal-striatal circuits. Neuron. 74:947–960.

Shen C-Y, Tyan Y-S, Kuo L-W, Wu CW, Weng J-C. 2015. Quantitative Evaluation of Rabbit Brain Injury after Cerebral Hemisphere Radiation Exposure Using Generalized q-Sampling Imaging. PloS One. 10:e0133001.

Shulman EP, Harden KP, Chein JM, Steinberg L. 2015. Sex differences in the developmental trajectories of impulse control and sensation-seeking from early adolescence to early adulthood. J Youth Adolesc. 44:1–17.

Shulman EP, Smith AR, Silva K, Icenogle G, Duell N, Chein J, Steinberg L. 2016. The dual systems model: Review, reappraisal, and reaffirmation. Dev Cogn Neurosci. 17:103–117.

Simmonds DJ, Hallquist MN, Asato M, Luna B. 2014a. Developmental stages and sex differences of white matter and behavioral development through adolescence: a longitudinal diffusion tensor imaging (DTI) study. NeuroImage. 92:356–368.

Simmonds DJ, Hallquist MN, Asato M, Luna B. 2014b. Developmental stages and sex differences of white matter and behavioral development through adolescence: a longitudinal diffusion tensor imaging (DTI) study. NeuroImage. 92:356–368.

Somerville LH, Casey BJ. 2010. Developmental neurobiology of cognitive control and motivational systems. Curr Opin Neurobiol. 20:236–241.

Sowell ER, Thompson PM, Holmes CJ, Jernigan TL, Toga AW. 1999. In vivo evidence for post-adolescent brain maturation in frontal and striatal regions. Nat Neurosci. 2:859–861.

Sowell ER, Trauner DA, Gamst A, Jernigan TL. 2002. Development of cortical and subcortical brain structures in childhood and adolescence: a structural MRI study. Dev Med Child Neurol. 44:4–16.

Spear LP. 2000. The adolescent brain and age-related behavioral manifestations. Neurosci Biobehav Rev. 24:417–463.

Stalnaker TA, Cooch NK, Schoenbaum G. 2015. What the orbitofrontal cortex does not do. Nat Neurosci. 18:620–627.

Stansfield KH, Kirstein CL. 2006. Effects of novelty on behavior in the adolescent and adult rat. Dev Psychobiol. 48:10–15.

Stehouwer JS, Goodman MM. 2009. Fluorine-18 Radiolabeled PET Tracers for Imaging Monoamine Transporters: Dopamine, Serotonin, and Norepinephrine. PET Clin. 4:101–128.

Steinberg L. 2008. A Social Neuroscience Perspective on Adolescent Risk-Taking. Dev Rev. 28:78–106.

Steinberg L. 2010. A dual systems model of adolescent risk-taking. Dev Psychobiol. 52:216–224.

Stüber C, Morawski M, Schäfer A, Labadie C, Wähnert M, Leuze C, Streicher M, Barapatre N, Reimann K, Geyer S, Spemann D, Turner R. 2014. Myelin and iron concentration in the human brain: A quantitative study of MRI contrast. NeuroImage. 93:95–106.

Supekar K, Musen M, Menon V. 2009. Development of large-scale functional brain networks in children. PLoSBiol. 7:e1000157.

Surmeier DJ, Ding J, Day M, Wang Z, Shen W. 2007. D1 and D2 dopamine-receptor modulation of striatal glutamatergic signaling in striatal medium spiny neurons. Trends Neurosci. 30:228–235.

Tamnes CK, Ostby Y, Fjell AM, Westlye LT, Due-Tonnessen P, Walhovd KB. 2009. Brain Maturation in Adolescence and Young Adulthood: Regional Age-Related Changes in Cortical Thickness and White Matter Volume and Microstructure. Cereb Cortex. Epub ahead of print.

Tamnes CK, Walhovd KB, Dale AM, Østby Y, Grydeland H, Richardson G, Westlye LT, Roddey JC, Hagler Jr. DJ, Due-Tønnessen P, Holland D, Fjell AM. 2013. Brain development and aging: Overlapping and unique patterns of change. NeuroImage. 68:63–74.

Tarazi FI, Baldessarini RJ. 2000. Comparative postnatal development of dopamine D1, D2 and D4 receptors in rat forebrain. Int J Dev Neurosci. 18:29–37.

Tarazi FI, Tomasini EC, Baldessarini RJ. 1998a. Postnatal development of dopamine D4-like receptors in rat forebrain regions: comparison with D2-like receptors. Brain Res Dev Brain Res. 110:227–233.

Tarazi FI, Tomasini EC, Baldessarini RJ. 1998b. Postnatal development of dopamine and serotonin transporters in rat caudate-putamen and nucleus accumbens septi. Neurosci Lett. 254:21–24.

Teicher MH, Andersen SL, Hostetter JC Jr. 1995. Evidence for dopamine receptor pruning between adolescence and adulthood in striatum but not nucleus accumbens. Brain Res Dev Brain Res. 89:167–172.

Telzer EH. 2016. Dopaminergic reward sensitivity can promote adolescent health: A new perspective on the mechanism of ventral striatum activation. Dev Cogn Neurosci. 17:57–67.

Todorich B, Pasquini JM, Garcia CI, Paez PM, Connor JR. 2009. Oligodendrocytes and myelination: the role of iron. Glia. 57:467–478.

Tziortzi AC, Searle GE, Tzimopoulou S, Salinas C, Beaver JD, Jenkinson M, Laruelle M, Rabiner EA, Gunn RN. 2011. Imaging dopamine receptors in humans with [11C]-(+)-PHNO: dissection of D3 signal and anatomy. NeuroImage. 54:264–277.

Unger EL, Bianco LE, Jones BC, Allen RP, Earley CJ. 2014. Low brain iron effects and reversibility on striatal dopamine dynamics. Exp Neurol. 261:462–468.

Unger EL, Wiesinger JA, Hao L, Beard JL. 2008. Dopamine D2 receptor expression is altered by changes in cellular iron levels in PC12 cells and rat brain tissue. J Nutr. 138:2487–2494.

van Duijvenvoorde ACK, Achterberg M, Braams BR, Peters S, Crone EA. 2016. Testing a dual-systems model of adolescent brain development using resting-state connectivity analyses. NeuroImage. 124:409–420.

van Leijenhorst L, Gunther Moor B, Op de Macks Z, Rombouts S, Westenberg PM, Crone E. 2010. Adolescent risky decision-making: Neurocognitive development of reward and control regions. NeuroImage. 51:345–355.

Vander Borght TM, Kilbourn MR, Koeppe RA, DaSilva JN, Carey JE, Kuhl DE, Frey KA. 1995. In vivo imaging of the brain vesicular monoamine transporter. J Nucl Med Off Publ Soc Nucl Med. 36:2252–2260.

Verstynen TD. 2014. The organization and dynamics of corticostriatal pathways link the medial orbitofrontal cortex to future behavioral responses. J Neurophysiol. 112:2457–2469.

Verstynen TD, Badre D, Jarbo K, Schneider W. 2012. Microstructural organizational patterns in the human corticostriatal system. J Neurophysiol. 107:2984–2995.

Vink M, Zandbelt BB, Gladwin T, Hillegers M, Hoogendam JM, van den Wildenberg WPM, Du Plessis S, Kahn RS. 2014. Frontostriatal activity and connectivity increase during proactive inhibition across adolescence and early adulthood. Hum Brain Mapp. 35:4415–4427.

Volkow ND, Wang GJ, Fowler JS, Logan J, Gatley SJ, MacGregor RR, Schlyer DJ, Hitzemann R, Wolf AP. 1996. Measuring age-related changes in dopamine D2 receptors with 11C-raclopride and 18F-N-methylspiroperidol. Psychiatry Res. 67:11–16.

Vossel S, Geng JJ, Fink GR. 2014. Dorsal and Ventral Attention Systems. The Neuroscientist. 20:150–159.
Vymazal J, Hajek M, Patronas N, Giedd JN, Bulte JW, Baumgarner C, Tran V, Brooks RA. 1995. The quantitative relation between T1-weighted and T2-weighted MRI of normal gray matter and iron concentration. J Magn Reson Imaging JMRI. 5:554–560.
Wager TD, Davidson ML, Hughes BL, Lindquist MA, Ochsner KN. 2008. Prefrontal-subcortical pathways mediating successful emotion regulation. Neuron. 59:1037–1050.
Wahlstrom D, Collins P, White T, Luciana M. 2010. Developmental changes in dopamine neurotransmission in adolescence: behavioral implications and issues in assessment. Brain Cogn. 72:146–159.
Walhovd KB, Tamnes CK, Bjørnerud A, Due-Tønnessen P, Holland D, Dale AM, Fjell AM. 2014. Maturation of Cortico-Subcortical Structural Networks—Segregation and Overlap of Medial Temporal and Fronto-Striatal Systems in Development. Cereb Cortex. bht424.
Wang J, Shaffer ML, Eslinger PJ, Sun X, Weitekamp CW, Patel MM, Dossick D, Gill DJ, Connor JR, Yang QX. 2012. Maturational and Aging Effects on Human Brain Apparent Transverse Relaxation. PLoS ONE. 7:e31907.
Wang Y, Adamson C, Yuan W, Altaye M, Rajagopal A, Byars AW, Holland SK. 2012. Sex differences in white matter development during adolescence: a DTI study. Brain Res. 1478:1–15.
Ward RJ, Zucca FA, Duyn JH, Crichton RR, Zecca L. 2014. The role of iron in brain ageing and neurodegenerative disorders. Lancet Neurol. 13:1045–1060.
Wiecki TV, Frank MJ. 2013. A computational model of inhibitory control in frontal cortex and basal ganglia. Psychol Rev. 120:329–355.
Wiesinger JA, Buwen JP, Cifelli CJ, Unger EL, Jones BC, Beard JL. 2007. Down-regulation of dopamine transporter by iron chelation in vitro is mediated by altered trafficking, not synthesis. J Neurochem. 100:167–179.
Willcutt EG. 2012. The prevalence of DSM-IV attention-deficit/hyperactivity disorder: a meta-analytic review. Neurother J Am Soc Exp Neurother. 9:490–499.
Wise RA. 2002. Brain reward circuitry: insights from unsensed incentives. Neuron. 36:229–240.
Wu Q, Reith ME, Kuhar MJ, Carroll FI, Garris PA. 2001. Preferential increases in nucleus accumbens dopamine after systemic cocaine administration are caused by unique characteristics of dopamine neurotransmission. J Neurosci Off J Soc Neurosci. 21:6338–6347.
Yablonskiy DA. 1998. Quantitation of intrinsic magnetic susceptibility-related effects in a tissue matrix. Phantom study. Magn Reson Med Off J Soc Magn Reson Med Soc Magn Reson Med. 39:417–428.
Yakovlev PI, Lecours AR, Minkowski A. 1967. The myelogenetic cycles of regional maturation of the brain. In: Regional Development of the Brain in Early Life. Oxford: Blackwell Scientific. p. 3–70.
Yeh F-C, Tseng W-YI. 2011. NTU-90: A high angular resolution brain atlas constructed by q-space diffeomorphic reconstruction. NeuroImage. 58:91–99.
Yeh F-C, Verstynen TD, Wang Y, Fernández-Miranda JC, Tseng W-YI. 2013. Deterministic diffusion fiber tracking improved by quantitative anisotropy. PloS One. 8:e80713.
Yeh F-C, Wedeen VJ, Tseng W-YI. 2010. Generalized q-sampling imaging. IEEE Trans Med Imaging. 29:1626–1635.

Yendiki A, Koldewyn K, Kakunoori S, Kanwisher N, Fischl B. 2014. Spurious group differences due to head motion in a diffusion MRI study. NeuroImage. 88:79–90.

Yeo BTT, Krienen FM, Sepulcre J, Sabuncu MR, Lashkari D, Hollinshead M, Roffman JL, Smoller JW, Zöllei L, Polimeni JR, Fischl B, Liu H, Buckner RL. 2011. The organization of the human cerebral cortex estimated by intrinsic functional connectivity. J Neurophysiol. 106:1125–1165.

Zhang H, Wang Y, Lu T, Qiu B, Tang Y, Ou S, Tie X, Sun C, Xu K, Wang Y. 2013. Differences between generalized q-sampling imaging and diffusion tensor imaging in the preoperative visualization of the nerve fiber tracts within peritumoral edema in brain. Neurosurgery. 73:1044–1053; discussion 1053.

Zucca FA, Segura-Aguilar J, Ferrari E, Muñoz P, Paris I, Sulzer D, Sarna T, Casella L, Zecca L. 2017. Interactions of iron, dopamine and neuromelanin pathways in brain aging and Parkinson's disease. Prog Neurobiol. 155:96–119.